Fermi National Accelerator Laboratory

FERMILAB-Pub-75/36-THY
April 1975

REGGEON FIELD THEORY: FORMULATION AND USE*

Henry D. I. Abarbanel
Fermi National Accelerator Laboratory
Batavia, Illinois 60510

John B. Bronzan
Department of Physics,
Rutgers, The State University,
New Brunswick, N.J. 08903

Robert L. Sugar
Department of Physics, University of California,
Santa Barbara, California 93106

Alan R. White
Department of Physics, University of California,
Berkeley, California 94720

*Work supported by the Atomic Energy Commission and the National Science Foundation.

ABSTRACT

We formulate and discuss Reggeon field theory, which enables one to systematically analyze the exchange of Regge poles and associated branch points in high energy hadron scattering. The field theory is first motivated by a consideration of hybrid Feynman graphs, and then a more general derivation from crossed-channel multiparticle unitarity relations is given. Rules for Reggeon interaction and propagation are formulated. We treat in some detail the problem of the Pomeron or vacuum pole which has $\alpha(0) = 1$ and is responsible for diffractive processes. In particular the renormalization group analysis of Reggeon field theory is presented and the structure of Pomeron partial wave amplitudes is elucidated. Also the question of Pomeron or absorptive corrections to secondary trajectories (both fermion and boson) is considered. We make some comments on important problems yet remaining in Reggeon field theory; in particular, we stress the study of its s-channel content.

I. INTRODUCTION

The development of the theory of complex angular momentum (J) and the notion of moving singularities in the J-plane has provided for many years an important framework for the theoretical and phenomenological analysis of high energy (s) and small momentum transfer (t) hadron scattering processes. An elastic amplitude $T^{\tau}_{AB}(z,t)$ has the Sommerfeld-Watson representation

$$T^{\tau}_{AB}(z,t) = \frac{-1}{2i}\int_{-\frac{1}{2}-i\infty}^{-\frac{1}{2}+i\infty} \frac{dJ(2J+1)}{\sin\pi J}\,[P_J(-z)+\tau P_J(z)]F^{\tau}_{AB}(J,t) \qquad (1.1)$$

where z is the cosine of the center of mass scattering angle, and so is linearly related to s, while $\tau = \pm 1$ and denotes signature. The initial hope, based on non-relativistic potential theory, was that the only singularities of the partial-wave amplitude $F^{\tau}_{AB}(J,t)$ would be simple poles[1-3] -Regge poles, whose position depends on t. (Fig. 1.1.) It is well-known that in a relativistic theory a Regge pole gives both resonance poles in the cross-channel (positive t) and high-energy power behavior, for fixed t, in the direct or s-channel. Both of these properties of a Regge pole can easily be obtained from (1.1) and their use to relate experimental results in channels related by crossing was one of the early triumphs of complex angular momentum theory.

Unfortunately it soon became clear, following the theoretical work of Amati, Fubini and Stanghellini,[4] Mandelstam,[5] and Polkinghorne[6] that in a relativistic theory Regge poles in $F^{\tau}_{AB}(J,t)$ must be accompanied by further branch-point singularities - Regge cuts. These branch-points can be viewed as resulting directly from

the exchange of two or more Regge poles at high energy. Alternatively they can be thought of as resulting from unitarity in the cross-channel, since this requires branch-points at the production thresholds for two or more Regge poles. (The branch-points do not produce singularities in the t-channel physical partial-waves and so, unlike Regge poles, Regge cuts are not directly observable in this channel.) The exchange of n Regge poles (Fig. 1.2), all of which have the same trajectory $\alpha(t)$ gives a branch-point at $\alpha^{(n)}(t)$:

$$\alpha^{(n)}(t) - 1 = n\,[\alpha(t/n^2)-1] \qquad (1.2)$$

If we assume the existence of a Pomeron pole ($\underset{\sim}{P}$), which carries vacuum quantum numbers and has intercept $\alpha_{\underset{\sim}{P}}(0) = 1$ then the branch-points involving a Regge pole $\alpha_R(t)$ (which may or may not be the $\underset{\sim}{P}$) and many accompanying $\underset{\sim}{P}$'s become particularly significant. This is because these branch-points lie to the right of the Regge pole in the J-plane for negative t (this is clear from (1.2) if we take $\alpha_R(t) = \alpha_{\underset{\sim}{P}}(t)$), and so, in the absence of special arguments to the contrary, ought to provide the dominant contribution to high-energy scattering. From a phenomenological point of view, the branch-points are very unattractive. While a pole has a residue, which, depending on t as it must, factorizes, a branch-point is characterized by a function of J and t representing the jump or discontinuity across the cut attached to the branch-point. In general there is no factorization and considerable freedom of parametrization. Not

surprisingly therefore, phenomenologists have avoided Regge cuts as far as possible, and in fact in some areas the experimental success of Regge poles is more striking today than at any time in the past decade. In particular the parametrization of πN charge exchange by a simple ρ-Regge pole exchange

$$\frac{d\sigma}{dt}\left(\pi^- p \to \pi^0 n\right) = \beta(t) s^{2\alpha_\rho(t)-2} \tag{1.3}$$

has recently been shown to hold over an enormous range of laboratory momentum.[7]

Nevertheless it has also become clear recently that both experimentally and theoretically Regge cuts are unavoidable and must be accounted for. The rise of total cross-sections through Fermi-Lab and ISR energy ranges[8-10] may well be parametrized by a single Pomeron pole ($\underset{\sim}{P}$) but this requires $\alpha_{\underset{\sim}{P}}(0) > 1$ and we know this is inconsistent with the Froissart bound. Therefore, any consistent parametrization of asymptotically rising cross-sections must make essential use of Regge cuts.

The advent of the active study of inclusive reactions, in particular the combination of the Mueller theorem[11-14] with the sum rules relating different inclusive cross-sections,[15-16] has also shown that an asymptotically constant total cross-section associated with an isolated $\underset{\sim}{P}$ pole, is inconsistent. It is first argued that if the total cross-section goes to a constant, then the triple $\underset{\sim}{P}$ coupling observed in the triple Regge region of the one-particle inclusive cross-section must vanish at zero momentum transfer.[15,17] A further sequence of arguments then leads to the

conclusion that the $\underset{\sim}{P}$ couplings (to particles) which appear in total cross-sections should also vanish.[18,19] Hence the total cross-section cannot go to a constant. Thus as a matter of principle, Regge cuts must play an essential role if the total cross-section is to rise indefinitely or approach a constant at asymptotic energies.

We have already pointed out that (1.2) implies the importance of multi-$\underset{\sim}{P}$ cuts if $\alpha_{\underset{\sim}{P}}(0) = 1$. We emphasize that from a purely theoretical viewpoint multiparticle t-channel unitarity[20,21] (if nothing else) requires, that if we wish to describe the Pomeron as a Regge pole then $n\underset{\sim}{P}$ cuts with $\alpha_{\underset{\sim}{P}}^{(n)}(0) = 1$ must also be present. The issue has been their relative experimental and theoretical importance. What we are now arguing is that for a completely self-consistent picture of the $\underset{\sim}{P}$ the cuts are absolutely essential. This is true whether we are discussing the theoretical constraints of s and t- channel unitarity on the $\underset{\sim}{P}$ or whether we are discussing experimental properties.

In this article we shall review the derivation and current status of the one theory whose aim is to correctly assess the effect of all multi-$\underset{\sim}{P}$ cuts. This theory was developed by V. N. Gribov[22] and his collaborators and has been variously called the Reggeon diagram technique or the Reggeon calculus. We have decided to call it Reggeon Field Theory (RFT) instead because this name accurately states that we are dealing with a field theory for quasi-particles (Reggeons) with a Lagrangian, field operators, Green's functions etc. In fact most of the recent progress in the subject has come from the use of currently popular field-theoretic

techniques based on the renormalization group. We should perhaps add that with our present understanding we believe the field-theoretical picture of Reggeons is only valuable in the scattering region. We do not expect it to be adequate to describe the t-channel creation of particles and resonances.

Our aim is to give a coherent account of RFT rather than a historical survey or a detailed account of technical points. We have attempted to discuss those subjects which seem central so that a general reader can learn the scope and technical rudiments of the theory. We hope that references will lead both the general reader and the expert to the current literature.

In RFT the t-channel or cross channel is stressed. In our view the best starting point for a model independent derivation of the RFT is the multi-particle unitarity relation for the t-channel partial wave amplitude.

That Regge cuts can be studied more directly in the t-channel unitarity relation than in the s-channel relation was first pointed out by Mandelstam.[5] In a fundamental paper Gribov, Pomeranchuk and Ter-Martirosyan[20] (GPT) extrapolated and generalized Mandelstam's work to show that a complete structure for Regge cuts could be obtained from the multiparticle unitarity relation for the t-channel partial-wave amplitude. (The ambiguities in the GPT work associated with problems of signature and complex helicity continuations have since been resolved by White.)[21,23,24] The result is that, in the angular momentum plane Reggeons look very much like quasi-particles. The multi-Reggeon branch-points can be regarded as Reggeon production thresholds. The discontinuities across the

attached cuts are given by formulae very similar to conventional unitarity relations and we therefore call them Reggeon unitarity relations.

It is our belief that a proper treatment of Reggeon unitarity is crucial for the study of scattering at large s, fixed t. Our conviction arises because all of the multi-$\underset{\sim}{P}$ channels are coupled by the discontinuity formulae, and for $t \to 0$, the thresholds of these channels approach each other. (In Eq. (1.2) when $\alpha(0) = 1$, $\alpha^n(0) = 1$.) The resulting strong coupling of many $\underset{\sim}{P}$ channels is a vital effect whose treatment is unique to the RFT.

Some time after the GPT work Gribov showed,[22] by studying classes of hybrid Feynman graphs, how an underlying field theory of strong interactions could be expected to satisfy Reggeon unitarity. He found a J-plane perturbation expansion which is analogous to the Feynman-Dyson perturbation solution of conventional unitarity. This was Gribov's original justification for the RFT. However the RFT is probably best thought of as a device for ensuring that the Reggeon unitarity relations are satisfied. From this point of view it is clear that the RFT may also be applicable to theories of strong interactions that are not simple local field theories (dual models, for example).

Reggeons are treated directly as quasi-particles by associating each of them with a field. No attempt is made to understand the spectrum of Regge trajectories; instead one attempts to study their interactions given that they exist. The philosophy here is the same as in the study of interactions among excitations such as phonons and plasmons in solid-state physics.

While care is taken to enforce t-channel unitarity, the constraints of s-channel unitarity are not explicitly built into the RFT. As a result one must verify that the theory does not violate these constraints. (Because of the limited phase-space region described by RFT a complete check of s-channel unitarity in the form "$SS^+ = 1$" is probably not possible.) When the renormalized $\underset{\sim}{P}$ singularity has intercept one, the $\underset{\sim}{P}$ interactions apparently remove the violation of the inclusive sum rules found for poles alone.[25] Furthermore when one tries to increase the $\underset{\sim}{P}$ intercept above one, model calculations suggest that after all cuts are summed, the Froissart bound is at most saturated, in fairly general circumstances.[26,27] As a result we believe that the theory is complete enough to satisfy the constraints of s-channel unitarity.

The above philosophy should be contrasted with that of s-channel models. In these models the constraints of s-channel unitarity are built into the elastic scattering amplitude by repeated iteration of t-channel exchanges. For example, in eikonal models, when the eikonal phase is given by Regge pole exchange,[28,29] one is summing the graphs of Fig. 1.2, which do not include any interactions among the Reggeons. Such interactions can be put in by hand, one at a time,[30] but not in such a way as to satisfy Reggeon unitarity. Note that the graphs of the s-channel models form a subset of the RFT graphs, which may help to explain why the RFT does appear to satisfy the constraints of s-channel unitarity. Models which satisfy full multiparticle s-channel unitarity have also been constructed[31-33] but again they do not satisfy Reggeon unitarity.

The RFT has one apparent limitation which would be fatal if it were unmitigated. There are interactions among any number of $\underset{\sim}{P}$'s or among $\underset{\sim}{P}$'s and Regge poles carrying quantum numbers. Each of these interactions is specified by an arbitrary function of the momentum and angular momentum of the $\underset{\sim}{P}$'s and Regge poles coming together at a point. In the same way, arbitrary functions are involved in the production and absorption of $\underset{\sim}{P}$'s by particles. The theory therefore has infinitely many parameters.

It is possible that these parameters can be calculated in terms of a smaller set of parameters of the (assumed) underlying strong interaction theory. We favor the view that all these parameters are unimportant if the energy is high enough, while at current energies a phenomenology involving only a few parameters can probably be constructed. The former statement is defended by renormalization group arguments to be discussed in detail later. These arguments tell us that total and elastic cross-sections should have the asymptotic forms

$$\sigma_{AB}(s) \underset{s \to \infty}{\sim} g_A g_B (\log s)^{\eta} \tag{1.4}$$

and

$$\left(\frac{d\sigma}{dt}\right)_{AB} \underset{s \to \infty}{\sim} g_A^2 g_B^2 (\log s)^{2\eta} \varphi(\rho/\rho_0) \quad , \tag{1.5}$$

where

$$\rho = t/(\log s)^{\nu} \quad . \tag{1.6}$$

This asymptotic behavior arises from diagrams in which the external particles couple through poles (Fig. 1.3) - called enhanced graphs in the Soviet literature.

The numbers g_A, g_B and the scale parameter ρ_0 in the "scaling function" φ will depend on the parameters of the RFT, but η and ν and the functional form of φ will not. This was found to be the case in the original papers of Abarbanel and Bronzan[34] who

considered the theory with just a triple $\underset{\sim}{P}$ interaction, and of Migdal, Polyakov and Ter-Martirosyan,[25] who considered both the pure triple $\underset{\sim}{P}$ theory and the general theory obtained by adding higher couplings. Actually η and ν are two of several exponents in the theory, that are analogous to the critical exponents which govern second-order phase transition theory.[35] The universality principle that the critical exponents of the theory are independent of the (unknown) underlying parameters is also directly analogous to the universality of critical exponents in phase transitions.[35] The universality of φ offers the possibility that we can calculate the shape (if not the scale) of the diffraction peak at very high energies. We are fortunate that in asking for the form of the high energy behavior of hadron scattering processes we are asking a question which can have an answer which is both simple and universal.

Our plan of presentation will be this: We begin in Section II with a brief review of Gribov's derivation of Reggeon calculus rules from hybrid Feynman graphs. These rules underlie the RFT one abstracts from the graphs. We believe the hybrid graph approach provides the best physical motivation for the RFT and this is why we begin with it. The hybrid graph approach has, however, suffered from criticisms of double counting (which are difficult, although, we believe, possible to resolve), and one can certainly question the generality of the rules extracted from a particular model field theory. As a matter of principle therefore we prefer to introduce the RFT as a solution of Regge cut discontinuity formulae, that is Reggeon unitarity.

The derivation of Regge cut discontinuity formulae using only the hallowed S-matrix principles of unitarity and analyticity is discussed in Section III. The discussion concentrates on the two-Reggeon cut, with the extension to the n-Reggeon cut covered briefly. We also discuss some points that are independent of RFT, for example the sign of the $2\underset{\sim}{P}$ cut and the use of a sum rule to relate its magnitude to inclusive reaction data.

Section IV is devoted to the problem of the Pomeron and its self-consistency within the RFT. We first review early work by Soviet workers and others which is based on the Schwinger-Dyson equations of the theory and is directed towards a "weak coupling" $\underset{\sim}{P}$ (that is asymptotically constant total cross-sections). We then discuss the application of the renormalization group to the problem. We show that an explicit solution for the $\underset{\sim}{P}$ exists which is actually a "strong-coupling" or "scaling" solution and gives (1.4) and (1.5). We then discuss the interaction of the "scaling" $\underset{\sim}{P}$ with boson and fermion Regge poles. The Section closes on a speculative note about the existence of further solutions to the RFT.

In Section V we review the use of the RFT to describe inelastic processes. We discuss the "cutting rules" of Abramovskii, Gribov and Kanchelli[36] which can be used to derive an RFT for inclusive production processes from that for the elastic amplitude bypassing both the hybrid Feynman graph and the Reggeon unitarity approaches. We discuss 2-N production processes using the hybrid graph approach and briefly discuss the triple Regge region from both this approach

and Reggeon unitarity. The rest of the Section is devoted to the general issue of the s-channel content of Reggeon field theories which we address incompletely while stressing its importance.

Section VI is a discussion of conclusions and views toward a phenomenology using the RFT. We discuss some orders of magnitude to indicate our conception of where "asymptopia" may lie. Our prejudice is that what we primarily see at present accelerator and colliding beam energies is a "bare" $\underset{\sim}{P}$, together with its "bare" couplings. We discuss briefly how one might attempt to make a phenomenology out of this observation. The final part of this Section is a resumé of our article emphasizing the important conclusions and giving our outlook for the future of Reggeon Field Theory.

II. HYBRID FEYNMAN GRAPHS AS MOTIVATION FOR REGGEON FIELD THEORY

RFT was first abstracted from a study of hybrid Feynman diagrams by Gribov[22] in 1967. Examples of such diagrams are shown in Figs. 2.1 and 2.3. Their importance is that they represent explicit examples of the general form of amplitudes that we expect to represent multiple Regge exchanges in a relativistic field theory. The circles represent off mass-shell two-body amplitudes that will eventually be represented by their Regge asymptotic form. The first step, however, is to find the relation between the asymptotic behavior of the circles and that of the entire graph. One can then study the interaction between J-plane poles and cuts by making appropriate choices for the asymptotic behavior of the circles.

In order to illustrate Gribov's procedure let us outline his discussion of the diagram of Fig. 2.1. We wish to calculate the asymptotic behavior of this diagram for large $s = (p_1+p_2)^2$ and fixed $t = (p_1-p_1')^2$. For simplicity we take all the particles to be spinless and to have equal mass, m. It is convenient to introduce Sudakov variables[37] by writing a general four-vector, k, in the form

$$k = \alpha\tilde{p}_2 + \beta\tilde{p}_1 + k_\perp \quad , \tag{2.1}$$

where

$$\begin{aligned} \tilde{p}_1 &= p_1 - \frac{m^2}{s} p_2 \\ \tilde{p}_2 &= p_2 - \frac{m^2}{s} p_1 \end{aligned} \tag{2.2}$$

and α and β can range from plus to minus infinity. The vectors $\tilde{p}_1$ and $\tilde{p}_2$ have length

$$\tilde{p}_1^2 = \tilde{p}_2^2 = \frac{2m^4}{s} + \frac{m^6}{s^2} \tag{2.3}$$

so that at large s we make an error of $0(\frac{1}{s})$ by setting

$$\tilde{p}_1^2 = \tilde{p}_2^2 = 0 \tag{2.4}$$

The vector $k_\perp$ is a two-dimensional space-like vector orthogonal to $\tilde{p}_1$ and to $\tilde{p}_2$. In particular

$$q = (p_1 - p_1') = \frac{2q^2}{s}(\tilde{p}_2 - \tilde{p}_1) + q_\perp \tag{2.5}$$

and so $q^2 \simeq q_\perp^2$. We shall nearly always neglect terms of order $(m^2$ or $t)/s$. (This means that in the J-plane any results we derive are accurate only within a neighborhood of at most one unit from the leading singularity.) In terms of the Sudakov variables we shall, however, write d^4k in the form

$$d^4k = \sqrt{s}\ p\ d\alpha d\beta\ d^2k_\perp \tag{2.6}$$

where $p = (\frac{s}{4} - m^2)^{\frac{1}{2}}$. Keeping the factor $p = \frac{1}{2}s^{\frac{1}{2}} + 0(\frac{1}{s})$ will enable us to make our treatment of absorptive parts straightforward at a later stage.

The two-body amplitudes in Fig. 2.1 will be denoted by $f_1(k_1,k,k_2)$ and $f_2(p_1-k_1,q-k,p_2-k_2)$. It will be assumed that f_1 and f_2 are large when their energies $s_1 = (k_1+k_2)^2 \simeq 2k_1,k_2$ and $s_2 = (p_1-k_1+p_2-k_2)^2 \simeq 2(p_1-k_1)\cdot(p_2-k_2)$ are large, that is $0(s)$. It will also be assumed that they fall off when the momentum transfers k^2 and $(q-k)^2$ and the masses $k_1^2, (p_1-k_1)^2, k_2^2$, --- become

much larger than m^2. These assumptions are certainly reasonable when the asymptotic behavior of the f_i is dominated by Regge pole exchange. In this case the f_i can be written in factorized form; for example

$$f_1(k_1,k,k_2) = g(k_1^2,(k-k_1)^2;k^2)\,g(k_2^2,(k+k_2)^2;k^2) \cdot G(k^2,2k_1\cdot k_2) \tag{2.7}$$

The Reggeon propagator G, has the Sommerfeld-Watson representation

$$G(k^2,2k_1\cdot k_2) = -\int_{c-i\infty}^{c+i\infty} \frac{d\ell}{4i}\,\xi_\ell G_\ell(k^2)\left|2(k_1\cdot k_2)\right|^\ell \tag{2.8}$$

where as usual the contour of integration runs to the right of all singularities of G_ℓ and crosses the real axis between $\ell=-1$ and $\ell=0$

$$\xi_\ell = \frac{e^{-i\frac{\pi}{2}(\ell+\frac{1-\tau}{2})}}{\sin\frac{\pi}{2}(\ell+\frac{1-\tau}{2})} = \frac{e^{-i\pi\ell}+\tau}{\sin\pi\ell} \tag{2.9}$$

with $\tau = \pm 1$ for even or odd signature.

In general, of course, cut contributions to the f_i cannot be written in factorized form. However, as we shall see cuts which arise from the interplay of two or more poles can be expressed as integrals over factorized forms. As a result it is sufficient to study hybrid diagrams using only expressions of the form of equation (2.7) for the f_i.

We are now in a position to read off the high-energy behavior of the diagram of Fig. 2.1. First consider the denominators arising from the left-hand cross. For $s >> m^2$

$$
\begin{aligned}
k_1^2-m^2+i\epsilon &\approx \alpha_1\beta_1 s+k_{1\perp}^2-m^2+i\epsilon \\
(p_1-k_1)^2-m^2+i\epsilon &\approx \alpha_1(\beta_1-1)s+k_{1\perp}^2-\beta_1 m^2+i\epsilon \\
(k-k_1)^2-m^2+i\epsilon &\approx (\alpha_1-\alpha)(\beta_1-\beta)s+(k_\perp-k_{1\perp})^2-m^2+i\epsilon \\
(p_1-k_1-q+k)^2-m^2+i\epsilon &\approx (\alpha_1-\alpha)(\beta_1-1-\beta)s+2q^2(\alpha-\alpha_1-1-\beta+\beta_1) \\
&\quad + (q_\perp-k_\perp+k_{1\perp})^2+m^2(\beta-\beta_1)+i\epsilon
\end{aligned}
\tag{2.10}
$$

Notice that the four-momenta squared which enter (2.10) also appear as mass variables in the f_i. The requirement that they and the momentum transfers be less than or order m^2 gives

$$
\begin{aligned}
k_{1\perp}^2 &\lesssim m^2 & k_\perp^2 &\lesssim m^2 \\
\alpha_1 &\approx m^2/s & \alpha &\approx m^2/s \\
\beta_1 &\gtrsim 1 & \beta &\gtrsim 1
\end{aligned}
\tag{2.11}
$$

A similar analysis of the right-hand cross gives

$$
\begin{aligned}
k_{2\perp}^2 &\lesssim m^2 & k_\perp^2 &\lesssim m^2 \\
\beta_2 &\approx m^2/s & \beta &\approx m^2/s \\
\alpha_2 &\gtrsim 1 & \alpha &\gtrsim 1
\end{aligned}
\tag{2.12}
$$

Finally the requirement that $2k_1\cdot k_2 \approx \beta_1\alpha_2 s$ and $2(p_1-k_1)\cdot(p_2-k_2) \approx (1-\beta_1)(1-\alpha_2)s$ be of order s gives

$$
\beta_1 \approx 1 \qquad \alpha_2 \approx 1 \tag{2.13}
$$

Since $\beta \ll \beta_1$ it can be neglected in the denominators of (2.10). Similarly α can be neglected in the corresponding terms arising from the right-hand cross.

Putting together all of the above results we obtain a complete factorization of the integral represented by Fig. 2.1 which can now be written in the form

$$T(s,q^2) = \frac{i\pi}{4\sqrt{s}\,p} \int \frac{d\ell_1}{2\pi i} \frac{d\ell_2}{2\pi i} \frac{d^2k_\perp}{(2\pi)^2} \xi_{\ell_1} \xi_{\ell_2} N_{\ell_1\ell_2}(q,k_\perp)^2 \cdot G_{\ell_1}(k_\perp^2)\, G_{\ell_2}((q-k_\perp)^2)\, s^{\ell_1+\ell_2} \quad , \tag{2.14}$$

where

$$N_{\ell_1\ell_2}(q,k_\perp) = \frac{\lambda^2(\sqrt{s}\,2p)^2}{4(4\pi)^2} \int \frac{d\alpha_1 d\beta_1 d\alpha d^2k_{1\perp}}{(2\pi)^4} g(k_1^2, (k-k_1)^2; k_\perp^2) \cdot g((p_1-k_1)^2, (p_1-k_1+k-q)^2; (q-k_\perp)^2) \cdot \beta_1^{\ell_1}(1-\beta_1)^{\ell_2}[k_1^2-m^2+i\epsilon]^{-1}[(p_1-k_1)^2-m^2+i\epsilon]^{-1} \cdot [(k_1-k)^2-m^2+i\epsilon]^{-1}[(p_1-k_1+k-q)^2-m^2+i\epsilon]^{-1} \quad . \tag{2.15}$$

λ is the coupling constant for the three-particle vertices. $N_{\ell_1\ell_2}(q,k_\perp)$ can, of course, also be expressed in terms of the quantities associated with the right-hand crosses.

Several features of equation (2.15) are worth noticing. First the g's depend on α_1, β_1, and α only through the mass variables $k_1^2, (p_1-k_1)^2, (k-k_1)^2$ and $(p_1-k_1+k-q)^2$. Since the $i\epsilon$ prescription for the singularities in these variables is the same as for the propagators we see from (2.10) that the α_1 and α integrals vanish unless $0 \le \beta_1 \le 1$. For β_1 outside of this range, all singularities of the α_1 integrand lie on one side of the contour. We also see that if the coupling between the two-body amplitudes, which determines $N_{\ell_1\ell_2}$, were planar, all singularities in the α-plane (in the region where α_1 and α are

of order m^2/s) would lie on the same side of the α contour. As a result, the asymptotic contribution of the graph would be negligible.

This last result is the connection between Regge cut asymptotic behavior and the presence of a third double spectral function in the associated "two-particle/two Reggeon amplitude" which we shall find from a different point of view in the next section. Note that since $M^2 = (p_1 - k)^2 \approx -\alpha s + m^2$, we can pick out the α-integration in (2.15) and write

$$N_{\ell_1\ell_2}(q,k_\perp) = \frac{1}{\sqrt{2}} \int_{-\infty}^{+\infty} \frac{dM^2}{2\pi i} T_{\ell_1\ell_2}(M^2,q,k_\perp) \tag{2.16}$$

where $T_{\ell_1\ell_2}(M^2,q,k_\perp)$ is defined by the remainder of the integrand in (2.15). The M^2-contour can now be rotated to give

$$N_{\ell_1\ell_2}(q,k_\perp) = \frac{1}{\sqrt{2}} \int_{4m^2}^{\infty} \frac{dM^2}{\pi} A_{\ell_1\ell_2}(M^2,q,k_\perp) \tag{2.17}$$

where $A_{\ell_1\ell_2}(M^2,q,k_\perp)$ is the absorptive part of $T_{\ell_1\ell_2}(M^2,q,k_\perp)$ in the M^2-variable. We shall comment further on (2.17) shortly.

Since the important singularities in α and α_1, in (2.15), occur when these variables are of order m^2/s, each of these integrals gives rise to a factor of $\frac{1}{s}$. Consequently, $N_{\ell_1\ell_2}$ becomes independent of s at high energies. In addition, for q^2 and $k_\perp^2$ negative, which is the region of interest, $N_{\ell_1\ell_2}$ is real. If the simple crosses of Fig. 2.1 are replaced by more general couplings we still expect (2.14) to hold. Of course, $N_{\ell_1\ell_2}$ will no longer be given by (2.15) but we still expect it to be independent of s asymptotically and real in the s-channel physical region (this is

provided that the couplings do not themselves contain Regge singularities - a circumstance we consider shortly).

Next we note that since $\sqrt{s}$ p does not change sign under $s \to -s$, the signature of the amplitude $T(s,q^2)$ given by (2.14) is determined by the product of the signature factors $\xi_{\ell_1}\xi_{\ell_2}$. This is a generalized form of the result that the signature of the two-Reggeon cut is given by the product of the signatures of the contributing Regge poles.

The Reggeon calculus has as its objective a set of rules for the calculation of the signatured partial-wave amplitude $F(J,q_\perp^2)$ which is related to $T(s,q_\perp^2)$ by the Sommerfeld-Watson integral

$$T(s,q_\perp^2) = \frac{i}{4}\int_{c-i\infty}^{c+i\infty} dJ\ \xi_J\ s^J\ F(J,q_\perp^2) \tag{2.18}$$

ξ_J being the signature factor corresponding to the signature of $T(s,q_\perp^2)$. (2.18) can be inverted to give

$$F(J,q_\perp^2) = \frac{2}{\pi}\int_1^\infty ds'(s')^{-(J+1)}A(s',q_\perp^2) \tag{2.19}$$

where

$$A(s,q_\perp^2) = \text{Abs}T(s,q_\perp^2) = \frac{1}{2i}[T(s+i\epsilon,q_\perp^2)-T(s-i\epsilon,q_\perp^2)] \tag{2.20}$$

(2.18) is equivalent to (1.1) to leading order in s. The Mellin transform (2.19) is more convenient for our purposes here than the Froissart-Gribov projection which appears in (1.1). In the next Section we shall use the Froissart-Gribov projection because it diagonalizes t-channel unitarity equations.

Using the facts that

$$\mathrm{Abs}(\xi_\ell s^\ell) = s^\ell , \quad \mathrm{Abs}\left(\frac{i}{2p\sqrt{s}}\right) = \frac{1}{2p\sqrt{s}} \simeq \frac{1}{s} \tag{2.21}$$

we see from (2.14) that

$$A(s,q_\perp^2) = \frac{\pi}{2} \int \frac{d\ell_1}{2\pi i} \frac{d\ell_2}{2\pi i} \frac{d^2k_\perp}{(2\pi)^2} \gamma_{\ell_1\ell_2} N^2_{\ell_1\ell_2}(q_\perp,k_\perp)$$

$$\cdot G_{\ell_1}(k_\perp^2) G_{\ell_2}((q_\perp-k_\perp)^2) s^{\ell_1+\ell_2-1} \tag{2.22}$$

with

$$\gamma_{\ell_1\ell_2} = \frac{1}{\zeta_{\ell_1}\zeta_{\ell_2}} \cos\left[\frac{\pi}{2}\left(\ell_1+\ell_2 + \frac{(1-\tau_1)}{2} + \frac{(1-\tau_2)}{2}\right)\right] \tag{2.23}$$

and

$$\zeta_{\ell_i} = \sin\left[\frac{\pi}{2}\left(\ell_i + \frac{1-\tau_i}{2}\right)\right] \tag{2.24}$$

Finally, (2.19) gives

$$F(J,q_\perp^2) = \int \frac{d\ell_1}{2\pi i} \frac{d\ell_2}{2\pi i} \frac{d^2k_\perp}{(2\pi)^2} \gamma_{\ell_1\ell_2} N^2_{\ell_1\ell_2}(q_\perp,\ k_\perp)$$

$$\cdot \frac{G_{\ell_1}(k_\perp^2) G_{\ell_2}((q_\perp-k_\perp)^2)}{J+1 - \ell_1 - \ell_2} \tag{2.25}$$

If the amplitudes f_1 and f_2 are dominated asymptotically by Regge pole exchange then

$$G_\ell(k_\perp^2) = \frac{1}{\ell_1-\alpha_1(k_\perp^2)} \quad , \quad G_{\ell_2}((q_\perp-k_\perp)^2) = \frac{1}{\ell_2-\alpha_2((q_\perp-k_\perp)^2)} \tag{2.26}$$

In this case

$$F(J,q_\perp^2) = \int \frac{d^2k_\perp}{(2\pi)^2} \frac{\gamma_{\alpha_1\alpha_2} N^2_{\alpha_1\alpha_2}}{J+1-\alpha_1(k_\perp^2)-\alpha_2((q_\perp-k_\perp)^2)} \tag{2.27}$$

$$= \int \frac{d\ell_1}{2\pi i} \frac{d^2k_\perp}{(2\pi)^2} \gamma_{\alpha_1\alpha_2} N^2_{\alpha_1\alpha_2} G_{\ell_1}(k_\perp^2) G_{J+1-\ell_1}((q_\perp-k_\perp)^2) \tag{2.28}$$

where the ℓ_1-contour runs to the right of the pole in G_{ℓ_1} and to the left of the pole in $G_{J+1-\ell_1}$.

(2.28) now corresponds directly to the Reggeon (Feynman) diagram of Fig. 2.2. The vertices where two particles produce or absorb two Reggeons represent the factor $N_{\alpha_1\alpha_2}\sqrt{\gamma_{\alpha_1\alpha_2}}$ (we absorb the signature factor into the vertices). The propagators represent the Reggeon propagators G_{ℓ_1}, $G_{J+1-\ell_2}$ and the loop represents the ℓ_1 and $k_\perp$ integrations. There is conservation of both one minus angular momentum and $k_\perp$ at the vertices if one pair of external particles is regarded as a source for angular momentum; and transverse momentum $q_\perp$, and the other pair is regarded as a sink for the same quantities. Both angular momentum and transverse momentum then flow through the diagram.

One is ordinarily interested in the behavior of $F(J,q_\perp^2)$ near the J-plane branch-point generated by (2.28). For the $\underset{\sim}{P}$-$\underset{\sim}{P}$ cut, where $\tau_1=\tau_2=1$, $\gamma_{\alpha_1\alpha_2} \approx -1$ in this domain. One sees then that the effective two particle $\rightarrow 2\underset{\sim}{P}$ coupling $\sqrt{\gamma_{\alpha_1\alpha_2}}\, N_{\alpha_1\alpha_2}$ is pure imaginary. Similarly we see from (2.23) that the two particle $\rightarrow \underset{\sim}{P}$ + meson trajectory coupling is also pure imaginary independent of the signature of the meson trajectory.

Note that if we put $\ell_1=\alpha_1$, $\ell_2=\alpha_2$ in (2.17) we have expressed the two-particle → two Reggeon coupling $N_{\alpha_1\alpha_2}$ as an integral over the absorptive part of the two particle/two Reggeon scattering amplitude $T_{\alpha_1\alpha_2}(M^2,q,k_\perp)$. Comparing this with (2.19) evaluated at $J = -1$ we see that (2.16) is analogous to evaluating the two particle/two Reggeon partial-wave amplitude at a nonsense point - in this case $J = \alpha_1+\alpha_2-1$. This is the connection of the coupling $N_{\alpha_1\alpha_2}$ with a "nonsense fixed-pole residue" which we shall find in the next section.

It is straightforward to generalize the above results to the three-Reggeon cut diagram shown in Fig. 2.3. One merely uses for $f_1(k_1,k_1k_2)$ the two-Reggeon cut amplitude of (2.14). Proceeding as before one finds that the contribution of Fig. 2.3 to the elastic amplitude is given by

$$T(s,q^2) = \frac{\pi}{2}\int \frac{d\ell_1}{2\pi i}\frac{d\ell_2}{2\pi i}\frac{d\ell_3}{2\pi i}\frac{d^2k_\perp}{(2\pi)^2}\frac{d^2k'_\perp}{(2\pi)^2}\,\xi_{\ell_1}\xi_{\ell_2}\xi_{\ell_3}\,s^{\ell_1+\ell_2+\ell_3-2}$$
$$\cdot\, N^2_{\ell_1\ell_2\ell_3}(q,k_\perp,k'_\perp)\,G_{\ell_1}(k'^2_\perp)\,G_{\ell_2}((k_\perp-k'_\perp)^2)\,G_{\ell_3}((q-k_\perp)^2) \tag{2.29}$$

where $N_{\ell_1\ell_2\ell_3}$ is obtained from (2.15) by replacing $g(k_1^2,(k-k_1)^2,k_\perp^2)$ by $N_{\ell_1\ell_2}$, ℓ_1 by $\ell_1+\ell_2-1$ and ℓ_2 by ℓ_3. Calculating the absorptive part of $T(s,q_\perp^2)$ as before then gives

$$F(J,q_\perp^2) = \int \frac{d\ell_1}{2\pi i}\frac{d\ell_2}{2\pi i}\frac{d^2k_{1\perp}}{(2\pi)^2}\frac{d^2k_{2\perp}}{(2\pi)^2}\,\gamma_{\alpha_1\alpha_2\alpha_3}\,N^2_{\alpha_1\alpha_2\alpha_3}$$
$$\cdot\, G_{\ell_1}(k^2_{1\perp})\,G_{\ell_2}(k^2_{2\perp})\,G_{J+2-\ell_1-\ell_2}((q_\perp-k_{1\perp}-k_{2\perp})^2) \tag{2.30}$$

which corresponds to the Reggeon (Feynman) diagram of Fig. 2.4.

The generalization to the case of n-Reggeons is immediate

$$F(J,q_\perp^2)=2\pi i\int\prod_{i=1}^{n}\frac{d\ell_i}{2\pi i}\frac{d^2k_{\perp i}}{(2\pi)^2}\,\gamma_{\alpha_1\ldots\alpha_n}N^2_{\alpha_1\ldots\alpha_n}\left[\prod_{i=1}^{n}G_{\ell_i}(k_{i\perp}^2)\right]$$

$$\cdot\,\delta\Big(J-1+\sum_{i=1}^{n}(\ell_i-1)\Big)\delta^2\Big(q_\perp-\sum_{i=1}^{n}k_{i\perp}\Big) \qquad (2.31)$$

where in both (2.30) and (2.31)

$$\gamma_{\ell_1\ldots\ell_n}=(-1)^{n-1}\sin\left[\frac{\pi}{2}\Big(\sum_{i=1}^{n}(\ell_i+\frac{1-\tau_i}{2})\Big)\right]\Big/\prod_{i=1}^{n}\zeta_{\ell_i} \qquad (2.32)$$

Note that we have written (2.31) in a symmetric form by introducing δ-functions conserving angular momentum and transverse momentum.

The interpretation of (2.31) is as follows: two particles act as a source of two momentum $q_\perp$ and "energy" $1-J$; from this source n-Reggeons with momentum $k_{i\perp}$ and energy $1-\ell_i$ $i=1,\ldots n$, emerge with amplitude $N_{\ell_1\ell_2\ldots\ell_n}\sqrt{\gamma_{\ell_1\ldots\ell_n}}$. Each Reggeon propagates with the amplitude $G(\ell_i,k_{i\perp})$ appropriate to it until they are all absorbed by two particles acting as a sink. At each stage energy and momentum have been conserved; the overall energy and momentum conservation δ-functions have been factored off.

This rather attractive description of the n-Reggeon diagram is supported by the study of more complicated hybrid diagrams. Consider Fig. 2.5 next. An extension of the foregoing Sudakov analysis shows that this corresponds to the Reggeon diagram of Fig. 2.6, and yields for $F(J,q_\perp^2)$

$$F(J,q_\perp^2) = \left\{ \int \frac{d^2k_{1\perp}}{(2\pi)^2} \frac{d^2k_{2\perp}}{(2\pi)^2} \frac{d\ell_1}{2\pi i} \frac{d\ell_2}{2\pi i} (2\pi)^2 \delta^2(q_\perp - k_{1\perp} - k_{2\perp}) \right.$$

$$\cdot 2\pi i \, \delta(1-J-(1-\ell_1)-(1-\ell_2)) N_{\ell_1\ell_2}(k_{1\perp}, k_{2\perp}) \gamma_{\ell_1\ell_2}$$

$$\left. \cdot r_{\ell_1\ell_2 J}(k_{1\perp}, k_{2\perp}, q_\perp) G_1(\ell_1, k_{1\perp}) G_2(\ell_2, k_{2\perp}) \right\} G_3(J, q_\perp)$$

(2.33)

The additional ingredient here is the triple Reggeon vertex r shown in the present calculation as Fig. 2.7. More complicated contributions will change the detailed form of r but leave $F(J,q_\perp^2)$ as in (2.33). Since the coupling of two particles to one $\underset{\sim}{P}$ is real and that of two particles to two $\underset{\sim}{P}$'s is pure imaginary, the triple $\underset{\sim}{P}$ coupling of Fig. 2.6 must be pure imaginary for $k_{1\perp}, k_{2\perp}, q_\perp \sim 0$, since $F(J,q_\perp^2)$ must be real below the t-channel threshold. This means that $\sqrt{\gamma_{\ell,\ell_2}} \, r_{\ell_1\ell_2 J}$ must be pure imaginary and so $r_{\ell_1\ell_2 J}$ must be real. The coupling of a meson trajectory to a $\underset{\sim}{P}$ plus a meson must similarly be pure imaginary.

To derive Reggeon rules from a general hybrid Feynman graph one identifies familiar elements, for example, G,r the N's, and writes the desired contribution to $F(J,q_\perp)$ as products of the basic building blocks put together with energy and momentum integrations. The final outcome is that to obtain the full partial-wave amplitude we must write down the complete set of "Feynman" Reggeon graphs including general interactions in which arbitrary numbers of Reggeons are destroyed and created.[38] The corresponding contributions to the partial-wave amplitude are then constructed by writing down vertex functions for all couplings, propagators for

each internal Reggeon line, and $\int \frac{d\ell}{2\pi i} \frac{d^2k_\perp}{(2\pi)^2}$ for each internal Reggeon loop. Energy, $E = (1-\ell)$ and momentum being conserved at each vertex.

Notice that because the Reggeon propagator is linear in E we must specify the direction of propagation of the Reggeons. Diagrams which are topologically identical, but which have one or more Reggeons propagating in opposite directions are distinct.[22]

Clearly we have arrived at a set of "Feynman" rules for writing down our partial-wave amplitude and we shall formalize this further in Section IV. We finish our description of the derivation of these rules from hybrid graphs by noting the rules for the phases of the $\underset{\sim}{P}$ couplings that we have found. From (2.32) and similar signature factors for Reggeon interaction diagrams we find that if N_m is the coupling (treated as a constant) of two particles to m $\underset{\sim}{P}$'s and λ_{mn} is the coupling of m $\underset{\sim}{P}$'s to n $\underset{\sim}{P}$'s then

$$N_m \alpha (i)^{m-1} , \quad \lambda_{mn} \alpha (i)^{m+n-2} \tag{2.34}$$

We have now given a bare outline of the arguments of Gribov to motivate a field theoretic description of Reggeons. We do not intend to attempt the complete decomposition of a relativistic field theory into hybrid diagrams. This would be required to turn our present heuristic justification of the RFT into a proper derivation. Clearly we would need as a starting point some picture of the initial process which generates an <u>isolated</u> $\underset{\sim}{P}$ pole with $\alpha_{\underset{\sim}{P}}(0) \sim 1$. The amplitude for this process would then provide the input two-body

amplitude for our hybrid diagrams. (Conceptually it is sometimes useful to picture this process as the familiar multiperipheral or ladder mechanism,[36] but this is not essential.) However, there are still problems associated with the breaking up of hybrid diagrams which correspond to Reggeon interactions, such as that of Fig. 2.5, into a part corresponding to the full Reggeon diagram (that of Fig. 2.6 for Fig. 2.5) and parts corresponding to renormalization of the original, or bare, pole and or vertices. To handle this problem correctly it is necessary to introduce a cut-off in the $\underline{\ell}$ and $\underline{k}$ integrations in Reggeon diagrams and to relate this cut-off directly to the break-up of the phase-space in hybrid diagrams. A discussion of how this can be done and how the accusations of double-counting at this stage can be avoided, has been given by DeTar.[39]

Fortunately we can avoid this problem by using Reggeon unitarity as a basis for the RFT, as we discuss in the next Section. The Reggeon unitarity equations are applicable once we know, or rather assume, that there is an isolated $\underset{\sim}{P}$ pole in the neighborhood of $J \sim 1$, $t \sim 0$. These equations reassure us that we have not been double-counting in discussing hybrid diagrams. Before leaving the counting problem altogether however, we note that we shall discuss the use of a cut-off RFT in relation to the renormalization group in Section IV. It is worth noting from the above discussion that the cut-off may well be an essential feature in ensuring that the RFT is well-defined both mathematically and physically.

The generality of the Reggeon unitarity approach to RFT gives a powerful logical basis to the apparently more model dependent,

albeit rather more physically motivated process described above. To compare the results of this section directly with those of the next section we briefly discuss taking the discontinuity across the cuts attached to the Reggeon branch points occurring in the partial-wave amplitudes we have obtained.

Consider first the n-Reggeon branch point generated in (2.31). This can be viewed as a "threshold" singularity generated by the poles of the propagators $G_{\ell_i}(k_{i\perp}^2)$. The discontinuity is obtained by the usual "Cutkosky rules" of putting each Reggeon on its "spin" (mass) shell:

$$\underset{n}{\mathrm{disc}}_J F(J,q_\perp^2) = (-1)^{n-1} 2\pi i \sin\left[\frac{\pi}{2}\left(J-\sum_i \frac{\tau_i-1}{2}\right)\right] \int \frac{d^2k_{1\perp}}{(2\pi)^2}\cdots\frac{d^2k_{n\perp}}{(2\pi)^2}\,\delta^2\left(q_\perp - \sum_{i=1}^{n} k_{i\perp}\right)$$
$$\times\ \delta\left(J-1-\sum_{i=1}^{n}[\alpha_i(k_{i\perp}^2)-1]\right)\left(\prod_i \zeta_{\alpha_i}\right)^{-1} N^2_{\alpha_1\ldots\alpha_n} \qquad (2.35)$$

This expression being simply obtained from (2.31) by writing $G_{\ell_i}(k_{i\perp}^2) \to 2\pi i\,\delta(\ell_i-\alpha_i(k^2{}_{i\perp}))$.

For more complicated Reggeon diagrams there will be a contribution to the n-Reggeon discontinuity from every n-Reggeon state that can be found by "cutting" the diagram vertically. (There will, as in a conventional field theory, be a renormalization of the pole position in each propagator by "self-Energy" insertions. This renormalization will only be unambiguously defined from hybrid diagrams once the cut-off is introduced as discussed above.) To take all these contributions into account we follow the usual unitarity prescription of complex-conjugating that part of the diagram to the right of the cutting line. More technically, the

part of the diagram to the left of the cutting line is evaluated above its J-plane branch cut, while that to the right is evaluated below the branch cut. After summing all contributions the final result is that the complete discontinuity has the same form as (2.35), except that

$$N^2_{\alpha_1\cdots\alpha_n} \to |N_{\alpha_1\cdots\alpha_n}(J)|^2 = N_{\alpha_1\cdots\alpha_n}(J+i\epsilon)N_{\alpha_1\cdots\alpha_n}(J-i\epsilon) \tag{2.36}$$

where $N_{\alpha_1\cdots\alpha_n}(J)$ is the complete two particle $\to$ n Reggeon amplitude.

The complete imaginary part of $F(J,q_\perp^2)$ arising from its Reggeon branch-points is given by the Reggeon unitarity relation

$$\text{disc}_J F(J,q_\perp^2) = \sum_{n=2}^{\infty} \text{disc}_J F(J,q_\perp^2) \tag{2.37}$$

where $\underset{n}{\text{disc}}_J F(J,q_\perp^2)$ is given by (2.35) with the substitution (2.36). The purpose of the next Section is to derive (2.37) directly from multiparticle t-channel unitarity. We can then argue that the procedure of the latter part of this Section can be reversed and the RFT viewed simply as a solution of (2.37).

III. REGGEON UNITARITY RELATIONS

In this section we discuss the derivation and implication of Reggeon cut discontinuity formulae from the point of view of t-channel unitarity. We use standard S-matrix methods and the results depend on conventional S-matrix assumptions of analyticity put together with the existence of moving poles in the J-plane. Briefly speaking we argue that branch points in J arise from the presence of two or more moving poles in J. If there are additional singularities in the J-plane, we will not find them. Indeed, in the spirit of "maximal analyticity in the J-plane" we assume them to be absent. The full treatment of multiparticle t-channel unitarity in the J-plane is rather complicated but we shall try to minimize the technical details without depriving the reader of all insight into the procedure.

To motivate the use of the t-channel as the correct place for an S-matrix analysis of J-plane branch points let us look at the Feynman graphs which were the original indication of the presence of cuts.[4,5] (Figure 3.1a and Figures3.1b.) Both graphs have many intermediate states in the s-channel gotten by cutting the ladders which give rise to the Regge behavior. A priori all possible numbers of particles in the s-channel must be considered at the same time to discuss the large s, fixed t behavior of these diagrams.[40] Since we are, however, interested in a fixed t limit, by continuing t from the scattering region, $t \leq 0$, to some finite time-like point we can restrict our attention to particular t-channel intermediate states. In the diagrams in Figure 3.1 the lowest intermediate state in t is the four particle state. This suggests we may be able to study the two Reggeon cut in the full partial wave amplitude by looking at the four particle unitarity integral in the t-channel. Indeed, this is so,[20,21] provided, of course, that the Reggeons involved

couple to some two-particle states.

Mandelstam[5] actually analyzed in detail the diagrams of Figure 3.2 where one of the ladders (Regge poles) of Figure 3.1 is replaced by a single particle. Neither Figures 3.1a nor 3.2a has a Regge cut while 3.1b and 3.2b do. Mandelstam showed this for Figures 3.2a and 3.2b by considering the three particle unitarity relation in the t-channel. He argued that only in the case that the five point amplitude shown in Figure 3.3 has both a right and left hand cut in the sub-energy s_1 could a J-plane branch point be present in the elastic amplitudes of Figure 3.2. Figure 3.2a has only a right hand cut and does not yield a J-plane cut; Figure 3.2b has both right and left and gives rise to a J-plane cut. In other words, a J-plane cut will only occur when the "three particle-Reggeon amplitude" of Figure 3.3 has a "third double spectral function." This part of Mandelstam's argument is independent of Feynman graphs as is the final form for the contribution of the cut to the partial wave amplitude

$$F(J,t) \sim \int_{(\sqrt{t}+m)^2} dt_1 \frac{\lambda^{\frac{1}{2}}(t_1 t_1, m^2)}{t} \frac{C(t,t_1)}{J+1-\alpha(t_1)} , \qquad (3.1)$$

where $C(t,t_1)$ is a smooth function of its arguments, $\alpha(t)$ is the pole trajectory coming from the ladder graphs, and $\lambda(x,y,z) = (x+y-z)^2-4xy$ is the familiar kinematic factor.

Subsequently, Gribov, Pomeranchuk, and Ter-Martirosyan (GPT)[20] compared the form of (3.1) with the contribution to the two particle unitarity relation for $F(J,t)$ coming from a spinless particle of mass m and a particle of mass m_1, spin J_1, helicity n_1. This is

$$\mathrm{Im}_t F(J,t) = \sum_{n_1=-J_1}^{+J_1} \frac{\lambda^{\frac{1}{2}}(t,m_1^2,m^2)}{t} \frac{\Gamma(J+1-n_1)}{\Gamma(J+1+n_1)} f_{J_1 n_1}(t) f^*_{J_1 n_1}(t) \ , \tag{3.2}$$

where $f_{J_1 n_1}(t)$ is a helicity partial wave amplitude for the transition: two spinless particles → spinless particle + particle of spin J_1, helicity n_1. This formula contains a fixed pole at $J = J_1 - 1$ arising from the helicity state with $n_1 = J_1$, and near this point strongly resembles (3.1). Further, it is known that the residue of this fixed pole will vanish unless the amplitude giving $f_{Jn}(t)$ has a third double spectral function. This is the usual connection between nonsense wrong-signature fixed poles and third double spectral functions. {There is a rather thick layer of jargon in this, and we are required to ask the reader's patience and refer him to standard references[41] for an explanation of terms.}

This comparison suggested to GPT that J-plane branch points could be viewed as resulting from the presence of a fixed-pole in Reggeon particle intermediate states all along the Regge trajectory. This observation was the key to subsequent analysis of J-plane cuts using t-channel unitarity. A complete analysis of three particle unitarity together with a discussion of the Reggeon-particle cut in (3.1) has been given by White.[21] This last cut moves off the physical sheet of the J-plane around the two Reggeon branch point when t becomes small. Since it, therefore, does not contribute to the large s, fixed t behavior we turn our attention to the two Reggeon cut.

To study the two-Reggeon branch-point we consider not the complete t-channel unitarity relation for $t \gtrsim 16\ m^2$, but instead

isolate the discontinuity across the four-particle threshold. This eliminates the need to discuss the two and three particle contributions to the unitarity relation. The Feynman graphs of Fig. 3.1 do not have two or three particle intermediate states in the t-channel and so for them the four-particle discontinuity would be the complete unitarity relation for $16\ m^2 \leq t \leq 25\ m^2$. In general the four-particle threshold discontinuity can be written in a fairly conventional S-matrix form[42,43]

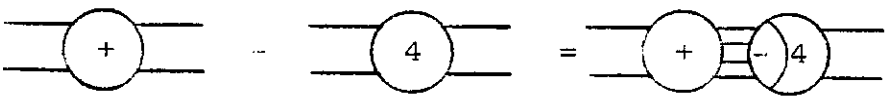

(3.3)

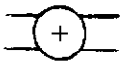

and 

are physical amplitudes, but the other amplitudes are defined by analytic continuation of these physical amplitudes. 

is 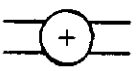

continued around the four-particle threshold as illustrated in Fig. 3.4. 

is 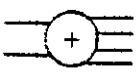

analytically continued around both the four-particle threshold in the total energy t (this is denoted by the 4) and around all phase-space thresholds in the sub-channels (this is denoted by 

and involves going around two-particle thresholds in all two-particle channels and three-particle thresholds in all three-particle channels). The integration implied by the right-hand side of (3.3) is over normal four-particle phase-space.

The next step is to project this unitarity relation onto partial waves. In Figure 3.5 a complete set of partial wave variables is given. Since the external particles are spinless we need only the total angular momentum J and $(\text{mass})^2 = t = Q^2$ of the four-particle state, J_i, $t_i = Q_i^2$ for the two pairs of particles

and n_i the helicity of each pair. The total helicity $n = n_1 + n_2$. One can now use these variables to construct the unitarity relation for partial waves coming from (3.3):[44]

$$F(J,t) - F^4(J,t) =$$

$$= \int d\rho \sum_{|n|\leq J} \sum_{\substack{J_1 \geq |n_1| \\ J_2 \geq |n_2|}} \Lambda(J,J_1,J_2,|n|,|n_1|n_2|) F(J,J_1,J_2,n_1,n_2,t,t_1,t_2)$$

$$F^{4-}(J,J_1,J_2,n_1,n_2,t,t_1,t_2) \tag{3.4}$$

with

$$\Lambda(J,J_1,J_2,t,t_1,t_2) = \frac{(2J_1+1)(2J_2+1)\Gamma(J_1-n_1+1)\Gamma(J_2-n_2+1)\Gamma(J-n+1)}{\Gamma(J_1+n_1+1)\Gamma(J_2+n_2+1)\Gamma(J+n+1)} , \tag{3.5}$$

and

$$d\rho = \frac{i}{(2\pi)^5 2^6 4!} \int_{4m^2}^{(\sqrt{t}-2m)^2} dt_1 \int_{4m^2}^{(\sqrt{t}-\sqrt{t_1})^2} dt_2 \frac{\lambda^{\frac{1}{2}}(t,t_1,t_2)}{t} \left[\frac{(t_1-4m^2)(t_2-4m^2)}{t_1 t_2}\right]^{\frac{1}{2}} . \tag{3.6}$$

Eq. (3.4) gives the discontinuity of the usual partial wave amplitude $F(J,t)$ across the four-particle threshold. The amplitude $F(J,J_1,J_2,n_1,n_2,t,t_1,t_2)$ is the helicity partial wave amplitude for two spinless particles to go to a particle of mass t_1, spin J_1, helicity n_1 plus a particle of (t_2,J_2,n_2). F^{4-} of the same arguments is the helicity partial wave amplitude of the analytically continued six point function.

We now focus on the "kinematic factor" Λ in (3.4). It contains the fixed pole at $J = n-1$. This is the singularity GPT expected to be present in order for the two Reggeon cut to appear in $F(J,t)$ when continued to complex J. GPT did not try to find the exact form of this continuation. They essentially tailored their assumptions on how to continue the sums in (3.4) to achieve the expected results. Since their work there has been considerable insight into the technical problems associated with analytic continuations of multiparticle amplitudes in angular momentum as well as helicity.[45]

For our purposes it is enough to know that the GPT program can be carried through although we shall need the exact form of the continuation of (3.4) to complex J. This has been given by White[21] and we follow his development. To continue $F(J,J_1,J_2,n_1,n_2,t,t_1,t_2)$ away from integer J,J_i, and n_i we must introduce signature as well as labels > or < telling us whether we have continued n_i into the right or left half helicity planes. We will collect these various labels into an index $\underset{\sim}{\eta}$ and refer to them only when essential.

The signature labels naturally refer to continuation in J-n, call the signature $\tilde{\tau}$; $J_i-n_i,\tilde{\tau}_i$; n_i,τ_i'. The signatures τ,τ_1,τ_2 for J,J_1,J_2 are

$$\tau = \tilde{\tau}\,\tau_1'\,\tau_2' \quad , \qquad \tau_1 = \tilde{\tau}_1\,\tau_1' \quad , \qquad \tau_2 = \tilde{\tau}_2\,\tau_2' \quad . \tag{3.7}$$

The contribution to the discontinuity in (3.4) from n_1, $n_2 > 0$ is now written

$$- \frac{\sin\frac{\pi}{2}(J-\hat{\tau})}{16}\int d\rho \sum_{\tau_i'=\pm 1}\int_{C_J}\frac{dn_1 dn_2}{\sin\frac{\pi}{2}(n_1-\hat{\tau}_1')\sin\frac{\pi}{2}(n_2-\hat{\tau}_2')\sin\frac{\pi}{2}\left[J-n-\hat{\tilde{\tau}}\right]}\times$$

$$\cdot \sum_{J_i-n_i=0}^{\infty} \Lambda(\underset{\sim}{J},\underset{\sim}{n})F^{\tau}_{\underset{\sim}{\eta}}(\underset{\sim}{J},\underset{\sim}{n})F^{\tau 4-}_{\underset{\sim}{\eta}}(\underset{\sim}{J},\underset{\sim}{n}) \quad , \tag{3.8}$$

where $\underset{\sim}{J} = (J,J_1,J_2)$, $\underset{\sim}{n} = (n_1,n_2)$, $\underset{\sim}{\tau} = (\tau,\tau_1,\tau_2,\tau_1',\tau_2')$, and $\hat{\tau} = \frac{1-\tau}{2}$, $\hat{\tau}_i' = \frac{1-\tau_i'}{2}$.

Clearly the sums over n_1 and n_2 in (3.4) have been converted to a contour integral over the contour C_J. Fig. 3.6 shows the projection of C_J in the n_1 plane at fixed n_2 and for fixed n_1 it would have the same form in the n_2 plane. That the contour is asymptotically parallel to both the n_1 and n_2 imaginary axes ensures that the integral converges and that the problem of divergent helicity sums in this context is avoided.[46-48] At integer J the two series of poles shown by crosses in Fig. 3.6 come together and pinch the contour C_J. The double integral over n_1 and n_2 develops a pole because of the pinching of the contour by the three sets of poles in the integrand coming from the factors of $\sin\frac{\pi}{2}(n_1-\hat{\tau}_1')$, $\sin\frac{\pi}{2}(n_2-\hat{\tau}_2')$, and $\sin\frac{\pi}{2}(J-n-\hat{\tilde{\tau}})$. The pole of the integral is cancelled by the "signature factor" $\sin\frac{\pi}{2}(J-\hat{\tau})$, which multiplies the integral and thus singles out the pole residue as the value of (3.8) at integer J. This residue contains just the requisite finite sum over helicity amplitudes.

We can now study the two Reggeon cut which arises from the presence of Regge poles at $J_i = \alpha_i(t_i)$, with signatures τ_i, in the J_i channels. Poles occur at $n_i = \alpha_i(t_i)$ in the term with $J_i-n_i=0$ in (3.8) provided $\tilde{\tau}_i = +1$. As shown in Fig. 3.6 these

poles lie on opposite sides of the C_J contour to the pole of Λ at $J = n-1$.

Therefore, unless there is a compensating "nonsense zero" in either $F^{\tau}_{\underset{\sim}{\eta}}(J,\underline{n})$ or $F^{\tau 4-}_{\underset{\sim}{\eta}}(J,\underline{n})$, there will be a pole in the helicity integral at $J = \alpha_1(t_1)+\alpha_2(t_2)-1$ as a result of the pinching of the Regge poles and the nonsense pole. For there to be no nonsense zero $J = n_1+n_2-1$ must be a <u>wrong-signature</u> nonsense point. This requires

$$\tilde{\tau} = +1 \implies \tau = \tau_1'\tau_2' \tag{3.9}$$

and since

$$\tilde{\tau}_1 = \tau_1\tau_1' = \tilde{\tau}_2 = \tau_2\tau_2' = +1 \tag{3.10}$$

we must have

$$\tau = \tau_1\tau_2 \ . \tag{3.11}$$

This is the S-matrix origin of the rule that the signature of a cut is the product of the signatures of the Regge poles building the cut.

Isolating the contribution of the pole at $J = \alpha_1(t_1) + \alpha_2(t_2)-1$ to (3.8), and taking $\tau_1 = \tau_2 = \tau = +1$ for simplicity, we obtain

$$-\frac{\pi^2}{4}\sin\frac{\pi}{2}J\int d\rho\ \frac{\Lambda'(J,\underset{\sim}{\alpha})R^{\tau}_{\underset{\sim}{\alpha}\underline{\eta}}(J,t)\ F^{\tau 4-}_{\underline{\eta}}(J,\underset{\sim}{\alpha},t)}{\sin\frac{\pi}{2}\alpha_1(t_1)\sin\frac{\pi}{2}\alpha_2(t_2)\,(J-\alpha_1(t_1)-\alpha_2(t_2)+1)} \tag{3.12}$$

where $\Lambda'(J,\underset{\sim}{\alpha})$ is the residue of $\Lambda(J,\underset{\sim}{n})$ at the pole at $J=n_1+n_2-1$ and $\underset{\sim}{R}^{\tau}_{\underset{\sim}{\alpha}\underset{\sim}{\eta}}(J,t)$ is the double Regge pole residue of $\underset{\sim}{F}^{\tau}_{\underset{\sim}{\eta}}(J,J_1=n_1,J_2=n_2,n_1,n_2)$. Note that we are using the fact that the Regge trajectories acquire imaginary parts at the lowest thresholds in the t_1 and t_2 channels so that $\underset{\sim}{F}^{\tau 4-}_{\underset{\sim}{\eta}}$ is not singular at $J_1=\alpha_1(t_1), J_2=\alpha_2(t_2)$, but instead has poles at $J_1=\alpha_1^*(t_1)$, $J_2=\alpha_2^*(t_2)$.

(3.12) already resembles (3.1) and we can improve the resemblance and simplify (3.12) by using two-particle unitarity in the t_1 and t_2 channels. It can be shown that we may write

$$\left(\frac{i}{16\pi}\right)^2\left(\frac{t_1-4m^2}{t_1}\right)^{\frac{1}{2}}\left(\frac{t_2-4m^2}{t_2}\right)^{\frac{1}{2}}\underset{\sim}{R}^{\tau}_{\underset{\sim}{\alpha}\underset{\sim}{\eta}}\underset{\sim}{a}^{\tau 4-}_{\underset{\sim}{\eta}}\rightarrow\underset{\sim}{N}^{\tau}_{\underset{\sim}{\alpha}\underset{\sim}{\eta}}\underset{\sim}{N}^{\tau 4}_{\underset{\sim}{\alpha}\underset{\sim}{\eta}} \tag{3.13}$$

in (3.12), where $\underset{\sim}{N}^{\tau}_{\underset{\sim}{\alpha}\underset{\sim}{\eta}}(J,t)$ is defined from $\underset{\sim}{R}^{\tau}_{\underset{\sim}{\alpha}\underset{\sim}{\eta}}(J,t)$ by factorizing off the two-particle/Reggeon vertex functions, if we replace the t_1 and t_2 integrations in $\int d\rho$ by contour integrals enclosing the two-particle thresholds in those channels - see Fig. 3.7. $\underset{\sim}{N}^{\tau 4}_{\underset{\sim}{\alpha}\underset{\sim}{\eta}}$ is simply the analytic continuation of $\underset{\sim}{N}^{\tau}_{\underset{\sim}{\alpha}\underset{\sim}{\eta}}$ around the four-particle thresholds in the t-channel. If we make the further simplification of absorbing $\sqrt{A'}$ into $\underset{\sim}{N}^{\tau}_{\underset{\sim}{\alpha}\underset{\sim}{\eta}}$ we obtain for ImF(J,t)

$$\frac{i}{\pi 2^5 4!}\sin\left(\frac{\pi}{2}J\right)\int_{\lambda(t,t_1,t_2)>0}dt_1dt_2$$

$$\frac{\lambda^{\frac{1}{2}}(t,t_1,t_2)\quad\underset{\sim}{N}^{\tau}_{\underset{\sim}{\alpha}\underset{\sim}{\eta}}(J,t)\underset{\sim}{N}^{\tau 4}_{\underset{\sim}{\alpha}\underset{\sim}{\eta}}(J,t)}{t\sin\frac{\pi}{2}\alpha_1(t_1)\sin\frac{\pi}{2}\alpha_2(t_2)\left(J-\alpha_1(t_1)-\alpha_2(t_2)+1\right)} \tag{3.14}$$

(3.12) is now clearly analogous to (3.1) except that the Reggeon-particle "fixed-pole" at $J=\alpha(t_1)-1$ has been replaced by the two-Reggeon fixed-pole at $J=\alpha_1(t_1)+\alpha_2(t_2)-1$.

The Reggeon-particle branch-point occurs in (3.1) when the fixed-pole hits the end-point of the t_1-integration - this gives a branch point at

$$J = \alpha((\sqrt{t}-m)^2) - 1 \qquad (3.15)$$

There are various end-point singularities generated in (3.14) but, apart from the two-Reggeon branch-point, they are not singular on the physical sheet of the full amplitude near t=0.[49,50] The two-Reggeon branch-point is generated when the pole at $J=\alpha_1(t_1)+\alpha_2(t_2)-1$ is tangential to the integration boundary at $\lambda(t,t_1,t_2)=0$. The position of the branch-point can therefore be formed by solving the Landau equations

$$\frac{\partial}{\partial t_1}(\mu_1[\alpha_1(t_1) + \alpha_2(t_2)] + \mu_2\lambda(t,t_1,t_2)) = 0 \qquad (3.16)$$

$$\frac{\partial}{\partial t_2}(\mu_1[\alpha_1(t_1) + \alpha_2(t_2)] + \mu_2\lambda(t,t_1,t_2)) = 0 \qquad (3.17)$$

together with the conditions

$$J_1 - \alpha_1(t_1)-\alpha_2(t_2)+1 = 0 , \quad \lambda(t,t_1,t_2) = 0 . \qquad (3.18)$$

If the two Regge trajectories are identical, the solution of these equations is $t_1=t_2=\frac{t}{4}$, with the branch-point occurring at

$$J = \alpha_c^{(2)} = 2\alpha(\tfrac{t}{4}) - 1 . \qquad (3.19)$$

For non-identical trajectories the branch-point trajectory will be more complicated.

Since the integration in (3.14) is two-dimensional and the trajectory functions are complex for $t_1, t_2 > 4m^2$, it is not straightforward to take the two-Reggeon cut discontinuity in (3.14). However, (3.14) becomes much easier to work with if we analytically continue it to $t < 0$.[50] The details of this continuation are complicated but the net result is that if we extract the "threshold" behavior of $\underset{\sim}{N}^{\tau}_{\underset{\sim}{\alpha},\underline{\eta}}(J,t)$ at $\lambda(t,t_1,t_2) = 0$ by writing

$$\underset{\sim}{N}^{\tau}_{\underset{\sim}{\alpha}\underline{\eta}}(J,t) = \underset{\sim}{C}^{\tau}_{\underset{\sim}{\alpha},\underline{\eta}}(J,t) \left[\frac{\lambda(t,t_1,t_2)}{t}\right]^{(J-\alpha_1-\alpha_2)/2} \tag{3.20}$$

then we can simply rotate the integration contour in (3.14) to the region $\lambda(t,t_1,t_2) < 0$ and write

$$[\lambda(t,t_1,t_2)]^{\frac{1}{2}} \to i[-\lambda(t,t_1,t_2)]^{\frac{1}{2}} \quad . \tag{3.21}$$

(For the purpose of studying the two-Reggeon branch-point we can ignore the fact that the original contour encircled the positive t_1 and t_2 thresholds.) For $t < 0$, then we obtain from (3.14)

$$\frac{1}{\pi 2^5 4!} \int_{\lambda<0} dt_1 dt_2 [-\lambda(t,t_1,t_2)]^{-\frac{1}{2}} \frac{\underset{\sim}{C}^{\tau}_{\underset{\sim}{\alpha}\underline{\eta}}\ \underset{\sim}{C}^{\tau 4}_{\underset{\sim}{\alpha}\underline{\eta}}}{\sin\frac{\pi}{2}\alpha_1(t_1)\sin\frac{\pi}{2}\alpha_2(t_2)\,(J-\alpha_1(t_1)-\alpha_2(t_2)+1)} \tag{3.22}$$

If the trajectory functions are real for negative t_1 and t_2 then the collision of the pole at $J=\alpha_1(t_1)+\alpha_2(t_2)-1$ with $\lambda(t,t_1,t_2)=0$ is now

straightforward - see Fig. 3.8 - and if $\underset{\sim}{C}^{\tau}_{\underset{\sim}{\alpha}\underset{\sim}{\eta}}$ and $\underset{\sim}{C}^{\tau 4}_{\underset{\sim}{\alpha}\underset{\sim}{\eta}}$ are both non-singular at $J = \alpha_c$ we obtain from (3.22)

$$\text{disc}_J F(J,t) = \frac{-i}{2^4 4!}\sin\tfrac{\pi}{2}J \int_{\lambda<0} dt_1 dt_2 \frac{\delta(J-\alpha_1(t_1)-\alpha_2(t_2)+1)\,\underset{\sim}{C}^{\tau}_{\underset{\sim}{\alpha}\underset{\sim}{\eta}}\underset{\sim}{C}^{\tau 4}_{\underset{\sim}{\alpha}\underset{\sim}{\eta}}}{[-\lambda(t,t_1,t_2)]^{\frac{1}{2}}\sin\tfrac{\pi}{2}\alpha_1 \sin\tfrac{\pi}{2}\alpha_2} \quad (3.23)$$

The discontinuity we have taken is

$$\text{disc}_J F(J,t) = F(J - i\epsilon, t) - F(J + i\epsilon, t) \quad (3.24)$$

since the sign of this discontinuity is the sign of the contribution of the cut to the total cross-section.

To obtain the complete discontinuity across the two-Reggeon cut we should actually multiply (3.23) by a factor of six. Firstly $F(J,J_1,J_2,n_1,n_2)$ is symmetric under $n_1,n_2 \to -n_1, -n_2$ and so we obtain an exactly similar contribution from that part of (3.4) in which $n_1,n_2 < 0$. Also the phase-space $\int d\rho$ we have used is that for four identical scalar particles. This was for simplicity, but it means that the same Reggeons can appear in channels defined by regrouping the four-particles to define new angular momentum states. Since there are three possible ways of pairing four particles, by repeating the foregoing analysis using different angular momentum states we obtain two more distinct contributions to the two-Reggeon cut.

By considering the exact form for the J-plane continuations of the parts of (3.4) for which $n_1>0$, $n_2<0$ or $n_1<0$, $n_2>0$ we can show that no two-Reggeon cut is generated.[21] Essentially this is because

the helicity-Regge poles and fixed-pole lie on the same side of the helicity contour and cannot generate a pole at $J=\alpha_1(t_1)+\alpha_2(t_2)-1$.

The next problem is to take account of the presence of the two-Reggeon branch-point in $\underset{\sim}{C}^{\tau}_{\underset{\sim}{\alpha\eta}}(J,t)$. $\underset{\sim}{C}^{\tau 4}_{\underset{\sim}{\alpha\eta}}(J,t)$ will be singular at $J=\alpha_c^*$, rather than $J=\alpha_c$, when $t > 16m^2$, and we shall exploit this. To study the branch-point in $\underset{\sim}{C}^{\tau}_{\underset{\sim}{\alpha\eta}}(J,t)$ we have to use the unitarity condition for $F(J,J_1,J_2,n_1,n_2)$. The four-particle threshold discontinuity formula that has to be partial-wave projected is[42,43]

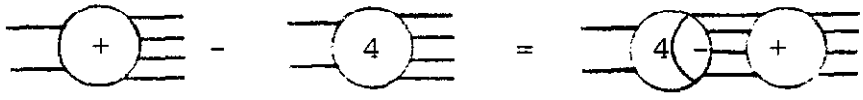

(3.25)

Proceeding through the analogous steps to those above we are finally led to study the two-Reggeon cut in a four-Reggeon amplitude $M_{\underset{\sim}{\alpha\alpha}'}(J,t)$ - shown pictorially in Fig. 3.9. This amplitude is defined as a double fixed-pole residue of a four-Reggeon amplitude defined by factorization at Regge-helicity poles. (The fixed-poles occur at $J=\alpha_1'(t_1')+\alpha_2'(t_2')-1$ and $J=\alpha_1(t_1)+\alpha_2(t_2)-1$, and the Regge-helicity poles occur at $J_i=n_i=\alpha_i(t_i)$ $i=1,2,1',2'$.) To study the two-Reggeon cut in $M_{\underset{\sim}{\alpha\alpha}'}$ we have to go to the discontinuity relation for the eight-point function[42,43]

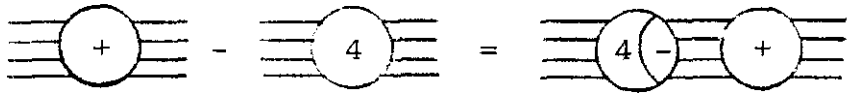

(3.26)

The procedure of projecting (3.23) and (3.24) onto partial-wave and continuing to complex helicity and angular momentum involves even more complicated expressions than those we have already considered,[21] mainly because of the proliferation of variables and indices. Therefore we shall not attempt to give the full details of the

manipulations of these equations, but instead illustrate only the formal structure that is used. We can write (3.14) in the form

$$F(J) - F^4(J) = N(J)\Gamma(J)N^4(J) \tag{3.27}$$

where $N(J) \equiv \underset{\sim}{N}^{\tau}_{\underset{\sim}{\eta\alpha}}(J,t)$ and $\Gamma(J)$ is a formal expression for the integration in (3.14) which generates the two-Reggeon cut discontinuity given by (3.23) From (3.25) and (3.26) we obtain analogous equations to (3.27)

$$N(J) - N^4(J) = N^4(J)\Gamma(J)N(J) \tag{3.28}$$

$$M(J) - M^4(J) = M^4(J)\Gamma(J)M(J) \tag{3.29}$$

The appearances of the same $\Gamma(J)$ in all three of (3.27) - (3.29) is vital. (3.27) - (3.29) are initially obtained for $t \gtrsim 16m^2$ and $ReJ > Re\alpha_c$. If we continue them to $ReJ < Re\alpha_c$ and use $\pm$ to denote a $\pm i\epsilon$ prescription in the J-plane with respect to the cut we obtain from (3.29)

$$M(J^{\pm}) - M^4(J) = M^4(J)\Gamma(J^{\pm})M(J^{\pm}) \tag{3.30}$$

From which we obtain

$$\delta M(J) = M(J^+) - M(J^-) = M^4(J)\Gamma(J^+)\delta M(J) + M^4(J)\delta\Gamma(J)M(J^-) \tag{3.31}$$

and so

$$(1 - M^4(J)\Gamma(J^+))\delta M(J) = M^4(J)\delta\Gamma(J)M(J^-) \tag{3.32}$$

$$= (1 - M^4(J)\Gamma(J^+))M(J^+)\delta\Gamma(J)M(J^-) \tag{3.33}$$

which has the solution

$$\delta M(J) = M(J^+)\,\delta\Gamma(J)\,M(J^-) \qquad (3.34)$$

Similarly we can obtain[51]

$$\delta N(J) = N(J^+)\,\delta\Gamma(J)\,M(J^-) \quad , \qquad (3.35)$$

and

$$\delta F(J) = N(J^+)\,\delta\Gamma(J)\,N(J^-) . \qquad (3.36)$$

For $t<0$ $\delta\Gamma(J)$ is given by (3.23) (apart from the factor of six) and so writing out (3.36) in full

$$\mathrm{disc}_J F(J,t) = \frac{-i}{2^5}\sin\tfrac{\pi}{2}J \int_{\lambda<0} dt_1 dt_2 \; \frac{\delta(J-\alpha_1(t_1)-\alpha_2(t_2)+1)\,\underset{\sim}{C}^{\tau}_{\underset{\sim}{\alpha}\underline{\eta}}(J^+,t)\,\underset{\sim}{C}^{\tau}_{\underset{\sim}{\alpha}\underline{\eta}}(J^-,t)}{[-\lambda(t,t_1,t_2)]^{\frac{1}{2}}\sin\tfrac{\pi}{2}\alpha_1(t_1)\sin\tfrac{\pi}{2}\alpha_2(t_2)} \qquad (3.37)$$

It is clearly straightforward to write out detailed versions of (3.34) and (3.35) giving the discontinuities across the two-Reggeon cut in $\underset{\sim}{N}^{\tau}_{\underset{\sim}{\alpha}\underline{\eta}}(J,t)$ and $\underset{\sim}{M}^{\tau}_{\underline{\eta}\underset{\sim}{\alpha}\underset{\sim}{\alpha}'}(J,t)$.

There are several important properties of (3.37) which we should note. The most immediate point is that since $\underset{\sim}{C}^{\tau}_{\underset{\sim}{\alpha}\underline{\eta}}(J,t)$ is real-analytic $\underset{\sim}{C}^{\tau}_{\underset{\sim}{\alpha}\underline{\eta}}(J^-,t)$ is the complex-conjugate of $\underset{\sim}{C}^{\tau}_{\underset{\sim}{\alpha}\underline{\eta}}(J^+,t)$ and so the sign of the two-Reggeon cut discontinuity is determined. If both α_1 and α_2 are Pomerons so that in (3.37)

$$J \sim 2\alpha(t) - 1 \sim \alpha(t) \sim 1 \quad \text{for } t \sim 0 \quad , \qquad (3.38)$$

the integrand is positive definite and the overall negative sign persists. A detailed analysis[50] shows that this negative sign can be traced to the fact that the "signature factor" $\sin\frac{\pi}{2}(J-n_1-n_2-[\hat{\tau}-(\hat{\tau}'_1+\hat{\tau}'_2)])$ in (3.8) is evaluated at a nonsense wrong-signature point where it gives - 1.

The next point we note is that the signature factor $\sin\frac{\pi}{2}J$ in front of the integral in (3.37) ensures that the branch-point is not present (as a fixed singularity) in the physical t-channel partial-waves - that is $F(J,t)$ evaluated at even integer J.

Another point is that the factors $\sin\frac{\pi}{2}\alpha_1$, $\sin\frac{\pi}{2}\alpha_2$ lead to the generation of the Reggeon-particle branch-point in (3.37). It is generated when α_1 or $\alpha_2 = 0$ (t_1 or $t_2 = m^2$), $\lambda(t,t_1,t_2) = 0$, and $J = \alpha_1 + \alpha_2 - 1$. Because of this the two-Reggeon cut is able to shield the Reggeon-particle cut from the physical sheet of the J-plane when $t \sim 0$, so that the Reggeon-particle cut does not contribute to the high-energy scattering.

A further point with important physical significance is that (3.37) shows that the cut discontinuity is entirely controlled by the fixed-pole residue of $\underset{\sim}{N}^{\tau}_{\underset{\sim}{\alpha}\underline{\eta}}(J,t)$. This residue has been defined in terms of the J-plane continuation of $\underset{\sim}{F}^{\tau}_{\underline{\eta}}(\underset{\sim}{J},\underline{n})$ by first continuing to Regge poles at $J_1=n_1=\alpha_1(t_1)$, $J_2=n_2=\alpha_2(t_2)$, and then to the fixed-pole at $J=\alpha_1+\alpha_2-1$. However, we can also regard $\underset{\sim}{N}^{\tau}_{\underset{\sim}{\alpha}\underline{\eta}}(J,t)$ as the Froissart-Gribov projection of a momentum-space helicity amplitude which describes the scattering of two particles into two Reggeons - see Fig. 3.10. This amplitude $\underset{\sim}{A}_{\underset{\sim}{\alpha}}(M^2,t)$ is commonly referred to as the maximum helicity-flip amplitude. This is because

in the t_1 and t_2 channels $n_1=J_1$ and $n_2=J_2$ would be the maximum values n_1 and n_2 could take if J_1 and J_2 were physical spins. (In the symmetric notation we have used, if n_1 is defined as the helicity of the J_1 - state then, $-n_2$ must be defined as the helicity of the J_2 - state.)

The Froissart-Gribov projection of $A_{\underset{\sim}{\alpha}}(M^2,t)$ satisfies the usual Froissart-Gribov formula (omitting $\underline{\eta}$ labels and the signature labels associated with $\underset{\sim}{\alpha}$ for simplicity)

$$N_{\underset{\sim}{\alpha}}(J,t) = \frac{1}{2\pi}\int_{z_o}^{\infty} dz Q_J^{\alpha_1+\alpha_2}(z)\,\mathrm{Im}A_{\underset{\sim}{\alpha}}(z,t) + \frac{1}{2\pi}\int_{-\infty}^{-z_o} dz Q_J^{\alpha_1+\alpha_2}(-z)\,\mathrm{Im}A_{\underset{\sim}{\alpha}}(z,t) \tag{3.39}$$

z being the center of mass scattering angle. At $J=\alpha_1+\alpha_2-1$, $Q_J^{\alpha_1+\alpha_2}(z) = (z^2-1)^{\frac{\alpha_1+\alpha_2}{2}}$, and since it is

$$F_{\underset{\sim}{\alpha}}(M^2,t) = (z^2-1)^{\frac{\alpha_1+\alpha_2}{2}} A_{\underset{\sim}{\alpha}}(z,t) \tag{3.40}$$

which has no kinematic singularities at $z = \pm 1$, the second integral in (3.39) can be first written as an integral around the left-hand cut of $F_{\underset{\sim}{\alpha}}(M^2,t)$ and then transformed to an integral over the right-hand cut using Cauchy's theorem. Thus we obtain the usual expression for fixed-pole residues of helicity amplitudes

$$N_{\underset{\sim}{\alpha}}(j = \alpha_1+\alpha_2-1,t) = \frac{1}{\pi}\int_{z_o}^{\infty} dz\,\mathrm{Im}F_{\underset{\sim}{\alpha}}(M^2,t)\ . \tag{3.41}$$

Now the Reggeon particle imaginary part is experimentally accessible in the single particle inclusive process shown in

Figure 3.11. In the regime where $s \to \infty$ with t and M^2 fixed, the inclusive cross section measures $\mathrm{Im}F_{\underset{\sim}{\alpha}}(M^2,0)$ given in (3.41). Inclusive cross section data provides us with a phenomenological handle on the strength of the discontinuity across Regge cuts.[52]

Our final point about these formulae for the two Reggeon cut concerns the phase space. In the neighborhood of $\alpha_i \sim J \sim 1$ which is the regime of the $\underset{\sim}{P}$, all factors besides the phase space are smooth. The phase space integration is two dimensional so we take advantage of this by defining two vectors $\vec{q}_i$ for each momentum transfer $t_i = -|\vec{q}_i|$. Further we note that the delta function on J can be written

$$\delta(J-\alpha_1(t_1)-\alpha_2(t_2)+1)$$

$$= \delta(1-J-(1-\alpha_1(\vec{q}_1)) - (1-\alpha_2(\vec{q}_2))) \ , \qquad (3.42)$$

which encourages us to write Reggeon energies $E_i = 1-\alpha_i(\vec{q})$ and $E=1-J$. The discontinuity across the two Reggeon cut in $F(E,\vec{q})$ is then (absorbing signature and such factors) (see Figure 3.12)

$$\mathrm{disc}_E F(E,\vec{q}) = -2i\int d^2q_1 dE_1 d^2q_2 dE_2 \delta(E-E_1-E_2)$$

$$\delta^2(\vec{q}-\vec{q}_1-\vec{q}_2)\delta(E_1-(1-\alpha_1(\vec{q}_1)))\delta(E_2-(1-\alpha_2(\vec{q}_2)))$$

$$N(E+i\epsilon,E_1,\vec{q}_1,E_2,\vec{q}_2)N(E-i\epsilon,E_1,\vec{q}_1,E_2,\vec{q}_2) \ , \qquad (3.43)$$

where N is the Reggeon particle amplitude as shown in Figure 3.12.

This discontinuity formula is identical to that given by (2.32) with n=2. It suggests that we treat the Reggeon as a quasi-particle living in two space and one time dimension carrying energy

$E(\vec{q}) = 1 - \alpha(\vec{q})$ when it is on the "mass shell." In this sense (3.43) is (apart from the negative sign) an ordinary unitarity relation giving the two quasi-particle intermediate state contribution to the imaginary part of $F(E,\vec{q})$. Note that we do not associate an energy with individual particles, instead pairs of particles are treated as sources of E and $\vec{q}$ for Reggeons which then propagate. Similar relations can be written for N(E) and M(E) appearing in (3.35) and (3.36). Perhaps the best viewpoint on the Reggeon field theories is that they are a compact device for providing automatically the correct phase space structure for Reggeons and satisfying these Reggeon unitarity relations.[34,53-55]

It is also possible to discuss the solution of (3.34)-(3.37) using "S-Matrix" methods rather than the field-theoretic methods which are the subject of this review. Such methods are likely to be limited in use to the situation where only a small number of Regge cuts need be considered. This may well be the situation for the weak-coupling $\underset{\sim}{P}$ (if it exists) but is clearly not the case for the strong-coupling $\underset{\sim}{P}$. (The reader is referred to the next section for precise definitions of weak and strong coupling.) We shall not discuss these methods here, but instead refer the reader to Refs. 51 and 55-57 for a detailed discussion of this subject.

The treatment we have given here of the two-Reggeon cut can be extended to all multi-Reggeon cuts.[20,21] The N-Reggeon cut can be studied through the 2N unitarity integral. As we have seen the four-particle unitarity integral is sufficiently complicated to handle technically and the higher unitarity integrals are worse. However, we can illustrate the general structure by looking briefly at the three-Reggeon cut (more details can be found in the GPT

paper). We analyze the six-particle unitarity integral using partial-wave amplitudes corresponding to the coupling scheme shown in Fig. 3.13. The three-Reggeon cut is generated by Regge poles at $J_i = n_i = \alpha_i(t_i)$ $i = 1,3,4$, together with nonsense wrong-signature poles at $J_2 = n_3 + n_4 - 1$, $J = n_1 + n_2 - 1$ in the amplitude with $J_2 = n_2 (= n_3 + n_4)$. A fixed-pole is then generated at

$$J = \alpha_1(t_1) + \alpha_3(t_3) + \alpha_4(t_4) - 2 \quad . \tag{3.44}$$

When this fixed-pole is tangential to the phase-space boundary at

$$t^{\frac{1}{2}} - t_1^{\frac{1}{2}} - t_3^{\frac{1}{2}} - t_4^{\frac{1}{2}} = 0 \quad , \tag{3.45}$$

the three-Reggeon cut is generated. For identical trajectories this occurs at $t_1^{\frac{1}{2}} = t_3^{\frac{1}{2}} = t_4^{\frac{1}{2}} = t/3$, giving a branch-point at

$$\alpha_c(t) = 3\alpha(t/9) - 2 . \tag{3.46}$$

In general the N-Reggeon cut is generated by N Regge-pole N-1 nonsense wrong-signature poles giving a fixed-pole at

$$J = \alpha_1(t_1) + \text{---} \quad \alpha_N(t_N) - (N-1) \tag{3.47}$$

which collides with the phase-space boundary at

$$t^{\frac{1}{2}} - t_1^{\frac{1}{2}} - \quad \text{---} \quad - t_N^{\frac{1}{2}} = 0 \tag{3.48}$$

and, for identical trajectories gives a branch-point at

$$\alpha_c^{(N)}(t) - 1 = N[\alpha(t/N^2) - 1] \tag{3.49}$$

To obtain the total discontinuity across the N-Reggeon cut it is, of course, necessary to add the contributions from all possible partial-wave coupling schemes. The form of the discontinuity is analogous to (3.37) being expressed as an integral of a sum of products of two multiple fixed-pole residues - one evaluated above the N-Reggeon cut and one below (boundary values of cuts in sub-channels must also be specified as for momentum space unitarity). The most important point is that the discontinuity can be expressed as the N - (quasi-)particle contribution to the quasi-unitarity relation for the scattering of quasi-particle Reggeons. The sign of the N-Pomeron cut is $(-1)^{N-1}$ because the cut is generated by (N-1) nonsense poles and there will be (N-1) factors of -1 coming from the corresponding signature factors.

The extension of Reggeon unitarity to production processes is complicated by the necessity to perform helicity as well as angular momentum continuations. Reggeon unitarity will initially determine Reggeon field theory rules for production processes when all azimuthal angles (the conjugate variables to helicities) are large. For $2 \to N$ processes the azimuthal angles cannot be taken large in the physical region and analytic continuation must be used to obtain the rules.[58] However, for inclusive processes this is not necessary and it can be shown that Reggeon unitarity determines the Reggeon rules for the triple Regge limit of the one-particle inclusive cross-section in a straightforward way.[59,60]

Finally we mention briefly some technical points that we have glossed over in our derivation of the two-Reggeon cut discontinuity formula. Firstly, because of physical region singularities of the six-point function in channels overlapping the t_1 and t_2 channels, the amplitude $F(J,J_1,J_2,n_1,n_2,t,t_1,t_2)$ will not be a single analytic function of t_1 and t_2 throughout the physical region. This problem

can be eliminated by using the Steinmann relations together with a multiple dispersion relation to separate out that part of the amplitude having singularities in the t_1 and t_2 channels. Secondly it can be shown that even when we separate out that part of the amplitude, the Froissart-Gribov amplitudes $F^{\tau}_{\underset{\sim}{\eta}}(J,\underset{\sim}{n})$ only satisfy the Carlson condition as a function of J for part of the physical region ranges of t_1 and t_2. Fortunately we can cover the whole physical region by using all possible partial-wave coupling schemes. Further the region in which $F^{\tau}_{\underset{\sim}{\eta}}(J,\underset{\sim}{n})$ does satisfy the Carlson condition includes the region where the two-Reggeon cut is generated.

As a final point we note that if the Pomeron has $\alpha_p(0) = 1$, then $\alpha_p(t)$ will have a complex part for $t < 0$ and so we cannot write the two-Pomeron discontinuity as a real integral for $t < 0$, as in (3.37). Therefore, there will be no range of t where the discontinuity can be expressed as a simple real integral. However, in a perturbation solution of the discontinuity formulae (such as the Reggeon field theory) which begins with bare analytic trajectory functions, perturbative unitarity will involve real discontinuity formulae.

IV. THEORETICAL DEVELOPMENTS IN REGGEON FIELD THEORY

(a) Opening Remarks

This section is devoted to a discussion first of the $\underset{\sim}{P}$ pole and all its cuts taken by themselves, and then the consequences of those $\underset{\sim}{P}$ interactions for the structure of secondary trajectories. It is useful to begin by explaining why the $\underset{\sim}{P}$ and its interactions must be studied first. The essential reason is contained back in Equations (3.47)-(3.49), for the position of branch points in J. When one has multiple exchange of $\underset{\sim}{P}$ with $\alpha(0) = 1$, the cuts and pole collide at t=0. This is certainly true for $\underset{\sim}{P}$'s alone. It is equally true for one secondary trajectory with $\alpha_R(0) \neq 1$ when it is exchanged in the t-channel with any number of $\underset{\sim}{P}$'s. In that case the cuts and pole collide at t=0 at $J=\alpha_R(0)$.

The notation developed in Section II is useful in this regard. There we learned that in the Reggeon unitarity relations a two-momentum $\vec{q}$ and an "energy" E=1-J were conserved for each Reggeon. For Reggeons on shell the $E,\vec{q}$ relation is

$$E(\vec{q}) = 1 - \alpha(\vec{q}) \tag{4.1}$$

so that $E(0) = 0$ for the $\underset{\sim}{P}$. This is just the $E,\vec{q}$ relation of a quasiparticle with no energy gap. Every other Reggeon has an energy gap of $\Delta=1-\alpha(0) > 0$. The addition of any number of $\underset{\sim}{P}$'s to some exchange process in the t-channel, then, does not alter the threshold for that process in the E plane since at $\vec{q}=0$ a zero energy quantum may be added. The addition of any other trajectory to an already existing t-channel exchange alters the threshold (position of branch point) because finite energy, Δ, is required at zero momentum. All

this is analogous to the positions of thresholds in conventional quantum field theory when massless particles are present. The $\underset{\sim}{P}$ is analogous to a massless particle, and the solution to the problem of the J plane singularity arising from multiple $\underset{\sim}{P}$ cuts is the solution to an infrared problem.

Now we understand how the thresholds of multiple $\underset{\sim}{P}$ exchange stand out and further we see why in the case of $\underset{\sim}{P}$ alone the thresholds all occur at J=1 (E=0) at t=0 ($\vec{q}$=0). From a physics point of view it is useful to recall at this juncture the significance of J=1, t=0 before we go on to the $\underset{\sim}{P}$ itself. The Froissart-Gribov formula for signatured partial wave amplitudes gives us a connection between the absorptive part of two body amplitudes AB → A'B' and the t-channel partial wave amplitude F(J,t). Schematically,

$$F(J,t) = \frac{2}{\pi} \int_1^\infty ds\ s^{-J-1}\ \text{Abs}\ T_{AB\to A'B'}(s,t). \tag{4.2}$$

Furthermore it is known for a variety of processes, called diffractive, that

$$\sigma_{AB\to A'B'}(s) \underset{s\ \text{large}}{\approx} s^{2\alpha(0)-2}(\log s)^{2\beta}\ g_{AA'}h_{BB'}\ , \tag{4.3}$$

with $\alpha(0) \approx 1$, β small, and $g_{AA'}$ or $h_{BB'}$ numbers which depend only on the properties of A and A' or only on B and B' respectively. In short, the behavior of diffractive amplitudes

1. is almost energy independent; $\alpha(0) \approx 1$;
2. shows factorization of vertices as expected from an elementary t-channel exchange.

On further inspection of the amplitudes which have diffractive behavior one learns

3. no quantum numbers are exchanged in the t-channel.

From an operational point of view this is the Pomeron. Equation (4.3) translates into the J plane as

$$F(j,0) = \frac{g_{AA'}\, h_{BB'}}{[J-\alpha(0)]^{1+\beta}} \quad ; \tag{4.4}$$

that is, a branch point at $J=\alpha(0)=1$ whose detailed nature governs the behavior in log s of elastic or quasi-elastic cross sections.

The optical theorem relates the behavior of elastic amplitudes to total cross sections; for (4.3) we have

$$\sigma_T^{AB}(s) \underset{s \text{ large}}{\sim} g_{AA} h_{BB}\, s^{\alpha(0)-1} (\log s)^{\beta} \quad , \tag{4.5}$$

and we know from the Froissart bound that

$$\alpha(0) \leq 1 \ , \tag{4.6}$$

and

$$\beta \leq 2, \text{ when } \alpha(0) = 1 \ . \tag{4.7}$$

The experimental behavior of amplitudes then chooses $\alpha(0) = 1$ as the point where we ought to concentrate our attention. The result of summing all colliding cuts at J=1 will be to determine the fine structure in J at J=1 and thus the log s behavior of cross sections. Furthermore any singularities in J away from J=1 will give contributions to cross sections which are negligible by powers of s when $\underset{\sim}{P}$

can be present; that is, vacuum quantum numbers are allowed in the t-channel. So we turn our attention to the problem of a $\underset{\sim}{P}$ singularity in the J plane which lies at J=1 at t=0.

(b) Formulation of the RFT

We have learned in Sections II and III that Reggeons propagate in two space, $\vec{x}$, and one time, τ, dimensions. These are conjugate to the two momentum, $\vec{q}$, and energy, 1-J, and are actually the impact parameter and rapidity of the Reggeon. The RFT describes this by a field amplitude $\varphi(\vec{x},\tau)$ for finding the Reggeon at $\vec{x}$ and τ. In the absence of interactions the Reggeon field satisfies the Schrödinger equation

$$i \frac{\partial}{\partial \tau} \varphi(\vec{x},\tau) = (1-\alpha_0(\frac{1}{i}\vec{\nabla}))\varphi(\vec{x},\tau) \quad , \qquad (4.8)$$

where $\alpha_0(\vec{q})$ is given by the choice of bare energy momentum relation; i.e., the non-interacting Reggeon. This function $\alpha_0(\vec{q})$ is a priori at our disposal; it specifies the nature of the $\underset{\sim}{P}$ or other Reggeon before interactions are accounted for. We must turn to physics to help us here.

The appropriate physics is the connection between bound states in the t-channel and large s behavior in the s channel. Fifteen years ago it became clear that the Regge pole at $J=\alpha(t)$ represents a bound state of hadrons whose mass squared has been continued from $m_B^2 > 0$ to the value t occurring in the scattering process, and, at the same time, whose spin J_B has been continued to $\alpha(t)$.[61] This connection between bound states and crossed channel large s behavior

is one of the deep attractive features of Regge theory. Now, what is important for us is that it follows from t-channel partial wave dispersion relations that $\alpha(t)$ is analytic at t=0 unless at t=0 there is a collision of this pole trajectory with some other singularity in the J-plane.[61] For a Reggeon in isolation, then, one expects $\alpha(t)$ to be regular at t=0. For the purposes of our present concern, which is the behavior near $\vec{q}=0$, J=1, we may expect that the non-interacting Reggeon is adequately represented by

$$\alpha_0(\vec{q}) = \alpha_0 - \alpha_0'\vec{q}^2 \quad , \tag{4.9}$$

where α_0 and α_0' are parameters which it may be possible to extract from a detailed knowledge of the way in which a Reggeon is constructed in the "correct" underlying field theoretic or S-matrix model. The free energy momentum relation is then

$$E(\vec{q}) = \alpha_0'\vec{q}^2 + (1-\alpha_0) \quad , \tag{4.10}$$

which is like a non-relativistic quasi-particle with mass gap $(1-\alpha_0) = \Delta_0$ and mass $= (2\alpha_0')^{-1}$. The mobility of a Reggeon in $\vec{x},\tau$ space depends on its effective mass $(2\alpha_0')^{-1}$, and the smaller α_0', the less mobile is the Reggeon. Since α' is known to be smaller for $\underset{\sim}{P}$ by about 1/3 compared to, say, the ρ trajectory, we may expect the $\underset{\sim}{P}$ to be very ponderous. If we now associate a field with this Reggeon, the free action will be

$$A_0 = \int d^2x d\tau \mathcal{L}_0(\vec{x},\tau) \quad , \tag{4.11}$$

with

$$\mathcal{L}_0(\vec{x},\tau) = \frac{i}{2}\,\varphi^+(\vec{x},\tau)\,\overleftrightarrow{\frac{\partial}{\partial\tau}}\,\varphi(\vec{x},\tau)$$

$$-\alpha_0'\,\vec{\nabla}\varphi^+(\vec{x},\tau)\cdot\vec{\nabla}\varphi(\vec{x},\tau) - \Delta_0\varphi^+(\vec{x},\tau)\varphi(\vec{x},\tau) \qquad (4.12)$$

the Lagrangian density. The next issue is the interaction.

To determine what interactions are allowed we turn to models which generate Reggeon interactions. In Section II φ^3 field theory models were studied to extract the RFT rules. Other natural models in which to examine this question are multiperipheral and dual models or perhaps more realistic field theories. In each of these it is possible to have four and five and higher point $\underset{\sim}{P}$ interactions as well as the simplest triple $\underset{\sim}{P}$ coupling discussed before. Four $\underset{\sim}{P}$ couplings arise, for example, in a φ^3 field theory, where the $\underset{\sim}{P}$ is generated via ladder graphs, as in Figure 4.1. Here two $\underset{\sim}{P}$'s can scatter, or one $\underset{\sim}{P}$ can make a transition into three $\underset{\sim}{P}$'s.

In any given model each N $\underset{\sim}{P}$ coupling, N=3,4,---, is in general a function of the energies $(1-J_i)$ and momenta of the $\underset{\sim}{P}$'s involved. This means that if we are to incorporate directly the content of an underlying theory into a RFT, we will have to construct a field theory which is both non-local and involves an infinite number of coupling functions, one for each independent n $\underset{\sim}{P} \rightarrow$ m $\underset{\sim}{P}$ transition. For 4 $\underset{\sim}{P}$ couplings, for example, we will have two independent functions

$$\mathcal{L}_{I4}(\vec{x},\tau) = \int d^2x_1 d\tau_1 \ldots d^2x_4 d\tau_4 \Big\{\varphi^+(\vec{x}_1,\tau_1)\varphi^+(\vec{x}_2,\tau_2)$$

$$\cdot\,\varphi^+(\vec{x}_3,\tau_3)\varphi(\vec{x}_4,\tau_4) + \text{h.c.}\Big\} F_1(\vec{x}-\vec{x}_1,\tau-\tau_1,\ldots\vec{x}-\vec{x}_4,\tau-\tau_4) \qquad (4.13)$$

$$+\,\varphi^+(\vec{x}_1,\tau_1)\varphi^+(\vec{x}_2,\tau_2)\varphi(\vec{x}_3,\tau_3)\varphi(\vec{x}_4,\tau_4)F_2(\vec{x}-\vec{x}_1,\tau-\tau_1,\ldots\vec{x}-\vec{x}_4,\tau-\tau_4)$$

Unless there is some simplification, we are faced with the prescription of an infinite number of arbitrary functions.

Since we are ultimately interested in the infrared ($E_i \approx 0$, $\vec{q}_i \approx 0$) behavior of any RFT we write down, as a first step we expand each of the coupling functions about this point. We begin the discussion by retaining only the first non-vanishing terms. This reduces the non-local theory to a local theory with coupling constants and maybe a few derivative interactions. This procedure applied to 3 $\underset{\sim}{P}$ and 4 $\underset{\sim}{P}$ interactions gives

$$\mathcal{L}_I(\vec{x},\tau) = -\frac{\lambda_0}{2!}\left[\varphi^+(\vec{x},\tau)\varphi^+(\vec{x},\tau)\varphi(\vec{x},\tau) + \text{h.c.}\right]$$
$$-\frac{\lambda_4}{3!}\left\{\varphi^+(\vec{x},\tau)^3\,\varphi(\vec{x},\tau) + \text{h.c.}\right\} - \frac{\lambda_{41}}{(2!)^2}\,\varphi^+(\vec{x},\tau)^2\varphi(\vec{x},\tau)^2 \tag{4.14}$$

for the interaction Lagrangian. This has improved the situation in the sense that we now have a local theory with an infinite number of coupling constants. However, there is one more level of heuristic argument we may use to eliminate from our preliminary consideration any but the 3 $\underset{\sim}{P}$ coupling. Essentially we argue that to emit and absorb $\underset{\sim}{P}$'s inside any diagram of our RFT costs a phase space factor dEd^2q each time. We are ultimately interested in the $E_i \to 0$, $\vec{q}_i \to 0$ limit of the RFT so each additional phase space factor decreases the importance of any given graph. N $\underset{\sim}{P}$ couplings with N > 3 require more phase space than N=3; therefore, one may ignore them. Later in this section we will return to reconsider the whole matter of higher point $\underset{\sim}{P}$ couplings and derivative couplings, and justify this heuristic argument.

We must incorporate a final point from Sections II and III before we begin the discussion of the various attacks on RFT. In those sections we learned that the two $\underset{\sim}{P}$ cut carries a minus sign relative to the contribution of a single $\underset{\sim}{P}$ exchange. A graph like Figure 4.2 must contain a minus sign. This is naturally incorporated as part of the Feynman rules of the RFT if the coupling λ_0 in (4.14) is pure imaginary: $\lambda_0 = ir_0$. The RFT now to be discussed has the Lagrange function

$$\mathcal{L}(\vec{x},\tau) = \frac{i}{2}\,\varphi^+ \overleftrightarrow{\frac{\partial}{\partial\tau}}\,\varphi - \alpha_0'\vec{\nabla}\varphi^+\cdot\vec{\nabla}\varphi - \Delta_0\varphi^+\varphi$$

$$- \frac{ir_0}{2}\left[\varphi^+\varphi^+\varphi + \text{h.c.}\right] \qquad (4.15)$$

The solution of this field theory with an anti-Hermitean interaction in the infrared limit is the central problem of RFT. The spectrum of the theory determines the Pomeron. This was first written down and studied by V. N. Gribov and A. A. Migdal.[62-64] It is with their work that we now concern ourselves.

(c) Early Developments in RFT for $\underset{\sim}{P}$

To review in detail the work of the Leningrad school would be a monumental task. Leaving this pleasure to the historians we will sketch the essential results of their calculations. To begin we established some notation that we will employ frequently.

The objects of primary interest in RFT, as in any field theory, are the Green's functions for the m $\underset{\sim}{P}$ → n $\underset{\sim}{P}$ transition

$$\tilde{G}^{(n,m)}(\vec{x}_1,\tau_{x_1},\ldots\vec{y}_m,\tau_{y_m}) =$$

$$\langle 0|T_\tau(\varphi^+(\vec{y}_1,\tau_{y_1})\ldots\varphi^+(\vec{y}_m,\tau_{y_m})\varphi(\vec{x}_1,\tau_{x_1})\ldots\varphi(\vec{x}_n,\tau_{x_n}))|0\rangle \tag{4.16}$$

where $|0\rangle$ is the no $\underset{\sim}{P}$ state. There is no crossing in RFT so both n and m must be given. The Fourier transform of $\tilde{G}^{(n,m)}$ is of interest also (Figure 4.3):

$$\delta\Big(\sum_{i=1}^{n} E_i - \sum_{j=n+1}^{n+m} E_j\Big)\delta^2\Big(\sum_{i=1}^{n}\vec{q}_i - \sum_{j=n+1}^{n+m}\vec{q}_j\Big)G^{(n,m)}(E_i,\vec{q}_i) =$$

$$\int d^2x_1 d\tau_{x_1}\ldots d^2y_m d\tau_{y_m}\, e^{-i\vec{q}_i\vec{x}_1+iE_1\tau_{x_1}-\ldots+i\vec{q}_{n+m}\vec{y}_m-iE_{n+m}\tau_{y_m}}\,\tilde{G}^{(n,m)}(\vec{x}_1,\tau_{x_1},\ldots\vec{y}_m,\tau_{y_m}) \tag{4.17}$$

The spectrum of the theory is specified by the zeroes of the inverse $\underset{\sim}{P}$ propagator

$$\Gamma^{(1,1)}(E,\vec{q}^2) = [G^{(1,1)}(E,\vec{q}^2)]^{-1} . \tag{4.18}$$

It is convenient to discuss the one $\underset{\sim}{P}$ irreducible proper vertex functions $\Gamma^{(n,m)}(E_i,\vec{q}_i)$ gotten by amputating the external legs of the one $\underset{\sim}{P}$ irreducible part of $G^{(n,m)}$. $\Gamma^{(1,1)}$ or $G^{(1,1)}$ and $\Gamma^{(1,2)}$, the 3 $\underset{\sim}{P}$ vertex function, are prominent in the analysis of Gribov and Migdal.

In the non-interacting theory $G^{(1,1)}$ takes the value

$$G_0^{(1,1)}(E,\vec{q}^2) = \frac{i}{E-\alpha_0'\vec{q}^2-\Delta_0+i\epsilon} , \tag{4.19}$$

where the $i\epsilon$ prescription means only retarded propagation. Its origin is the requirement that, in the Sommerfeld-Watson integrals defining the theory, the integration contour in J lies to the right of all singularities in $F(J,t)$.

When all interactions of $\underset{\sim}{P}$'s are summed, the inverse propagator takes the form

$$i\Gamma^{(1,1)}(E,\vec{q}^2) = E-\alpha_0'\vec{q}^2-\Delta_0-\Sigma(E,\vec{q}^2) \quad , \tag{4.20}$$

where the proper self energy Σ must satisfy the Schwinger-Dyson equation (Figure 4.4)

$$\Sigma(E,\vec{q}^2)$$

$$= \frac{ir_0}{2}\int \frac{d^2q'dE'}{(2\pi)^{3/2}} [\Gamma^{(1,1)}(E',\vec{q}^2)\Gamma^{(1,1)}(E-E',(\vec{q}-\vec{q}')^2)]^{-1}$$

$$\cdot \Gamma^{(1,2)}(E',E-E',\vec{q}',\vec{q}-\vec{q}')+(\text{terms due to } \Gamma^{(1,n)} \text{ with } n \geq 3). \tag{4.21}$$

The Soviet workers discussed in detail two possible solutions to the RFT we have posed:

(a) The <u>weak coupling solution</u>, wherein for small E and $\vec{q}^2$

$$\Sigma_{w.c.}(E,\vec{q}^2) << E,\vec{q}^2 \rangle \tag{4.22}$$

so that the resulting propagator is very much the same as the unperturbed propagator (4.19) and the $\underset{\sim}{P}$ spectrum is a simple pole still, constrained now to have $\Delta=1-\alpha(0) = 0$, so

$$i\Gamma^{(1,1)}_{w.c}(E,\vec{q}^2) \underset{E,\vec{q}^2=0}{\approx} E-\alpha_0'\vec{q}^2 \quad . \tag{4.23}$$

This cannot come about if the higher order vertex functions are arbitrary since they are linked to $\Gamma^{(1,1)}$ via the representation In particular if $\Gamma^{(1,2)}$ - the three $\underset{\sim}{P}$ vertex function - took on the constant value of lowest order perturbation theory, the right-hand side of (4.21) would be infra-red divergent. $\Gamma^{(1,2)}$ must therefore vanish at the infra-red point where all of its arguments are zero. Gribov and Migdal suggested that the zero of $\Gamma^{(1,2)}$ should be sufficiently strong that the infra-red regions in (4.21) and the analogous equation for $\Gamma^{(1,2)}$ shown graphically in Fig. 4.5,, be completely suppressed. This requires the leading behavior of $\Gamma^{(1,2)}$ to be analytic at the infra-red point, since the only possible source of non-analyticity - the infra-red regions - are suppressed in the integral equations it satisfies. Therefore

$$\Gamma^{(1,2)}_{w.c.}(E_1,\vec{q}_1,E_2,\vec{q}_2) = a(E_1+E_2)+b(\vec{q}_1+\vec{q}_2)^2 + c(\vec{q}_1^{\,2}+\vec{q}_2^{\,2}) + \text{higher order terms} \tag{4.24}$$

and the detailed form of $\Gamma^{(1,1)}$ is then

$$i\Gamma^{(1,1)}_{w.c.}(E,\vec{q}^2) = E-\alpha_0'\vec{q}^2 + \frac{(aE+b\vec{q}^2+CE/\alpha_0')^2}{16\pi\alpha_0'}\log(\tfrac{1}{2}\alpha_0'\vec{q}^2-E) \tag{4.25}$$

where a and b appear in $\Gamma^{(1,2)}_{w.c.}$ and contributions from further terms in (4.21) are negligible in the infrared limit. Note that $\Gamma^{(1,3)}$ and $\Gamma^{(2,2)}$ are also required to vanish when their arguments[20] are zero if (4.24) and (4.25) hold.

(b) The <u>strong coupling solution</u>[64] in which for small E and $\vec{q}^2$

$$\Sigma_{s.c.}(E,\vec{q}^2) \geq E,\vec{q}^2 \tag{4.26}$$

and both the propagator and vertex function have a scaling form for small values of their arguments

$$i\Gamma^{(1,1)}_{s.c.} \sim -(-E)^{1-\gamma}\varphi(\vec{q}^2/(-E)^z),\quad \Gamma^{(1,2)}_{s.c.} \sim (-E)^{-\mu} F\left(\frac{\vec{q}^2}{(-E)^z}, \frac{\vec{q}_1^2}{(-E_1)^z}, \frac{\vec{q}_2^2}{(-E_2)^z}, \frac{E_1}{E_2}\right) \tag{4.27}$$

where $3\gamma+z-2\mu=2$. In this case the infra-red regions of the Schwinger-Dyson equations are not suppressed, but instead the scaling forms of $\Gamma^{(1,1)}_{s.c.}$ and $\Gamma^{(1,2)}_{s.c.}$ combine so that these regions scale consistently throughout the equations.

The weak coupling solution leaves the $\underset{\sim}{P}$ pole essentially unchanged. The gap Δ_0 (or intercept of the $\underset{\sim}{P}$ pole α_0) is shifted to zero (or $\alpha(0)=1$), but basically a pole at t=0 is left a pole. The three $\underset{\sim}{P}$ coupling function, however, changes quite drastically. In lowest order perturbation theory one has

$$\Gamma^{(1,2)}_{w.c.} = r_0/(2\pi)^{3/2} \quad , \tag{4.28}$$

while the fully interacting solution to the RFT vanishes at $E_i, \vec{q}_i \to 0$, as in (4.24). Such a phenomenon is possible because of the imaginary triple $\underset{\sim}{P}$ coupling. Formally, the full $\Gamma^{(1,2)}$ is defined by an infinite series in r_0 with terms of alternating signs, so a cancellation or extinction of the lowest order term is possible at isolated points in momentum space. Physically one argues that $\underset{\sim}{P}$ exchange is absorptive, a fact which is embodied in the imaginary nature of the coupling of three $\underset{\sim}{P}$'s, and that the sum of all absorptive corrections (Figure 4.5) cancels up the leading constant. This solution is also called a quasi-stable Pomeron because the rate for the decay of a $\underset{\sim}{P}$ into two $\underset{\sim}{P}$'s vanishes abnormally rapidly as energy tends to zero. This argument of Gribov and Migdal[62] was the earliest argument for the vanishing of the triple $\underset{\sim}{P}$ vertex.

The dynamics underlying a quasi-stable $\underset{\sim}{P}$ was later studied in a ladder graph model in RFT by Bronzan.[65] He wrote an integral equation for $\Gamma^{(1,2)}$ of the symbolic form (see Figure 4.6)

$$\Gamma^{(1,2)} = r_0 + \Gamma^{(1,2)}\, G^{(1,1)} G^{(1,1)} V^{(2,2)} \tag{4.29}$$

where $V^{(2,2)}$ is the two $\underset{\sim}{P}$ irreducible part of $\Gamma^{(2,2)}$. It is the RFT counterpart of the Bethe-Salpeter irreducible kernel encountered in conventional field theory. The model consisted of approximating $V^{(2,2)}$ by the one $\underset{\sim}{P}$ exchange graphs of Figure 4.7. This yields $\Gamma^{(1,2)}$ as an infinite series of RFT ladder graphs. The potential, $V^{(2,2)}$, in this model is very singular in the infrared limit. Then (4.29) can hold only if $\Gamma^{(1,2)}$ vanishes as E_i, $\vec{q}_i \to 0$ from almost all directions, as in the weak coupling solution. There is also an infinite number of new $\underset{\sim}{P}$ poles in $G^{(1,1)}$ all of which accumulate at E=0. This last result shakes one's confidence in the weak coupling solution. It is true that bare vertices have been used in Fig. 4.7, so $V^{(2,2)}$ is probably overly singular. On the other hand, if (4.24) holds, and complete vertices are used in Fig. 4.7, $V^{(2,2)}$ is non singular, and there is no reason for $\Gamma^{(1,1)}$ to vanish. Either way, the weak coupling solution does not occur in detail in this model.

The weak coupling solution is subject to other difficulties. One line of argument notes that if the $\underset{\sim}{P}$ is a pole passing through j=1, t=0, then the vanishing of $\Gamma^{(1,2)}$, which may be demonstrated in marvelous generality using tools which blossomed in the study of inclusive reactions,[17] requires the vanishing of large numbers of other $\underset{\sim}{P}$ couplings at t=0,[18] including the coupling to particles[19] which is supposed to set the scale for asymptotic hadron total cross sections.

This apparent disaster has been circumvented by arguments by Gribov[66] and by Cardy and White.[53,67] The former examines the vertex function for two hadrons and a $\underset{\sim}{P}$ when the hadrons are considered as composite systems. He finds that there is a very neat cancellation due to $\underset{\sim}{P}$ interaction with the constituents so that the particle-particle-$\underset{\sim}{P}$ coupling need not vanish at t=0. One of the conclusions he draws, however, is that all hadron cross sections must be asymptotically equal as well as constant. If this is indeed the case, then the asymptotic regime where this takes place is a long way away.

Cardy and White pointed out that if, as in Bronzan's model, an infra-red singular $V^{(2,2)}$ was responsible for the zero of $\Gamma^{(1,2)}$ then the decoupling arguments based on the relation of pole contributions in inclusive cross-sections[7] via the inclusive sum rules, would not go through. This is because the singular potential will also contribute to the vertices appearing in cut contributions to the two-particle inclusive cross-section. Consequently the cut contributions are enhanced and not suppressed relative to the pole contributions. The sum rules can no longer be used to relate pole contributions. Therefore the vanishing of the triple-$\underset{\sim}{P}$ vertex no longer requires the couplings of the $\underset{\sim}{P}$ to other Reggeons or to hadrons to vanish.

A further point noted by Cardy and White was that if the complete two particle/two $\underset{\sim}{P}$ amplitude is separated into its one $\underset{\sim}{P}$ irreducible and reducible parts then the one $\underset{\sim}{P}$ irreducible part satisfies the same integral equation as $\Gamma^{(1,2)}$, that is (4.29), except that the inhomogeneous term is different. Therefore an infra-red singular $V^{(2,2)}$ will also produce an infra-red zero of the one $\underset{\sim}{P}$ irreducible amplitude. The leading contribution of the two $\underset{\sim}{P}$ cut to the total cross-section then comes from the one $\underset{\sim}{P}$ reducible amplitude - that is the cut couples through the pole and factorises, hence

$$\sigma_T^{AB}(s) \sim g_{AA\underset{\sim}{P}} g_{BB\underset{\sim}{P}} (1-\gamma^2/\log s) + O\left(\frac{1}{(\log s)^2}\right). \qquad (4.30)$$

However, as noted above $V^{(2,2)}$ is only singular in Bronzan's model when vertex renormalisation is ignored. In fact since we have no complete weak coupling model we cannot say whether a singular $V^{(2,2)}$ is the answer to the decoupling problems. If it is, it seems that the higher-order $\underset{\sim}{P}$ couplings must play an essential role in producing the singularity.

The weak coupling or quasi-stable solution to the $\underset{\sim}{P}$ problem in RFT is attractive for a number of physical reasons: (1) It is rather simple. (2) It has an immediate implication for the detailed processes in the s-channel which produce it; namely, some sort of generalized ladder or multiperipheral graph. The single particle inclusive spectrum will have a rapidity plateau and the cross sections for n particles, $\sigma_n(s)$, will be more or less that of the multiperipheral model with small corrections due to the two $\underset{\sim}{P}$ exchange cut.[36] One may hope to parametrize the cut in terms of a small number of undetermined constants. Since the weak coupling solution satisfies *t-channel unitarity* and apart from the decoupling problem seems to be otherwise self-consistent, it is certainly attractive. We will argue, however, that the weak coupling "solution" is not the solution to the problem set by Eq. (4.15).

The strong coupling scaling solution was not favored by Gribov and Migdal.[62,64] Their argument began with the observation that near $E=\vec{q}^2=0$, one has

$$i\Gamma^{(1,1)}_{s.c.}(E,\vec{q}^2) = -\Sigma(E,\vec{q}^2) \quad . \tag{4.31}$$

Let us accept Eq. (4.31) and then examine Eq. (4.21) together with the Schwinger-Dyson equation for $\Gamma^{(1,2)}$. We now substitute $\Gamma^{(1,1)}_{s.c.} \to \tilde{\Gamma}^{(1,1)}_{s.c.} = -\Gamma^{(1,1)}_{s.c.}$. This transforms the Schwinger-Dyson equations into those for a strong coupled field theory with Hermitean coupling. (The role of Eq. (4.31) in this is that when it holds, changing the sign of $\Gamma^{(1,1)}$ is equivalent to changing the sign of Σ.) For the Hermitean theory we can invoke the Källen-

Lehmann representation to learn that $\mathrm{Im}\Gamma^{(1,1)}$ has a definite sign. The sign is such that the contribution of Fig. (4.9a) to σ_T^{AB} is negative. Clearly this is unacceptable and were this the way a strong coupling, scaling form for $\Gamma^{(1,1)}(E,\vec{q}^2)$ is in fact achieved by the RFT we consider, one would be forced to reject it.

Development beyond the work of Gribov and Migdal has been possible because there is an alternative infrared behavior to that of Eqs. (4.22) and (4.26):

$$\Sigma(E,\vec{q}^2) = E-\alpha_0'\vec{q}^2-\Delta_0-\sigma(E,\vec{q}^2),$$
$$\sigma(E,\vec{q}^2) \ll E,\vec{q}^2 \quad . \tag{4.32}$$

The bare $\underset{\sim}{P}$ pole is extinguished, and a stronger singularity is present in $G^{(1,1)}$ at $E=\vec{q}^2=0$. This singularity represents the confluence of the $\underset{\sim}{P}$ pole and cuts at $E=\vec{q}^2=0$. (For $\vec{q}^2\neq 0$, there is still a $\underset{\sim}{P}$ pole.) Note that the weak coupling solution has a pole as the leading singularity at $E=\vec{q}^2=0$, while the Gribov-Migdal strong coupling solution, Eq. (4.31) has a weaker singularity than a pole. We now turn to what may be termed "recent developments" of RFT to see how Eq. (4.32) emerges.

(d) Recent Developments in the RFT for the Pomeron

In the work of Gribov and Migdal[62-64] it was assumed that the interacting Pomeron has $\Delta=1-\alpha(0)=0$. Because there is no energy gap, one must either sum the full perturbation series to learn the infrared behavior of $\Gamma^{(n,m)}$, or have compelling arguments for any omissions. Faced with this, Gribov and Migdal studied the Schwinger-Dyson equations for the complete proper vertex functions. The solutions they found were therefore not calculated directly from the Lagrangian, Eq. (4.15), but were based on self-consistency conditions.

There is another way to calculate the infrared behavior of the RFT which avoids perturbation theory in the three-$\underset{\sim}{P}$ coupling. This approach uses the constraints of the renormalization group to yield the allowed forms of the $\Gamma^{(n,m)}$ in certain regions of $E_i, \vec{q}_i$ phase space. This approach was used by Migdal, Polyakov, and Ter-Martirosyan, and by Abarbanel and Bronzan.[34] In describing it we will use the notation of the latter authors, although the Soviet results are identical where they overlap.

The philosophy of the renormalization group approach to the study of quantum field theories is described at some length in summer school lectures by Coleman[68] and by Abarbanel.[69] Here we confine ourselves to the outlines and concentrate on the results for the $\underset{\sim}{P}$.

Our RFT has in the Lagrangian of (4.15) four parameters: the scale of the term involving ∂_τ, which is taken to be 1; the slope parameter α_0'; the bare mass gap Δ_0; and the bare coupling constant r_0. When the full proper vertex functions are evaluated they again may be parametrized in terms of four numbers: 1, α', Δ, and r which replace the bare parameters. These four numbers are specified by the value of $\Gamma^{(1,1)}$ and its E and $\vec{q}^2$ derivatives and the value of $\Gamma^{(1,2)}$ at some convenient, but arbitrary, point of $E, \vec{q}$ space. We follow Ref. 34 by taking $E_i \propto -E_N < 0$, and $\vec{q}_i = 0$ as this point. Physics dictates that a change in $E_N \to E_N + \delta E_N$ must have no consequences for the physical content of the RFT. We can compensate for the change in E_N by the substitutions $\alpha' \to \alpha' + \zeta \frac{\delta E_N}{E_N}$, $\Delta \to \Delta + \eta \delta E_N$, $1 \to 1 + \gamma \frac{\delta E_N}{E_N}$, and $r \to r + \tilde{\beta} \delta E_N / E_N$, which are chosen in such a way that the vertex functions computed from our Lagrangian are unchanged.

How is this done in practice? The fields φ which enter the Lagrangian have their scale (normalization) altered by the interaction so that the unrenormalized φ_u becomes

$$\varphi(\vec{x},\tau) = Z^{-\frac{1}{2}}\varphi_u(\vec{x},\tau) \quad , \tag{4.33}$$

while α_0' , Δ_0, and r_0 become α', Δ, and r respectively. The $\Gamma_u^{(n,m)}$ expressed in terms of φ_u are functions of α_0' , Δ_0, r_0 and a possible cutoff to define the integrals in perturbation theory. The $\Gamma^{(n,m)}$ expressed in terms of φ are functions of α', Δ, r and E_N. The relation between them is

$$\Gamma^{(n,m)}(E_i,\vec{q}_i,\alpha',\Delta,r,E_N)=Z^{(n+m)/2}\Gamma_u^{(n,m)}(E_i,\vec{q}_i,\alpha_0',\Delta_0,r_0,\Lambda) \tag{4.34}$$

where Λ represents some form of cutoff. Since $\Gamma_u^{(n,m)}$ has no knowledge of E_N, it must not change when $E_N \to E_N + \delta E_N$. $\Gamma^{(n,m)}$, however, must satisfy

$$\left[E_N \frac{\partial}{\partial E_N} + \tilde{\beta}(r,\alpha') \frac{\partial}{\partial r} + \eta(r,\alpha')\Delta \frac{\partial}{\partial \Delta} + \zeta(r,\alpha') \frac{\partial}{\partial \alpha'} - \frac{(n+m)}{2}\gamma(r,\alpha')\right]\Gamma^{(n,m)}(E_i,\vec{q}_i,\alpha',\Delta,r,E_N) = 0 \quad . \tag{4.35}$$

This clearly puts a constraint on the way the parameters can enter $\Gamma^{(n,m)}$.

The $\underset{\sim}{P}$ problem requires $\Delta=0=1-\alpha(0)$ for the fully interacting $\underset{\sim}{P}$. This, as in the earlier Soviet work, is taken as given and is not derived. Clearly this requirement demands a special relation between α_0', r_0, and Δ_0. We will return to that relation. For the moment, however, we imagine that this relation can be and has been arranged, and continue to seek the consequences of a theory with $\Delta=0$.

The solution to the constraint (4.35) - known as the renormalization group equation - is

$$\Gamma^{(n,m)}(\xi E_i, \vec{q}_i, g, \alpha', E_N) = \Gamma^{(n,m)}(E_i, \vec{q}_i, \tilde{g}(-\log\xi), \tilde{\alpha}'(-\log\xi),$$

$$\cdot \exp \int_{-\log\xi}^{0} \frac{d\xi'}{\xi'} \left[1 - \frac{n+m}{2} \gamma(\tilde{g}(\log\xi'))\right] \quad , \tag{4.36}$$

where we have introduced the dimensionless coupling

$$g = \frac{r}{(\alpha')^{\frac{1}{2}}} E_N^{-\frac{1}{2}} \quad ; \tag{4.37}$$

and the auxiliary functions $\tilde{g}(\eta)$ and $\tilde{\alpha}'(\eta)$ satisfy

$$\frac{d\tilde{g}}{d\eta} = -\beta(\tilde{g}(\eta)) \quad , \quad \tilde{g}(0)=g \tag{4.38}$$

and

$$\frac{1}{\tilde{\alpha}'(\eta)} \frac{d\tilde{\alpha}'(\eta)}{d\eta} = 1 - \frac{\zeta(\tilde{\alpha}'(\eta), \tilde{g}(\eta))}{\tilde{\alpha}'(\eta)} = z(\tilde{g}(\eta)), \qquad \tilde{\alpha}'(0)=\alpha' \tag{4.39}$$

In these we find the crucial function $\beta(g)$ which measures the response of the dimensionless coupling constant to a change in the normalization point.

The utility of the renormalization group approach is now explicit. We want to study $\Gamma(E_i, \vec{q}_i)$ as $E_i \to 0$ or in (4.36) as $\xi \to 0$. This means we need to know $\tilde{g}(\eta)$ as $\eta = -\log\xi \to +\infty$. For this we need to know $\beta(\tilde{g}(\eta))$. The key observation is that if $\beta(g)=0$ at $g=g_1$, say, then $\tilde{g}(\eta)$ approaches g_1 since $d\tilde{g}/d\eta$ vanishes there. Whether $\tilde{g}$ goes to g_1 as $\eta \to \pm\infty$ depends on the slope $\beta_1 = \left.\frac{d\beta}{dg}\right|_{g_1}$ For the infrared, $\eta \to +\infty$, limit, we require $\beta_1 > 0$. In this case

$$\tilde{g}(-\log\xi) = g_1 + (g-g_1)\xi^{\beta_1} \tag{4.40}$$

as $\xi \to 0$.

The $\Gamma^{(n,m)}$ are constrained by Equation (4.36) to then have the form

$$\Gamma^{(n,m)}(E_i,\vec{q}_i,g,\alpha',E_N) = C_\gamma E_N \left(\frac{E_N}{C_{\alpha'}}\right)^{(2-n-m)\frac{1}{2}} \tag{4.41}$$

$$\left(\frac{-E}{E_N}\right)^{1+z(g_1)\frac{(2-n-m)}{2}-\left(\frac{n+m}{2}\right)\gamma(g_1)} \varphi_{n,m}\left(\frac{E_i}{E_N}, \left(\frac{-E}{E_N}\right)^{-z(g_1)} \frac{C_{\alpha'}\vec{q}_i\cdot\vec{q}_j}{E_N}, g_1\right)$$

where

$$E = \sum_{i=1}^{n} E_i \tag{4.42}$$

and C_γ and $C_{\alpha'}$ are some constants while $\varphi_{n,m}$ is an unknown function. For $\Gamma^{(1,1)}$ this means

$$i\Gamma^{(1,1)}(E,\vec{q}^2,g,\alpha',E_N) = \tag{4.43}$$

$$C_\gamma E_N \left(\frac{-E}{E_N}\right)^{1-\gamma(g_1)} \varphi_{1,1}\left(\frac{C_{\alpha'}\vec{q}^2}{E_N}\left(\frac{E_N}{-E}\right)^{z(g_1)}, g_1\right),$$

which is precisely the scaling form suggested in the earlier strong coupling solution.

Now we have to inquire into the possible values of g_1. Suppose $g_1=0$; then the theory is a free theory in the infrared limit and $\gamma(g_1) = 0$ while $z(g_1) = 1$. This is the weak coupling or quasi-stable $\underset{\sim}{P}$. If $g_1 \neq 0$, only the strong coupling solution is chosen. From a

computational point of view, then, the nature of the $\underset{\sim}{P}$ reduces to the study of the zeroes of $\beta(g)$ and the evaluation of $\gamma(g_1)$ and $z(g_1)$. This is a task not much less complicated than solving the full RFT. There are two modes of attack which we know. One is likely to be unreliable; the second is complicated in procedure, but likely to be reliable.

The first technique is to use perturbation theory to learn $\beta(g)$. In lowest order we need the graphs shown in Figure 4.5 and 4.8 which yields

$$\beta(g) = -\frac{(4-D)}{4} g + Kg^3 \quad , \quad K > 0 \ , \tag{4.44}$$

when the phase space has D space dimensions. This $\beta(g)$ has a zero with positive slope at

$$g_1^2 = \frac{4-D}{4K} \quad . \tag{4.45}$$

If $D \approx 4$, then g_1 would be very small and having evaluated only the lowest graphs for $\beta(g)$ would be extremely reliable. Physics requires D=2, however and the accuracy of keeping only these graphs is at best problematic.

Indeed, only the graphs shown lead to

$$-\gamma(g_1) = +1/6 \approx 0.17 \ , \tag{4.46}$$

and

$$z(g_1) = 13/12 \approx 1.08 \tag{4.47}$$

for D=2. To next order in an expansion in 4-D it is found that[70,71]

$$-\gamma(g_1) = \left(\frac{4-D}{12}\right) + \left(\frac{4-D}{12}\right)^2 \left[\frac{257}{12} \log \frac{4}{3} + \frac{37}{24}\right] + \ldots \qquad (4.48)$$

and

$$z(g_1) = 1 + \left(\frac{4-D}{12}\right) \frac{1}{2} + \left(\frac{4-D}{12}\right)^2 \left[\frac{155}{24} \log \frac{4}{3} + \frac{79}{48}\right] + \ldots \qquad (4.49)$$

or

$$-\gamma(g_1) \approx 0.38 \ , \qquad (4.50)$$

and

$$z(g_1) \approx 1.18 \ . \qquad (4.51)$$

It would seem, therefore, that this series in 4-D or equivalently in g_1^2 is unreliable at 4-D = 2. Such series expansions are employed in statistical physics for the critical indices in second order phase transitions. It is possible that the $0((4-D)^3)$ terms might be small, but we know no way to be sure except by direct (laborious) calculation. From this procedure, then, one has definite, albeit unreliable, values for γ and z.

If one reformulates RFT on a lattice, then one can envision using techniques developed in statistical mechanics to evaluate γ and z directly in two-dimensions.[72-74] It has been possible to show that if there is an infra-red stable fixed point of the type discussed above, $-\gamma \leq z \leq 2$; so the Froissart bound is satisfied and $\sigma_{el} \leq \sigma_{tot.}$[74] Numerical calculations of γ and z are presently in progress.[72-74]

Here let us comment on the physical implications of the existence of a zero of $\beta(g)$ at $g_1 \neq 0$. First of all, of course, we have the scaling form which is similar to the strong coupling

solution of Gribov and Migdal.[64] Indeed, the weak coupling or quasi-stable $\underset{\sim}{P}$ would appear to be out. There is a very significant difference, however, since in the present solution $\Gamma^{(1,1)}$ is not equal to $-\Sigma$, but has the value $-\sigma$, where σ is small, as in (4.32). By computation, the problem of negative total cross sections does not arise. Second, even though the bare Pomeron pole is extinguished there is a moving pole, on the trajectory

$$\alpha(t) = 1 + Ct^{1/z(g_1)} \quad . \tag{4.52}$$

This can be shown either by a perturbative evaluation of $\varphi_{1,1}$,[25,34] or by a more accurate evaluation using the full power of the renormalization group.[60] In either evaluation of $z(g_1)$ given above, $z(g_1) > 1$, so any trajectory has a cusp at t=0. Third, when one couples particles back into the theory, one finds a hierarchy of contributions to $\sigma_T^{AB}(s)$ for A+B → anything (see Figure 4.9):

$$\sigma_T^{AB}(s) \underset{s\to\infty}{\sim} g_A g_B \, (\log s)^{-\gamma(g_1)} \tag{4.53}$$

$$- f_{AB}(\log s)^{-1} + k_{AB}(\log s)^{-2+\gamma(g_1)} + \ldots$$

It is important to note that the dominance, by powers of logs, of the generalized "pole" graph of Figure 4.9a, yields a <u>factorized asymptotic total cross section</u>. Since $-\gamma(g_1) > 0$, <u>this cross section rises</u>.

(e) Secondary Trajectories and Multi-Pomeron Corrections

Having in hand a theory of the $\underset{\sim}{P}$ by itself it becomes quite natural to ask what will be the structure of partial wave amplitudes with quantum number exchange or, like the $\underset{\sim}{P}'$, with $\alpha(0)<1$. This has direct application to experimental fact in the case of the ρ trajectory with $\alpha_\rho(0) \approx 1/2$ since experiments on $\pi^- p \to \pi^0 n$ for a large range of incident beam momentum show an s and t dependence consistent with the exchange of a simple ρ Regge pole with trajectory[7]

$$\alpha_\rho(t) = \frac{1}{2} + t/\left(\frac{GeV}{c}\right)^2 \quad . \tag{4.54}$$

Also in the case of Fermion trajectories there is the long standing problem of parity doublets - we will come to this.

Since the exchange of any Reggeon with $\alpha_R(0) < 1$ requires an energy gap $E(0) = 1-\alpha_R(0) > 0$, the important processes which determine the singularity near $J = \alpha_R(0)$ are one Reggeon-multiple $\underset{\sim}{P}$ exchanges. All such processes have an infinite number of thresholds at $E=1-\alpha_R(0)$. If we restrict ourselves to triple couplings by phase space or simplicity arguments, then only graphs such as Figure 4.10 will occur and we have two couplings: r_0 from our earlier work and a Reggeon-Reggeon-$\underset{\sim}{P}$ (RR$\underset{\sim}{P}$) coupling which must be pure imaginary for the same signature reason. Because Reggeons with $\alpha_R(0) < 1$ are to occur only once, their number operator is conserved and we may solve for the coupled $\underset{\sim}{P}$-Reggeon Green's functions as all $\underset{\sim}{P}$ energies $= 1-J_i \to 0$ and all shifted Reggeon energies $\varepsilon_i = \alpha_R(0)-J_i \to 0$.

First we consider the case of Boson trajectories ($\underset{\sim}{P}$, A_2, ρ, ω, or what have you). This was studied in the early Soviet work by Gribov, Lenin and Migdal.[75] They rather casually treated the ratio of slopes for the $\underset{\sim}{P}$ and Reggeon and neglected the triple $\underset{\sim}{P}$ coupling altogether. This latter point is certainly in the spirit of the quasi-stable $\underset{\sim}{P}$. They found that by using a "Ward identity" they were able to determine almost on dimensional grounds that an originally linear Reggeon trajectory

$$\alpha_{R0}(t) = \alpha_{R0} + \alpha'_{R0}\, t \tag{4.55}$$

was strongly modified by the $RR\underset{\sim}{P}$ interaction to

$$\alpha_R(t) = \alpha_R(0) \pm i\kappa\sqrt{-t} \quad , \tag{4.56}$$

or if there were no $RR\underset{\sim}{P}$ coupling but only a $RR\underset{\sim}{\underset{\sim}{P}}$ quartic coupling, the resulting trajectory was

$$\alpha_R(t) = \alpha_R(0) + \alpha'_R t - Ct/(\log t)^3. \tag{4.57}$$

Both these solutions are at best true in the weak coupling case. In the case of strong coupling no solution was presented.

The renormalization group approach[76] does not presuppose the absence of a triple $\underset{\sim}{P}$ coupling; indeed, it is a crucial element. From a field theory of $\underset{\sim}{P}$'s and Reggeon one finds scaling laws for the Green's functions as before. There turn out to be three zeros of

the beta function for the $\underset{\sim}{P}$-Reggeon vertex which could yield the infrared behavior of the coupled $\underset{\sim}{P}$-Reggeon vertex functions. Two of these yield Reggeon trajectories which have cusps at t=0. One gives a linear trajectory, with renormalized intercept and slope, near t=0

$$\alpha_R(t) = \alpha_R(0) + \alpha_R' t + 0(t^2) \tag{4.58}$$

which in light of the experimental facts on πN charge exchange is an attractive result. The amplitude, for charge exchange for example, would read in this last case

$$T_{AB\to A'B'}(s,t) \underset{\substack{s\to\infty \\ t\ \text{small}}}{=} g_{AA'R}(t) g_{BB'R}(t)\ s^{\alpha_R(t)} \cdot (e^{-i\pi\alpha_R(t)} + \tau_R)(\log s)^{-\gamma_R} , \tag{4.59}$$

where τ_R is the Reggeon signature and $\alpha_R(t)$ is given in (4.58). The index γ_R is in the expansion about D=4 described above

$$-\gamma_R = 1/12 \quad . \tag{4.60}$$

In any case it is not unreasonable to expect γ_R to be small in magnitude. This leaves the result of the boson trajectory with all $\underset{\sim}{P}$ corrections in fine shape as far as experiment goes. It is quite surprising that the collision of all the multiple $\underset{\sim}{P}$ cuts has so mild an effect.

The problem of Fermion trajectories is enormously more complicated in detail although it conceptually is the same as the boson secondary trajectory.[77] The key experimental fact is

that fermion trajectories are essentially linear in the Mandelstam variable u appropriate for backward scattering

$$\alpha_F(u) = \alpha_F(0) + \alpha_F' u \ , \tag{4.61}$$

and since both positive and negative parity trajectories must be present to maintain the Mandelstam analyticity of the scattering amplitude, both trajectories would seem to be present. Only trajectories carrying either positive or negative parity are known; never, both. A successful theory of Fermion trajectories must, therefore, avoid these parity doublets.

Starting with the standard $\underset{\sim}{P}$ theory described before and positive and negative parity trajectories of the form

$$\alpha_F(0) \pm \beta_0' \sqrt{u} + \alpha_{0F}' u \ , \tag{4.62}$$

one finds, through the usual renormalization group procedure, a renormalized trajectory almost linear in u. Furthermore for $u < 0$ in the scattering region both parity poles are on the physical sheet of the J plane. For $u > 0$ in the regime where particles lie on the Regge trajectories, one of the parity partners slips onto an unphysical sheet through the $\underset{\sim}{P}$-F cuts. Both important observed properties of fermion trajectories are thus achieved. An "unnatural" aspect of the treatment of fermion trajectories is that the fixed points in the space of coupling constants are only conditionally stable. This means that the results we have stated only if there is a certain relation among the couplings and slopes.

The results of the calculations of the multiple $\underset{\sim}{P}$ corrections to secondary trajectories, by their accord with observed facts give support to the solution to the $\underset{\sim}{P}$ problem by itself. To test any of these in detail is difficult because of the present uncertainties in the actual values of the indices such as γ, not even to mention the experimental problems in differentiating among various variations in log s. Clearly the whole package has an attractiveness and coherence which is quite pleasing.

(f) Higher Point $\underset{\sim}{P}$ Couplings

In setting up the RFT as summarized in the Lagrange function (4.15) we briefly discussed and then ignored four and more point $\underset{\sim}{P}$ couplings as well as derivative couplings. An heuristic argument based on phase space was given for this. It is possible to make a stronger case. Within the context of the weak coupling or quasi-stable $\underset{\sim}{P}$, Gribov and Migdal were able to use ordinary perturbation theory to evaluate corrections to their leading $\underset{\sim}{P}$ structure.[62] Here the phase space arguments are both correct and persuasive. Typical of the results obtained are the corrections to the inverse propagator as given in (4.25) where a linear trajectory is modified by a $t^2 \log t$ correction - a harmless addition.

In the case of the latter day renormalization group strong coupling solution, as discussed above, the problem is again non-perturbative. Migdal, Polyakov and Ter-Martirosyan gave a number of arguments why four point and higher and derivative couplings would become negligible in the infrared limit.[25] Abarbanel and Bronzan showed that when the triple $\underset{\sim}{P}$ coupling vanishes, the fixed

value of the renormalized four $\underset{\sim}{P}$ coupling is zero, so that the $\underset{\sim}{P}$ is weak coupling.[78] This is consistent with the notion of a dominant triple $\underset{\sim}{P}$ coupling.

Finally Brower and Ellis demonstrated that the simplest derivative couplings were harmless in the infrared limit.[79] Basically the task of each of these calculations was to show that the effective coupling constants, like the $\tilde{g}(\eta)$ of the three $\underset{\sim}{P}$ case, for higher point or derivative couplings were driven to zero in the infrared limit while the triple $\underset{\sim}{P}$ coupling approached the same zero g_1 of $\beta(g)$. In short, both the stability of the original calculation and the ignorability of higher order couplings - all in the infrared limit - were suggested by these exercises.

A much more complete treatment of this matter was given by Jengo and Calucci.[80,81] They considered, at once, an infinite set of n $\underset{\sim}{P}$ couplings, n = 3,4,...., and all derivative couplings. If the $E_i, \vec{q}_i$ phase space integrals were always extended to infinity, then such a theory would certainly be non-renormalizable. However, since we are here involved with an infrared phenomenon it is natural to introduce a cut-off. As we discussed in Section II such a cut-off is almost certainly required to consistently extract the RFT from an underlying theory. The action of this theory is

$$A = \int d\tau d^2x \Big\{ \Big[\frac{i}{2} \varphi^\dagger \overleftrightarrow{\partial}_\tau \varphi - \alpha_0' \nabla\varphi^\dagger \cdot \nabla\varphi - \Delta_0 \varphi^\dagger\varphi - \alpha_0'' (\nabla^2\varphi^\dagger)(\nabla^2\varphi) + \ldots \Big] - i \Big[\frac{r_0}{2} (\varphi^\dagger + \varphi)(\varphi^\dagger\varphi) + \frac{r_0'}{2} (\varphi^{\dagger 2}\nabla^2\varphi + \varphi^2\nabla^2\varphi^\dagger) + \ldots$$
$$- \frac{\lambda_0}{(2!)^2} \varphi^{\dagger 2}\varphi^2 + \frac{\lambda_1}{3!}(\varphi^{\dagger 3}\varphi + \varphi^3\varphi^\dagger) + \frac{\lambda_2}{(2!)^2}(\varphi^{\dagger 2}\nabla^2\varphi + \varphi^2\nabla^2\varphi^\dagger) + \ldots$$
$$+ \ldots . \qquad (4.63)$$

with the prescription that in momentum space all integrals are to be cutoff at $|\vec{q}_i| = \Lambda$, $|E_i| = \alpha_0' \Lambda^2$. The infrared behavior of the theory ought to be independent of the cutoff Λ. Now one scales the cutoffs to $|\vec{q}_i| = \Lambda/A$, $|E_i| = \alpha_0' \Lambda^2/B$ and expresses the scaled theory in terms of new constants $\tilde{\alpha}_0'$, $\tilde{\Delta}_0$, $\tilde{\alpha}_0''$, $\tilde{r}_0$, etc. which are functions of A, B, α_0' , Δ_0 , ... (Scaling the cutoffs, as indicated above, is equivalent to holding the cutoffs fixed and scaling momenta and energies; thus A or B play the role of ξ in (4.36).)

Carrying out this procedure it is found that if one only requires $\tilde{\Delta}_0$ to be stable at zero, that is, α_0=1, then the renormalization group strong coupling solution is reproduced with all couplings except $\tilde{r}_0$, the three $\underset{\sim}{P}$ coupling, going to zero in the infrared limit. If one puts further constraints on the couplings, then it is possible to find other solutions to the RFT including, strikingly enough, the quasi-stable $\underset{\sim}{P}$. To achieve that, however one must essentially require that r_0, be specially chosen so that it maps into zero under the scalings of the cutoff. From the point of view of physics there is no special motivation to further constrain the theory in this way. Indeed, if we do so and launch upon the pathway of the quasi-stable $\underset{\sim}{P}$, then we are plagued with the various decouplings of $\underset{\sim}{P}$. This rather general treatment of all couplings at once provides a posterori support for the model Lagrangian of (4.15).

(g) The Formal Status of the RFT

There are two points that are essential to our understanding of the solution of the RFT with the Lagrangian of (4.15) provided by the renormalisation group. Firstly we need to know that the theory is renormalisable in the conventional sense, so that the formalism of the renormalisation group is applicable. In particular we would like to be sure that we can safely set $\Delta=0$, since this is essential to the dimensional analysis used. Secondly we need to know how the theory can be constructed perturbatively since this is the only way we can explicitly check Reggeon unitarity. These two points are not unrelated.

In the original study of the RFT it was found useful to generalise the two space dimensions to D dimensions. There are two reasons for this. Firstly in a general, non-integer number of dimensions all Feynman graphs can be defined by analytic continuation from $D < 2$ the ultra-violet divergences are relegated to poles in the variable D and a simple regularisation procedure is provided in principle by subtracting such poles, with their (real) residues, from the Green's functions in which they occur. However, the RFT is actually super-renormalisable in terms of simple power counting for $D < 4$. This means that the subtraction of the poles has to be equivalent to an intercept (mass) renormalisation and it is not clear then that this subtraction is compatible with the $\Delta=0$ condition.

The second reason for varying D is that at D=4, a clearly unphysical situation, the theory possesses a (broken) scale invariance in separate space, $\vec{x}$, and "time," τ scalings. This manifests itself in the fact that the dimensionless coupling constant, $g = (r/\alpha'^{D/4})E_N^{(D-4)/4}$, has no explicit dependence on the normalisation point E_N. As a consequence there is a zero of $\beta(g)$ at $g_1=0$ which governs the infra-red behavior of the theory. It is this latter fact which motivates the expansion of the theor around D=4 in powers of 4-D.

The poles from the ultra-violet divergences occur at

$$4 - D = \frac{2}{n}, \qquad n = 1,2,.... \tag{4.64}$$

and a series expansion in powers of (4-D) actually hides the poles since

$$\frac{1}{4-D-\frac{2}{n}} = -\frac{n}{2} - \frac{n^2(4-D)}{4} \quad .... \tag{4.65}$$

Therefore the expansion of the theory around D=4 sidesteps the problem of the intercept renormalisation. In fact for D < 4 the problem of the ultra-violet divergences of the theory cannot be separated from the infra-red behaviour if we set $\Delta=0$. The theory cannot be renormalised order by order in perturbation theory. This problem has been studied in detail by Sugar and White, both for the present RFT,[82,83] and for conventional $\lambda\varphi^4$ theories,[82] where the problems are very similar.

The essence of the difficulty is that for $\Delta=0$, the intercept renormalization counter-term, $\delta\Delta$, has the form

$$\delta\Delta = (r_0/\alpha_0'^{D/4})^{4/(4-D)} \quad f(4-D), \tag{4.66}$$

where f is dimensionless. This follows from dimensional analysis only. Clearly $\delta\Delta$ cannot have a power series expansion in r_0, and any perturbative construction of the propagator must necessarily involve a re-ordering of standard perturbation theory. Sugar and White provided such a scheme using renormalization group apparatus. The derivative renormalization condition on $\Gamma_u^{(1,1)}$ is

$$\frac{\partial}{\partial E}\, i\Gamma_u^{(1,1)}(E,0)\Big|_{E=-E_N} = Z(x_N)^{-1} \tag{4.67}$$

where Z is the wave function renormalization constant and

$$x_N = [r_0/\alpha_0'^{D/4}]^{4/(4-D)}\, E_N^{-1} \quad . \tag{4.68}$$

Eq. (4.67) can be integrated to give

$$i\Gamma_u^{(1,1)}(E,0) = -E_N x_N \int_x^\infty dx_N\, x_N^{-2}\, Z(x_N)^{-1} \tag{4.69}$$

with $x=x_N E_N/(-E)$. When this integral representation is combined with the formulae

$$Z(g) = \exp\left[\int_0^g dg'\, \gamma(g')/\beta(g')\right] \tag{4.70}$$

$$(r_0/\alpha'^{D/4})\, E^{(D-4)/4} = g\, \exp\left[-\int_0^g dg'\, (g'^{-1} + \tfrac{\epsilon}{4}\beta(g')^{-1})\right]$$

which are fairly easily derived from the renormalization group equations, we obtain a complete set of equations for calculating $\Gamma^{1,1}(E,0)$ given $\gamma(g$ and $\beta(g)$. Provided that $\beta(g)$ has a zero with positive slope this set of equations solves all of the above problems. The infra-red behavior of $\Gamma_u^{(1,1)}$ follows immediately and when the representation of $\Gamma_u^{(1,1)}$ is compared with perturbation theory we find

$$\delta\Delta = (r_0/\alpha_0'^{D/4})^{4/(4-D)} \int_0^\infty dx_N \, x_N^{-2}[1-Z(x_N)^{-1}] \qquad (4.71)$$

which does indeed contain all of the ultra-violet poles (as divergences at $x_N=0$). When the equations are generalised to non-zero $\vec{q}^2$ they can be combined with perturbation theory for $\Gamma^{(1,2)}$ to provide a complete iterative scheme for constructing $\Gamma^{(1,1)}$ in such a way that it always satisfies $\Delta=0$ and has the correct infra-red scaling behavior.

Finally the representation of $\Gamma^{(1,1)}(E,\vec{q}^2)$ allows us to show that perturbation theory can be used for large $(-E)$ and $(-\vec{q}^2)$ showing that $\Gamma^{(1,1)}(E,\vec{q}^2)$ has a leading $\underset{\sim}{P}$ pole and Reggeon unitarity is satisfied.

Note also that when the representation of $\delta\Delta$ is modified to allow for the presence of a cut-off it can be shown that $\delta\Delta$ is positive and so (to the extent that higher $\underset{\sim}{P}$ couplings can be ignored) we must have $\alpha_0 > 1$ to obtain a renormalised intercept at one. In this case each term of the perturbation expansion will appear to violate the Froissart bound, even though the sum respects it.

(h) Ideas about $\alpha_0 > 1$

We have seen that the requirement $\Delta=0$ is met only if Δ_0, r_0 and α_0' are related in a special manner. Since this relationship is not automatically satisfied, the requirement $\Delta=0$ might be termed "unnatural" even though it is indicated experimentally. One alternative to this situation is to ask what happens when Δ_0 becomes arbitrarily large and negative. In model calculations in which an infinite set of cuts is summed, the Froissart bound is not violated, even though every individual cut violates the bound.[26,27] Instead, the new "$\underset{\sim}{P}$" is a pair of branch points at

$$\alpha(t) = 1 \pm 2[\alpha_0'(\alpha_0 - t)t]^{\frac{1}{2}} \quad . \tag{4.72}$$

The "$\underset{\sim}{P}$" resembles the Pomeron of the Regge-eikonal model[29,33] in some some respects. It comes from a pole with $\alpha_0 > 1$, and in impact parameter space it is a disk whose radius grows like $\ell n s$. However, the disk is gray, not black, and total cross sections factorize in the high energy limit rather than approaching a common value. $\sigma_T(s) \sim (\ell n s)^2$ has the maximum rate of increase allowed by the Froissart bound. This seems to be fortuitous because s-channel unitarity is not imposed in RFT.

On the other hand, it may not be accidental that it is impossible to have a renormalized $\Delta < 0 (\alpha > 1)$ within the RFT, even though s-channel unitarity is not explicitly imposed. $\Delta < 0$ represents a negative mass gap, which is akin to a negative $(\text{mass})^2$ in relativistic field theory. Putting $\Delta_0 < 0$ makes perturbation theory around $\varphi=0$ unstable in much the same manner as so-called spontaneous symmetry breaking in conventional field theory. This means one must shift the field φ to a minimum of the field potential and compute corrections about that.[84,85] The result of such a shift is to produce another Lagrange density where the terms quadratic in the oscillating field, call it χ, are

$$\mathcal{L}_\chi = \frac{i}{2}\chi^\dagger \overleftrightarrow{\partial_\tau}\chi - \alpha_0'\nabla\chi^\dagger\cdot\nabla\chi - \eta_0\chi^\dagger\chi - a_0(\chi^{\dagger 2}+\chi^2) \quad , \tag{4.73}$$

where a_0 and η_0 are proportional to $-\Delta_0$ and depend in detail on the Lagrangian before shifting. This new "free" Lagrangian has $E(\vec{q})$ spectrum

$$E(\vec{q})^2 = (1-\alpha(\vec{q}))^2 = (\eta_0+\alpha_0'\vec{q}^2)^2 - 4a_0^2 \tag{4.74}$$

where when $\eta_0 = 2a_0$,

$$\alpha(\vec{q}) = 1 \pm 2\sqrt{\alpha_0' a_0 \vec{q}^2} \tag{4.75}$$

for small $\vec{q}^2$. This, in general features, resembles the results of Refs. 26 and 27.

The more general problem of why $\Delta=0$ or how one can incorporate it in a "natural" way into the RFT remains open and inviting.

(i) Other "Weak Coupling" Ideas

The idea that the solution to our RFT is strong coupling in the infrared limit, namely $\beta(g_1)=0$, $g_1\neq 0$, has certain unattractive features from an aesthetic point of view even though the physics is certainly sound. The reasoning is more or less that since we had to begin our RFT by a choice of bare trajectory correct near $J=1$ and $t=0$ it is perhaps discomforting that we did not reproduce that singularity after summing all graphs. To do so would require that the $\beta(g)$ for the RFT must have a zero at $g=0$ which governs the infrared behavior, for then all Green's functions become the original Green's functions plus small corrections. Such a RFT could be said to bootstrap itself near E_i, $\vec{q}_i \to 0$. Some examples of such theories have been given by Abarbanel.[86] One which has the scaling form similar to the Moscow-Batavia strong coupling theory is

$$G^{(1,1)}(E,\vec{q}^2)^{-1} = E^p\left(1 + \frac{a_0\vec{q}^2}{E^{3p-1}}\right) \quad , \qquad (4.76)$$

where the power p is undetermined. This theory bootstraps itself in the sense stated above when a constant triple $\underset{\sim}{P}$ coupling is present.

A serious fault of these and any other theories which begin with non-linear bare trajectories is that demonstrating that multiparticle t-channel unitarity is satisfied is a difficult task. It should be recalled from Section III that t-channel unitarity is nothing less than the foundation of RFT.

V. INELASTIC PROCESSES IN RFT

In this Section we consider particle production processes in the RFT. This is a very important problem in its own right, and it is crucial for studying the internal consistency of the RFT. In constructing the RFT for the elastic amplitude t-channel unitarity was built in from the start, but the constraints of s-channel unitarity were not. One must verify a posteriori that these constraints are satisfied, and in most cases this requires some information about production processes.

One approach to the problem is to derive RFT rules for the production amplitudes and then use the techniques of Section IV to study their asymptotic behavior. As indicated in Section II, it is difficult to apply Reggeon unitarity to 2-N production amplitudes; however, it has been possible to study the asymptotic behavior of these amplitudes in the multi-Regge region of phase space using the hybrid Feynman diagram procedure. Drummond[87] and Campbell[88] have studied hybrid diagrams which lead to reggeon graphs with one closed loop, and recently Bartels[89] has obtained the rules for a general Reggeon diagram. Here we will briefly discuss the results for the two-to-three amplitude.

First, one must identify the counterparts of the signatured partial wave amplitudes encountered in the elastic process. We refer to the kinematics of Figure 5.1. In the double Regge limit we consider the five point amplitude A_5 with $s_{12}, s_{13}, s_{23} \to \infty$ and $t_1 = Q_1^2$, $t_2 = Q_2^2$, and $\eta_{12} = s_{12}/s_{13}s_{23}$ fixed. When we have Regge poles $\alpha_i(t_i)$ in the t_i channel, study of a hybrid graph as in Figure 5.2 leads to

$$A_5(s_{12},s_{13},s_{23},\eta_{12},t_1,t_2)$$

$$= \beta_1(t_1)\beta_2(t_2)\Big\{ s_{12}^{\alpha_1}\, s_{23}^{\alpha_2-\alpha_1}\, \xi_{\alpha_1}\xi_{\alpha_2-\alpha_1}\, V_1(t_1,t_2,\eta_{12})$$

$$+ s_{12}^{\alpha_2}\, s_{23}^{\alpha_1-\alpha_2}\, \xi_{\alpha_2}\xi_{\alpha_1-\alpha_2}\, V_2(t_1,t_2,\eta_{12})\Big\} \qquad (5.1)$$

with

$$\xi_{\alpha_1-\alpha_2} = \frac{e^{-i\pi(\alpha_1-\alpha_2)} + \tau_1\tau_2}{\sin\pi(\alpha_1-\alpha_2)} \quad .$$

The decomposition of A_5 indicated in Eq. (5.1) is consistent with the Steinman relations, which tell us that A_5 cannot have simultaneous discontinuities in s_{13} and s_{23}. The two particle-Reggeon coupling β is real. The two Reggeon-particle couplings V_i are real and, in models, are analytic at $\eta_{12}=0$. This suggests that the appropriate partial wave amplitudes are the generalizations of V_1 and V_2. It also suggests that one will require two kinds of two Reggeon-particle couplings to build a calculus for evaluating Reggeon cut contributions to the $2 \to 3$ process. These expectations are borne out by the study of more complicated hybrid graphs; for example, those which correspond to the Reggeon graph of Figure 5.3. This and fancier graphs yield the form for A_5

$$A_5 = \int \frac{dJ_1}{2\pi i}\frac{dJ_2}{2\pi i}\Big\{ s_{12}^{J_1}\, s_{23}^{J_2-J_1}\, \xi_{J_1}\xi_{J_2-J_1}\, V_1(J_1,J_2,t_1,t_2,\eta_{12})$$

$$+ s_{12}^{J_2}\, s_{13}^{J_1-J_2}\, \xi_{J_2}\xi_{J_1-J_2}\, V_2(J_1,J_2,t_1,t_2,\eta_{12})\Big\} \quad , \qquad (5.2)$$

in the double Regge limit. The Reggeon graph rules yields V_1 and V_2.

Bartels has generalized the above results to the multiparticle production amplitudes, A_{4+n}.[89] The only new difficulty is that the decomposition of the amplitudes required by the Steinman relations becomes cumbersome. However, for processes in which only the $\underset{\sim}{P}$ singularity is important, one only needs the small E and k^2 behavior of the multiparticle partial wave amplitudes. In this case it sufficies to approximate the bare vertices and coupling functions by constants, and only one independent amplitude enters for each n.

In some cases the analysis of inclusive cross sections is even cleaner than that of exclusive cross sections. For example, the RFT rules for the single particle inclusive cross section in the triple Regge limit have been obtained both from the hybrid graph approach[60] and from the Reggeon unitarity relations.[59] Further work on inclusive cross sections is presently in progress.

Another approach to the s-channel content of a Reggeon calculus has been given by Abramovskii, Gribov and Kanchelli (AGK).[36] They bypass RFT by studying the s-channel absorptive part of two-body amplitudes directly. Since such absorptive parts are immediately related to production processes in the s-channel, we gain directly the information desired. However, one must pay a certain price for this splendid efficiency since it is necessary to specify how one cuts through Reggeons in extracting absorptive parts. The formulation of AGK assumes that the Reggeon, in particular the $\underset{\sim}{P}$ is given by a set of generalized ladder graphs as in Figure 5.4. The cut through this $\underset{\sim}{P}$ is, up to considerations of signature to be treated in a moment, just as in the familiar multiperipheral model shown in Figure 5.5. It gives rise to a uniform distribution in produced

particle rapidity in the central region for single particle inclusive production; it yields multiplicity of produced particles proportional to log s, etc. With cutting rules in hand, one may cut up any given Reggeon graph to find the contribution to the desired s-channel process. Clearly this method is most attractive when only a small number of Reggeon graphs need be treated. As such it lends itself well to the so-called weak coupling $\underset{\sim}{P}$ discussed in the last section. That $\underset{\sim}{P}$ is without terribly high regard at the time of this writing and summation of infinite sets of $\underset{\sim}{P}$ graphs appears rather necessary. These caveats exposed we turn to a description of the AGK cutting rules and some consequences thereof.

Given the rules for cutting a $\underset{\sim}{P}$, AKG argue that the details of the basic production mechanism need not be specified. With the cutting rules they study the effects on the generalized ladder $\underset{\sim}{P}$ arising from multiple $\underset{\sim}{P}$ exchange and from $\underset{\sim}{P}$ interactions. Two low order graphs are shown in Figure 5.6 along with the contributions to production amplitudes generated by cutting them. The features revealed in this manner are absorptive corrections to the ladder-like production amplitude of Figure 5.5, production from more than one (multiperipheral like) chain, and the possibility of large rapidity gaps between produced particles.

One can already make some qualitative statements from Figure 5.6. First, if the average number of particles arising from the exchange of the basic $\underset{\sim}{P}$ is $\bar{n}_1 \approx$ a log s, then $\bar{n}$ from the exchange of k non-interacting $\underset{\sim}{P}$'s will be of order $k\bar{n}_1$. In the absence of $\underset{\sim}{P}$ interactions then, the multiplicity distribution will be as shown in Figure 5.7a with $\sigma_{\bar{n}}/\sigma_{k\bar{n}} \approx (\log s)^{k-1}$. $\underset{\sim}{P}$ interactions will fill in the gaps

and smooth out σ_n to look more like Figure 5.7b. The actual possibility of seeing the peaks in σ_n at $k\bar{n}$ rests on model dependent couplings not estimated by AGK or anyone else. Furthermore production from k independent $\underset{\sim}{P}$'s is expected to give rise to the order of ka particles per unit rapidity interval. In individual events one expects to encounter long range fluctuations in the rapidity distribution. Calculation of fluctuation probabilities have been made by AGK for the weak coupling $\underset{\sim}{P}$.[36]

The detailed cutting rules depend crucially on the observation that for a particular discontinuity to be non-negligible, the cut must go completely through any Reggeon in the graph or not cut it at all. As an example of this consider the cut of the two Reggeon graph of Figures 2.1 and 2.2 as shown in Figure 5.8. In order for it to be interpreted as a cut through a Reggeon the rapidity spread y across the cut lines must be large. In that case the particle line carrying momentum q will have an enormous mass $q^2 = e^y$. However, it is a basic assumption of the hybrid graph approach that any diagram is negligible when a line carries a large mass. For small values of y the cut is interpreted as passing through the Regge vertex functions $N^{(n)}$. This argument applies to any Reggeon diagram, for a partially cut Reggeon leaves a hanging chain and yields an unacceptably large q^2 somewhere.

For diagrams involving the exchange of k non-interacting $\underset{\sim}{P}$'s the analysis is straightforward. The contribution to the amplitude $T(s,\underset{\sim}{q}^2)$ from k $\underset{\sim}{P}$'s is

$$T^{(k)}(s,q_\perp^2) = -i\frac{\pi}{2}s\int \prod_{j=1}^{k} \frac{d^2q_{j\perp}}{(2\pi)^2}\,\delta^2\Big(q_\perp - \sum_{j=1}^{k} q_{j\perp}\Big)$$

$$\cdot N^{(k)}_{\alpha_1\ldots\alpha_k}(q_{1\perp},\ldots q_{k\perp})^2 \prod_{j=1}^{k} \frac{i}{s}\,G_j(s,q_{j\perp}^2) \quad , \tag{5.3}$$

where

$$G_j(s,q_\perp^2) = -\,s^{\alpha_j(q_\perp^2)}\,\frac{e^{-i\frac{\pi}{2}\alpha_j(q_\perp^2)}}{\sin\frac{\pi}{2}\,\alpha_j(q_\perp^2)} \quad . \tag{5.4}$$

Cutting through $N^{(k)}$ should have no effect on them. Recall that $N^{(2)}$ can be written as in Eq. (3.41) as an integral over the Reggeon-particle absorptive part. Since such an absorptive part involves only on-shell intermediate states, cutting does nothing. For $N^{(k)}$, $k > 2$, the argument is more formal, requiring an elaborate excursion into Sudakov land. The conclusion is that cut N's are the same as uncut N's.

The s-channel absorptive part of $T^{(k)}(s,q_\perp^2)$ is now reduced to a combinatorial problem in enumerating the ways of and weights associated with cutting 0, 1, ... k $\underset{\sim}{P}$'s in all possible ways. Take $T^{(2)}(s,q_\perp^2)$ for example:

$$\text{Abs}\,T^{(2)}(s,q_\perp^2) = \frac{\pi}{2s}\int \frac{d^2k_{1\perp}}{(2\pi)^2}\,\frac{d^2k_{2\perp}}{(2\pi)^2}\,\delta^2(q_\perp - k_{1\perp} - k_{2\perp})\,N^2_{\alpha_1,\alpha_2}$$

$$\Big\{[G_1G_2^* + G_2G_1^*] + [\text{Abs}G_1(iG_2)^* + iG_2\text{Abs}G_1 + \text{Abs}G_2(iG_1)^* +$$

$$iG_1\text{Abs}G_2] + [2\text{Abs}G_1\text{Abs}G_2]\Big\} \quad , \tag{5.5}$$

where

$$\text{Abs}G_i = \text{Im}G_i = s^{\alpha_i} \quad . \tag{5.6}$$

The terms in square brackets result respectively from cutting first 0, then 1, and finally 2 $\underset{\sim}{P}$'s. Note that for identical Reggeons the signs and weights of these contributions are +2, -8, and +4 yielding an overall negative two $\underset{\sim}{P}$ cut term in the elastic process.

Diagrams involving only triple $\underset{\sim}{P}$ vertices can also be easily dealt with since cutting across this vertex leaves it unchanged. However, the discontinuity across the general $n\underset{\sim}{P} \rightarrow m\underset{\sim}{P}$ vertex cannot be expressed in terms of the vertex itself when $n_1 m > 1$. As a result in order to calculate individual contributions to s-channel discontinuities from Reggeon diagrams containing such vertices, it is necessary to have greater knowledge of the vertex than is required to evaluate the Reggeon graph itself. (A theory with only triple $\underset{\sim}{P}$ vertices as building blocks for $n \rightarrow m$ transitions is thus quite attractive.)

The cutting rules were employed by AGK in studying single particle inclusive cross sections in the central region. This is the regime of the process $a+b \rightarrow c+X$ where in the center of mass frame of a+b, the rapidity y of c is finite as the rapidity of $a, y_a = \frac{\log s}{2}$ or of $b, y_b = -\frac{\log s}{2}$ grows large. Taking the diagram of Figure 5.9a and cutting it gives the leading contribution to the distribution in y and p_T, the transverse momentum of c:

$$\frac{d\sigma(a+b \rightarrow c+X)}{dyd^2p_T} = g_a g_b f_c(p_T^2)\,\text{Im}G(y_a-y,0)\,\text{Im}G(y-y_b,0) \quad , \tag{5.7}$$

which is precisely the flat rapidity distribution expected when $\alpha(0) = 1$ for the $\underset{\sim}{P}$. Corrections to (5.7) result from Reggeon graphs as in Figures 5.9b and 5.9c. They add up to be proportional to

$$f_c(p_T^2)\left[\frac{1}{(y_a-y)} + \frac{1}{(y-y_b)}\right] \tag{5.8}$$

after a variety of marvelous cancellations.

It is worth emphasizing once again that results like (5.8) are useful only when a small number of Reggeon diagrams make the major contribution to some process. The signal of the weak coupling $\underset{\sim}{P}$, which allows a small number of graphs, is the appearance of corrections as in (5.8) which are only of order $(\text{logs})^{-1}$ or equivalently $(\text{rapidity})^{-1}$.

The corresponding calculations with the strong coupling $\underset{\sim}{P}$ are far more difficult. In this case one must sum an infinite set of cut Reggeon diagrams, and as yet no convincing method has been presented for identifying the ones which make the leading contributions to the inclusive cross section. A start in this direction has been made by the Moscow group,[25] and by Caneschi and Jengo,[90] who consider a theory with both cut and uncut $\underset{\sim}{P}$'s. The Russians argue that the leading contribution to the single particle inclusive cross section is again given by Eq. (5.7) except that G is now to be interpreted as the full $\underset{\sim}{P}$ propagator. For large values of y $\text{Im}G(y,0)$ grows like $y^{-\gamma}$, so in this case the rapidity distribution is not flat.

One of the most important open questions concerning the strong coupling solution of the RFT is whether the constraints

of s-channel unitarity are in fact satisfied. Although a definitive answer cannot be given at the present time, the preliminary indications are very encouraging. First, the Froissart bound in D dimensions requires that

$$\sigma_{tot} \leq c(\log s)^D \quad , \tag{5.9}$$

where c is a constant. The bound is satisfied for small values of ϵ (see eqs. (4.46) and (4.53)), and it will be satisfied at D=2 provided an infra-red stable fixed point exists.[74] The crucial test must await the completion of the direct calculations in two dimensions which are now in progress.[72-74]

A closely related test comes from the calculation of the exclusive cross sections in the multi-Regge region of phase space. Long ago Finkelstein and Kajantie[91] showed that if the $\underset{\sim}{P}$ were a simple pole with intercept one and if the $\underset{\sim}{P}$-$\underset{\sim}{P}$-particle coupling did not vanish at zero momentum transfer, then one was led directly to a violation of the Froissart bound. The Moscow group has repeated this calculation for the strong coupling $\underset{\sim}{P}$ and found[25]

$$\sigma_{n+2} \underset{s\to\infty}{\longrightarrow} c_n (\ln s)^{-\alpha - n\beta} \quad , \tag{5.10}$$

where σ_{n+2} is the cross section to produce n+2 particles, c_n is a constant, and to first order in ϵ

$$\alpha = 2 - \frac{7\epsilon}{12} \tag{5.11}$$

$$\beta = 1 - \frac{\epsilon}{4} \tag{5.12}$$

So, at least for small values of ϵ, there is no Finkelstein-Kajantie disease. The calculation leading to Eq. (5.10) starts with a constant bare $\underset{\sim}{P}$-$\underset{\sim}{P}$-particle vertex functions, but because of the absorptive nature of the $\underset{\sim}{P}$ the renormalized vertex function vanishes when all transverse momenta go to zero. Similarly when one calculates the single particle inclusive cross section in the triple Regge limit,[25,59,60] a constant bare triple $\underset{\sim}{P}$ vertex leads to a renormalized one which vanishes when the momentum transfer does. For small values of ϵ there is no violation of the energy conservation sum rule.

Finally Caneschi and Jengo[90] have calculated the moments of the multiplicity distribution in models with cut and uncut $\underset{\sim}{P}$'s. They find no contradiction with the constraints arising from the positivity of the partial cross sections.

VI. CONCLUSIONS, OUTLOOK AND CRITICAL PROBLEMS

Up to now our discussion has been primarily concerned with the theoretical development of Reggeon field theories rather than with their consequences for phenomenology. There are several reasons for this. First, until the development of the Moscow-Batavia strong coupling solution it was not at all clear that a self-consistent theory of the Pomeron, its self interactions, and its interactions with other Reggeons was available, even in the RFT. It is an exceedingly doubtful business to do phenomenology with so uncertain a foundation. Second, a real feeling for the size of $\underset{\sim}{P}$ interactions has only been available since the study of high energy inclusive processes began at the CERN-ISR and at the Fermi National Accelerator Laboratory. We are not going to attempt here either a review of or a construction of a phenomenology of hadron reactions at very high energies on the basis of RFT, but we will indicate what in our opinion are the lessons we have learned that will play a basic role in any such description of phenomena.

The first issue concerns the size of the triple $\underset{\sim}{P}$ coupling and the energy domain in which it is necessary to sum the full series of $\underset{\sim}{P}$ graphs. We will concentrate on the graphs in Fig. 6.1 which we know will contribute to the dominant term in the total cross section (see Fig. 4.8). The order of magnitude of the corrections to the single $\underset{\sim}{P}$ exchange is set by the dimensionless parameter $g_0 = r_0^2/\alpha_0' E$. In terms of s this means that

$$\frac{r_0^2}{\alpha_0'} \log s \tag{6.1}$$

sets the scale for the convergence of the $\underset{\sim}{P}$ series. The best estimate of the size of the bare triple $\underset{\sim}{P}$ coupling, r_0, comes from the single particle inclusive experiment A + B → A + X (see Fig. 6.2) in the triple Regge region (s, m^2, $s/m^2 \to \infty$ with t fixed). If the triple $\underset{\sim}{P}$ coupling is small, one may use the lowest order term in the $\underset{\sim}{P}$ series to estimate its size. Under this assumption one finds from pp → p + X and pd → d + X data that

$$r_0^2/\alpha_0' \approx \frac{1}{50} \quad , \tag{6.2}$$

and guessing that when $\frac{r_0^2}{\alpha_0'}$ ℓns $\approx \frac{1}{2}$ we will need a large number of terms in the $\underset{\sim}{P}$ series, we learn that

$$\text{logs} \approx 25 \tag{6.3}$$

is where the whole sum given by the Moscow-Batavia scaling solution, will certainly be necessary. Now the logs values available at the CERN-ISR are only 8 or 8.5 at the most, and at FNAL they range up to about 7. At the energies of these devices the full sum of $\underset{\sim}{P}$ graphs would not appear to be necessary. This conclusion is certainly in line with the fashionable phenomenology based on s-channel approaches such as the multiperipheral model, which is motivated by the apparent "short-range rapidity correlation" nature of production processes observed experimentally.

We cannot completely rule out the possibility that the scaling solution is applicable at ISR-FNAL energies. If it were, then in the calculation of the inclusive eross section the quantity r_0^2/α_0' would be replaced by an effective coupling which is independent of r_0.[25] This alternative seems unlikely because we expect this

effective coupling to be of order of magnitude unity; however, this question cannot be fully resolved until we have reliable calculations of the critical exponents and scaling functions in two-dimensions. Work in this direction is presently in progress.

When only a few terms in the $\underset{\sim}{P}$ series are required for a good numerical estimate of the process under study then in the small logs regime one must face squarely the matter of secondary contributions from N $\underset{\sim}{P}$ coupling with N > 3 and from possible derivative couplings. We know of no way to choose among the alternatives which present themselves except by a trial and error approach. However, we are encouraged by the fact that it has been possible to fit the pp, $\bar{p}p$, $\pi^{\pm}p$ and $K^{\pm}p$ elastic scattering data over a wide range of energies with only a few terms in the $\underset{\sim}{P}$ series.[92,93] There is a nice feature to having only a finite number of terms to address. In such a case the AGK construction, even with its need for a specific assumption on the result of cutting $\underset{\sim}{P}$'s,[40] will be a useful tool in relating specific s-channel production processes to the J-plane physics.

Another lesson that we learned in Section IV was that when we required $\Delta = 1-\alpha(0) = 0$, as we desire for the full sum of $\underset{\sim}{P}$ graphs, the bare gap, $\Delta_0 = 1-\alpha_0(0) < 0$, so the bare $\underset{\sim}{P}$ has $\alpha_0(0) > 1$. (Happily the best fits in Refs. 92 and 93 also require $\alpha_0(0) > 1$, with Δ_0 having the right order of magnitude.[94]) In making the estimate in Eq. (6.3) we followed the approach where the perturbation series was developed using propagators with the renormalized intercept gap, $\Delta = 0$. Since we expect the bare $\underset{\sim}{P}$ to be observable at present accelerator

energies, it may be more appropriate to rearrange the perturbation series so that the bare gap enters the propagators. In this case each term in the series violates the Froissart bound, but the sum is constructed to satisfy it. Actually the value of Δ_0 is on the order of 5×10^{-2} which means a very slow growth in s from any $\underset{\sim}{P}$ graph. Taking this effect into account we may boldly imagine that the estimate in Eq. (6.3) is too large by a factor of as much as two. Then the need for the full $\underset{\sim}{P}$ series might set in at $\log s \sim 12\text{-}15$. If this were to be so, the use of the scaling form for the $\underset{\sim}{P}$ propagator might well be an attractive, compact expression to use at finite energies. To really be of use, however, we would again need reliable values of the scaling indices and reliable knowledge of the scaling functions.

Despite our cautious almost pessimistic view toward the utility of a Reggeon calculus phenomenology at the present stage of theoretical development, there have been several attempts at fitting real data. Serious evaluation of these, often attractive, phenomenological essays is difficult. We pass this task on to the reader by providing a few references from which he or she can begin.[92,93,95]

Here we turn our attention to a resumé of the ideas covered in this article and to a cheerful view of the progress achieved in the developments we have reported. We began by recalling the necessity of branch points in the J-plane arising from the combination of moving poles in J with unitarity. We assumed that the only branch points were those coming from the presence of multiple moving poles in the t-channel. This assumption is actually extremely conservative. It resembles almost in detail the experience of many years in locating

the position of branch points in the energy planes arising in conventional field theories. There, of course, one has a variety of dispersion relations and sum rules which allow a direct positive assessment of the validity of this assumption. We are not so fortunate here. We are forced to fall back on the (never entirely convincing, however persuasive and attractive) observation that satisfying t-channel multiparticle unitarity is straightforward and natural when branch points arise via moving poles and difficult, if possible at all, otherwise. Clearly if there are branch points in J arising from other sources, we have missed them.

We next saw how to obtain expressions for the discontinuities across the J-plane cuts from the multiparticle t-channel relations. These Reggeon unitarity relations are crucial for an understanding of the $\underset{\sim}{P}$ near J=1 and t=0 since they lead to strong couplings among the multi-$\underset{\sim}{P}$ channels whose thresholds all collide at this point. In order to insure that the full Reggeon unitarity relations are satisfied, we introduced a field theory to describe the emission, absorption and propagation of Reggeons. The Reggeon field $\varphi(\vec{x},\tau)$ operates in a world with two space and one time dimension. The branch points in the J-plane arise naturally as singularities in the Feynman integrals of the perturbation expansion of the field theory. These singularities represent, as in conventional field theories, thresholds for the production of the quanta (Reggeons) described by φ.

When the renormalized intercept gap vanished, we found that the RFT exhibited infra-red behavior analogous to that of conventional field theories with massless particles. In this case one

could use the renormalization group to study the behavior of the theory near J=1 and t=0. When an infra-red stable fixed point exists, the Reggeon Green's functions and the total and elastic cross-sections satisfy scaling laws which are given in Eqs. (1.4), (1.5), and (4.41). We saw that such a fixed point does exist in $D = 4 - \epsilon$ space dimensions, and attempted to extrapolate to the physically interesting case, D=2.

How are we to view the field $\varphi(\vec{x},\tau)$? Since the Reggeons it describes are composite states of the observed hadrons, it represents some averaged or mean behavior of the underlying hadrons. This mean behavior is likely to be rather independent of the constituent hadrons if the distances $|\vec{x}|$ and "times" τ represented in the field $\varphi(\vec{x},\tau)$ are large compared to the scales of the hadrons. The natural scales for hadrons are $|\vec{x}| \sim (m_{proton})^{-1}$ and $\tau = \log s \approx 1$ when s is measured in units of $(m_{proton})^2$. So for $|\vec{x}| >> (m_{proton})^{-1}$ and $\tau >> 1$, the average field may be expected to be a good representative of the collective behavior of the underlying hadronic matter. Now this translates into small momentum, $|\vec{q}|$, and energy E for the quanta described by the field. This is just the limit where we employed our RFT to learn in detail about $\underset{\sim}{P}$ interactions and amplitudes. In a sense this is very attractive, and in another sense this is terribly disappointing. The latter comes because we are saying that in large s, small t processes we will not be learning about the basic structure of hadrons; indeed, we are averaging over the hadron coordinates in a grand fashion.

There is a very persuasive analogy for this point of view. In many body problems near critical points one describes the free energy of the system in terms of mean fields which average over

large blocks of local, more fundamental coordinates. These mean fields interact; their quanta are emitted, are absorbed, and propagate. They are the clear analogue of our Reggeon field. One never produces the quanta of the mean field as free states outside the medium (electrons and ion cores) which gives them life. One never produces Reggeons as free states outside the medium (particles acting as sources) which gives them life.

At the critical temperature the correlation length for static correlation functions goes to infinity. This as usual, is the signal for a long range interaction mediated by a massless particle. We, too, have a massless excitation called the Pomeron. It provides for infinite range correlations in rapidity, the time dimension. The universality of scaling functions and critical exponents in the theory of second order phase transitions carries over directly into our Reggeon langauge. We, when $\alpha(0) = 1$, sit precisely at the analogue of $T = T_{critical}$. This marvelous universality means that phase transition phenomena near critical points will not teach one about the detailed dynamics underlying the observed phenomena. So, too, are we not learning about the detailed dynamics underlying the Pomeron by studying very large s, small t elastic amplitudes.

This brings us to the first of our critical problems now open for discussion in Reggeon physics; namely, the s-channel content of the theory we have built with quite explicit t-channel unitarity. Since the Reggeons reflect an infinite number of s-channel production processes, there is clearly a rich well of information on the structure of the Reggeons to be plumbed by the detailed study of

s-channel phenomena. We can say this in a language rather well adapted to the view of the generation of long range correlations in rapidity by Reggeon interactions. In the elastic amplitudes which have been the primary concern of our report, one probes the amplitude for a source (two particles) to emit Reggeons and then at a later time (rapidity) for another set of two particles acting as a sink to absorb them (Figure 6.3). In an s-channel production process such as single particle inclusive reactions in the triple Regge region there are three times involved $\log(m_{proton})^2 = 1$, $\log M^2$, and $\log s$. [Fig. 6.4] $_{\Lambda}$ [The energy scale is always $m_{proton} \approx 1$ GeV/c^2.] We, by studying this inclusive process, are probing intermediate times, which requires the Pomeron to reveal some of its short range (in rapidity) structure. Other examples of intermediate time probes will come directly to mind. Each has its counterpart in an s-channel process which is part of the building up of the Reggeons. Study of these many time correlation functions should provide a systematic method to learn how to put together Reggeons. It has the incidental, highly non-trivial attractiveness of discussing experimentally accessible s-channel processes. The elucidation of these s-channel properties is then an issue of the first importance in Reggeon theories.

Another issue, slightly more elusive perhaps, is that of the nature of bare Reggeons. The bare Pomeron is an important example. This is the quantity that is probed at present machine and colliding beam energies. Its structure is sure to reflect the detailed hadron dynamics of whatever theory, one chooses as an attractive candidate.

We haven't really much of an informative nature to say about the building of Reggeons. Despite decades of clever work on the matter, the issue of how hadrons bind to form hadrons and Reggeons remains open and enticing. The importance of the matter clearly transcends the somewhat circumscribed set of problems this report has been able to bring out and, indeed, seems a challenging note on which to finish.

REFERENCES

1. T. Regge, Nuovo Cimento 14, 951 (1959); 18, 947 (1960).
2. G. F. Chew and S. Frautschi, Phys. Rev. Lett. 7, 394 (1961); R. Blankenbecler and M. L. Goldberger, Phys. Rev. 126, 766 (1962).
3. V. N. Gribov, Soviet Physics JETP, 14, 478, 1395 (1962).
4. D. Amati, A. Stanghellini, S. Fubini, Nuovo Cimento 26, 896 (1962), S. Mandelstam, Nuovo Cimento 30, 1113, 1127, 1148 (1963).
6. J. C. Polkinghorne, J. Math. Phys. 4, 1396 (1963).
7. D. J. Mellema et al., Proceedings of the XVII International Conference on High Energy Physics, I-37, J. R. Smith, editor, London (1974). See also V. Barger-Plenary Report on Reaction Mechanisms at High Energy - same proceedings.
8. U. Amaldi et al., Phys. Lett. 44B, 112 (1973).
9. S. R. Amendolia et al., Phys. Lett. 44B, 119 (1973).
10. T. K. Kycia et al., Proceedings of the XVII International Conference on High Energy Physics, I-32, J.R.Smith, editor, London (19
11. A. H. Mueller, Phys. Rev. D2, 2963 (1970).
12. C. I. Tan, Phys. Rev. D4, 2412 (1971).
13. H. P. Stapp, Phys. Rev. D3, 3177 (1971).
14. J. C. Polkinghorne, Nuovo Cimento 7A, 555 (1972).
15. C. E. DeTar, D. Z. Freedman, and G. Veneziano, Phys. Rev. D4, 906 (1971).
16. G. Veneziano, Phys. Lett. 36B, 397 (1971).
17. H. D. I. Abarbanel, G. E. Chew, M. L. Goldberger and L. M. Saunders, Phys. Rev. Lett. 26, 937 (1971).
18. C. E. Jones, F. E. Low, S. H. Tye, G. Veneziano and J. E. Young, Phys. Rev. D6, 1033 (1972).
19. R. C. Brower and J. H. Weis, Phys. Lett. 41B, 631 (1972).

ACKNOWLEDGMENTS

We would like to thank our Reggeon Field Theory colleagues for countless discussions which clarified our thinking on the ideas presented here. Unfortunately they are too numerous to cite individually. We are particularly indebted to Esther Singer for her extraordinary efforts in preparing this manuscript. Finally, three of us, (J. B. B., R. L. S. and A. R. W.) would like to express our appreciation for the hospitality extended to us at Fermilab, where this work was begun.

20. V. N. Gribov, I. Ya. Pomeranchuk and K. A. Ter-Martirosyan, Phys. Rev. 139, B184 (1965).

21. A. R. White, Nucl. Phys. B50, 93, 130 (1972).

22. V. N. Gribov, Soviet Physics, JETP, 26, 414 (1968).

23. P. Goddard and A. R. White, Nuovo Cimento, 1A, 645 (1971).

24. A. R. White, Nucl. Phys. B39, 432, 461 (1972).

25. A. A. Migdal, A. M. Polyakov, K. A. Ter-Martirosyan, Phys. Lett. 48B, 239 (1974), Zh. Eksp. Teor. Fiz. 67, 84 (1974).

26. J. B. Bronzan, Phys. Rev. D9, 2397 (1974).

27. J. L. Cardy, Nucl. Phys. B75, 413 (1974).

28. S. Frautschi and B. Margolis, Nuovo Cimento, 56A, 1155 (1968).

29. H. Cheng and T-T. Wu, Phys. Rev. Lett. 24, 1456 (1970).

30. R. Blankenbecler, J. R. Fulco and R. L. Sugar, Phys. Rev. D9, 736 (1974).

31. G. Calucci, R. Jengo, C. Rebbi, Nuovo Cimento, 4A, 330 (1971), 6A, 601 (1971).

32. R. Aviv, R. Blankenbecler and R. L. Sugar, Phys. Rev. D5, 3252 (1972); S. Auerbach, R. Aviv, R. Blankenbecler and R. L. Sugar, Phys. Rev. D8, 2216 (1972).

33. S. J. Chang and T. M. Yan, Phys. Rev. D4, 537 (1971).

34. H. D. I. Abarbanel and J. B. Bronzan, Phys. Lett. 48B, 345 (1974); Phys. Rev. D9, 2397 (1974).

35. For a review of this subject and further references see J. Kogut and K. G. Wilson, Physics Reports 12C, 77 (1974).

36. V. A. Abramovskii, V. N. Gribov and O. V. Kanchelli, Yad. Fiz. 18, 595 (1973) [Sov. J. Nucl. Phys. 18, 308 (1974)].

37. V. V. Sudakov, Sov. Physics - JETP 3, 65 (1956).

38. Of course, hybrid diagrams corresponding to all possible graphs have not been considered. The general rules are obviously an extrapolation of the results obtained for simple diagrams. An infinite set of diagrams involving four-Reggeon interactions has been considered by P. V. Landshoff and J. C. Polkinghorne, Phys. Rev. 181, 1989 (1968). Again the general rules are confirmed.

39. C. E. DeTar, M.I.T. Preprint, MIT-CTP 421 (1974).

40. A detailed study of these graphs in the weak coupling limit by I. T. Halliday and C. J. Sachrajda, Phys. Rev. D8, 3598 (1973), has shown that there is some simplification and the cutting rules of Ref. 36 hold. There is, however, still some dispute about what s-channel states contribute to the two-Reggeon cut in general. (See T. DeGrand MIT preprint,,1975.)

41. P. D. B. Collins, Physics Reports 1, 104 (1971); Sec. 2.8.

42. R. J. Eden, P. V. Landshoff, D. I. Olive and J. C. Polkinghorne, The Analytic S-Matrix (Cambridge University Press, 1966).

43. J. Coster and H. P. Stapp, Journ. of Math. Phys. 11, 1441 (1970).

44. (3.4) can be obtained directly from (3.3) by diagonalizing the momentum-space integrations using partial-wave projections of the six-point function. The details of this procedure are given in the appendices of Ref. 21.

45. The results directly relevant for our purpose here can be found in Refs. 23 and 24. Other related papers on complex helicity are: C. E. Jones, F. E. Low and J. E. Young, Phys. Rev. D4, 2358 (1971); J. H. Weis, Phys. Rev. D6, 2823 (1972); H. D. I. Abarbanel and A. Schwimmer, Phys. Rev. D6, 3018 (1972); A. R. White, Nucl. Phys. B67, 189 (1973).

46. R. L. Omnes and V. A. Alessandrini, Phys. Rev. 136B, 1137 (1964).

47. Ya. I. Azimov, A. A. Anselm, V. N. Gribov, G. S. Danilov and I. T. Dyatlov, Sov. Phys. JETP 21, 1189 (1965), 22, 383 (1966).

48. I. T. Drummond and G. A. Winbow, Phys. Rev. 161, 1401 (1967).

49. Ya. A. Simonov, JETP 21, 160 (1965).

50. A. R. White, Phys. Rev.D10, 1236 (1974).

51. This procedure for isolating a discontinuity is the conventional one used in S-Matrix theory. In particular it is analogous to that used in non-relativistic scattering theory for finding the discontinuity across the elastic cut in the T-matrix. The analogy is drawn in H. D. I. Abarbanel, Phys. Rev. D10, 2788 (1972) where the two Reggeon cut discontinuity is discussed this way.

52. This observation was first made by V. N. Gribov and A. A. Migdal, Sov. Journ. Nucl. Phys. 8, 583 (1969) on the basis of equation (2.17) which is sometimes referred to as the Gribov-Migdal sum rule. It was first used by A. B. Kaidalov, Sov. J. Nucl. Phys. 13, 226 (1971) and later by others including I. J. Muzinich, F. E. Paige, T. L. Trueman and L. L. Wang, Phys. Rev. D4, 1048 (1972).

53. J. L. Cardy and A. R. White, Nucl. Phys. B80, 12 (1974).

54. H.D.I. Abarbanel, Proceedings of the XVII International Conference on High Energy Physics, I-136, J.R.Smith, editor, London (1974).

55. J. B. Bronzan, Phys. Rev. D4, 1097, 2569 (1971).

56. J. B. Bronzan and C. S. Hui, Phys. Rev. D5, 964 (1972).

57. K. Kang and A. R. White, Phys. Rev. D10, 983 (1974).

58. A complete description of the cross-channel unitarity constraints on multiparticle partial-wave amplitudes together with the related Reggeon unitarity relations will be given in a forthcoming series of papers - A. R. White, in preparation.

59. J. L. Cardy, R. L. Sugar and A. R. White, U. C. Berkeley - Santa Barbara preprint (1974) to be published in Physics Letters.

60. H. D. I. Abarbanel, J. Bartels, J. B. Bronzan and D. Sidhu, to be published.

61. See, for example, R. Oehme, "Complex Angular Momentum in Elementary Particle Scattering," in Strong Interactions and High Energy Physics, pp. 129-222, R. G. Moorhouse, editor (Oliver and Boyd, Edinburgh and London) 1964.

62. V. N. Gribov and A. A. Migdal, Yad. Fiz. 8, 1002 (1968) [Sov. J. Nucl. Phys. 8, 583 (1969)].

63. V. N. Gribov and A. A. Migdal, Yad. Fiz. 8, 1213 (1968) [Sov. J. Nucl. Phys. 8, 703 (1969)].

64. V. N. Gribov and A. A. Migdal, Zh. Eksp. Teor. Fiz. 55, 1498 (1968) [Sov. Phys. JETP 28, 784 (1969)].

65. J. B. Bronzan, Phys. Rev. D7, 480 (1973).

66. V. N. Gribov in Proceedings of the XVI International Conference on High Energy Physics, p. 491, Vol. 3, J. D. Jackson, A. Roberts and R. Donaldson, editors, National Accelerator Laboratory, Batavia, Illinois (1973).

67. J. L. Cardy and A. R. White, Phys. Letters 47B, 445 (1973).

68. S. Coleman, Lectures at the 1970 International Summer School of Physics Ettore Majorana.

69. H. D. I. Abarbanel, Proceedings of Summer Institute on Particle Physics, Vol. I, p. 399, SLAC PUB-179, 1974.

70. M. Baker, Phys. Letters 51B, 158 (1974); and Moscow (ITEP) preprint.

71. J. B. Bronzan and J. W. Dash, Phys. Letters 51B, 496 (1974), and Phys. Rev. D10, 4208 (1974).

72. R. C. Brower, J. Ellis, R. Savit and W. J. Zakrzewski, "Reggeon Field Theory on a Lattice: A Formulation," CERN preprint TH.1973 (February, 1975).

73. J. Ellis and R. Savit, "Phase Transitions and the High Temperature Expansion for the Reggeon Calculus," CERN preprint TH.1974 (March, 1975).

74. J. L. Cardy and R. L. Sugar, "Reggeon Field Theory on a Lattice, I", UCSB preprint (March 1975).

75. V. N. Gribov, E. M. Levin and A. A. Migdal, Yad. Fiz. 12, 173 (1970) [Sov. J. Nucl. Phys. 12, 93 (1971)].

76. H. D. I. Abarbanel and R. L. Sugar, Phys. Rev. D10, 721 (1974).

77. J. Bartels and R. Savit, Fermilab preprints FNAL-Pub-74/60-THY and FNAL-Pub-74/61-THY.

78. H. D. I. Abarbanel and J. B. Bronzan, Phys. Rev. D9, 3304 (1974).

79. R. C. Brower and J. Ellis, Phys. Lett. 51B, 242 (1974).

80. R. Jengo, Phys. Letters 51B, 143 (1974).

81. G. Calucci and R. Jengo, Nucl. Phys. B84, 413 (1975).

82. R. L. Sugar and A. R. White, Phys. Rev. D10, 4063 (1974).

83. R. L. Sugar and A. R. White, Phys. Rev. D10, 4074 (1974).

84. H. D. I. Abarbanel, Phys. Letters 49B, 61 (1974).

85. S. S. Pinsky and V. Rabl, Ohio State University preprint COO-1545-140 (1974).

86. H. D. I. Abarbanel, Fermilab preprint NAL-Pub-74/42-THY (1974).

87. I. T. Drummond, Phys. Rev. 176, 2003 (1968).

88. D. K. Campbell, Phys. Rev. 188, 2471 (1969).

89. J. Bartels, Fermilab-Pub. 74/94-THY and 74/95-THY.

90. L. Caneschi and R. Jengo, CERN preprint, TH. 1939-CERN (1974).

91. J. Finkelstein and K. Kajantie, Phys. Lett. 26B, 305 (1968); Nuovo Cimento 56A, 659 (1968).

92. P. D. B. Collins, F. D. Gault and A. Martin, Nuc. Phys. B83, 241 (1974).

93. A. Capella and J. Kaplan, Phys. Lett. 52B, 448 (1974).

94. A. R. White, Proceedings of the SLAC Summer Institute on Strong Interactions, August (1974).

95. N. S. Craige and G. Preparata, Phys. Lett. 45B, 487 (1973); C. Pajares and D. Schiff, Nuovo Cim. Lett. 8, 237 (1973); J. N. Ng and V. P. Sukhatme, Nuc. Phys. B55, 253 (1973); P. D. B. Collins, F. D. Gault and A. Martin, Phys. Lett. 47B, 171 (1973); Nuc. Phys. B80, 135 (1974).

FIGURE CAPTIONS

Figure 1.1 Exchange of a Regge pole in an elastic process giving rise to $s^{\alpha(t)}$ behavior of the elastic amplitude $T_{AB}(s,t)$. The residue of the pole factorizes.

Figure 1.2 Exchange of N Regge poles with trajectory $\alpha(t)$ giving rise to a branch point at $\alpha^{(N)}(t)-1=N[\alpha(t/N^2)-1]$.

Figure 1.3 The dominant term in the solution to RFT which sums all the multi-$\underset{\sim}{P}$ cuts.

Figure 2.1 The hybrid Feynman graph which produces the two Reggon cut contribution to the elastic process $p_1 + p_2 \to p_1' + p_2'$ at large $s = (p_1 + p_2)^2$, fixed $t = (p_1 - p_1')^2$. The blobs represent generalized ladder graphs and have power behavior in their sub-energies; for example, $f_1 \approx [(k_1 + k_2)^2]^{\alpha_1(k^2)}$. All momentum transfers and particle masses are presumed to remain $\lesssim m^2$, some characteristic finite mass, in the dominant region of integration.

Figure 2.2 The Reggeon graph contribution to the t-channel partial wave amplitude coming from the hybrid graph of Figure 2.1. N is a two particle-two Reggeon transition amplitude; G is a Reggeon propagator. See Eq. (2.14)

Figure 2.3 A hybrid Feynman graph which gives a three Reggeon cut contribution to $F(J,q_\perp^2)$.

Figure 2.4 The Reggeon graph which comes from the hybrid Feynman graph of Fig. 2.3.

Figure 2.5 A hybrid Feynman graph which introduces Reggeon interactions.

Figure 2.6 The Reggeon graph contribution to $F(J_1 q_\perp^2)$ from the hybrid Feynman diagram of Fig. 2.5. The triple Reggeon coupling $r_{\alpha_1\alpha_2\alpha_3}$ appears here.

Figure 2.7 The simplest contribution to the triple Reggeon coupling $r_{\alpha_1\alpha_2\alpha_3}$. This will appear as a building block in more complicated Reggeon graphs.

Figure 2.3 A hybrid Feynman graph which gives a three Reggeon cut contribution to $F(J, q_\perp^2)$.

Figure 2.4 The Reggeon graph which comes from the hybrid Feynman graph of Fig. 2.3.

Figure 3.1 (a) A planar Feynman graph with two Reggeons, represented by ladders, in the t-channel. This planar graph does not give rise to a branch point in the J-plane at $\alpha^{(2)}(t)$, Eq. (1.2).

(b) The simplest non-planar Feynman graph which does yield the two Reggeon branch point.

Figure 3.2 (a) A planar Feynman graph with one particle and one Reggeon in the t-channel. This planar graph does not give rise to a branch point in J.

(b) The simplest non-planar graph which does give a Reggeon-particle branch point in J. It is the presence of a left and right right hand cut in the sub-energy s_1 which guarantees the existence of the cut. This Reggeon-particle cut is shielded by the

two Reggeon cut (Fig. 3.1b) in the scattering region, $t \leq 0$.

Figure 3.3 The two particle → one particle + Reggeon graph which is contained in the two particle → three particle amplitude. The Reggeon is represented by a ladder.

Figure 3.4 The path of continuation in the t-plane to reach the amplitude ⊐④⊏ needed in the unitarity formula Eq. (3.3).

Figure 3.5 A set of variables for the partial wave projection of the 2 → 4 amplitude needed in the study of the four particle contribution to the partial wave unitarity relation. J is angular momentum and n is helicity.

Figure 3.6 The contour in the helicity plane required in Eq. (3.8) for the four particle contribution to partial wave unitarity.

Figure 3.7 The t_1 or t_2 plane in the four particle phase space showing how the t_i integration is deformed to enclose the two particle threshold.

Figure 3.8 The position of the factors in Eq. (3.22) in the t_1, t_2 plane. The intersection of $\lambda(t,t_1,t_2)$ and $J - \alpha_1(t_1) - \alpha_2(t_2) + 1$ gives rise to the branch point at $J = \alpha_c(t)$.

Figure 3.9 The two Reggeon → two Reggeon amplitude $M_{\underset{\sim}{\alpha},\underset{\sim}{\alpha}'}(J,t)$.

Figure 3.10 The two particle → two Reggeon amplitude. The net helicity in the t-channel is $\alpha_1(t_1) + \alpha_2(t_2)$.

Figure 3.11 The single particle inclusive process in the limit $s \to \infty$, t, M^2 fixed. The Reggeon-particle absorptive part $\mathrm{Im}A_{\underset{\sim}{\alpha}}(M^2,0)$ is measured here.

Figure 3.12 The discontinuity across the two Reggeon cut in the particle partial wave amplitude $F(E = 1-J, t = -|\vec{q}|^2)$. The vertical dotted line across the blob in the left hand part of the figure indicates a discontinuity in E for fixed $\vec{q}$ has been taken. In the right half of the figure the Reggeons carrying two momentum $\vec{q}_i$ are "on-shell" and thus have "energy" equal to $1 - \alpha_i(\vec{q}_i)$. The vertical dotted line indicates this.

Figure 3.13 The angular momentum (J_i) and helicity (n_i) and mass (t_i) configuration used in studying the six particle contribution to the partial wave amplitude. This is the way to study the three Reggeon cut generated at $J = \alpha_1(t_1) + \alpha_2(t_2) + \alpha_3(t_3) - 2$.

Figure 4.1 Four $\underset{\sim}{P}$ couplings allowed in a RFT of $\underset{\sim}{P}$'s. They are abstracted from hybrid Feynman graphs, or the multiperipheral model, or any theory having Regge poles.

Figure 4.2 A Reggeon graph contribution to the elastic particle amplitude. This contains the two $\underset{\sim}{P}$ cut and must contribute negatively to the total cross section. We arrange this by writing the triple $\underset{\sim}{P}$ coupling to be purely imaginary = ir.

Figure 4.3 The notation for a n→m Reggeon Green's function.

Figure 4.4 The Schwinger-Dyson equation for the Pomeron proper self energy. $G^{(1,1)}$ is the full $\underset{\sim}{P}$ propagator and $\Gamma^{(1,2)}$ is the triple $\underset{\sim}{P}$ proper vertex function.

Figure 4.5 The graphical representation of the triple $\underset{\sim}{P}$ vertex function $\Gamma^{(1,2)}$.

Figure 4.6 The integral equation for the triple $\underset{\sim}{P}$ vertex function. $V^{(2,2)}$ is the two $\underset{\sim}{P}$ irreducible Bethe-Salpeter kernel.

Figure 4.7 The lowest order contributions to $V^{(2,2)}$.

Figure 4.8 The lowest order contributions to $\Gamma^{(1,1)}$.

Figure 4.9 The hierarchy of contributions to the total cross section for A+B→ anything coming from the strong coupling, scaling solution to the Pomeron RFT. γ is the anomalous dimension of the $\underset{\sim}{P}$ field. In an expansion of the RFT about a scale invariant theory γ is found (possibly unreliably) to be about -3/8.

Figure 4.10 Reggeon graphs for the propagator of a secondary trajectory, dotted line, coming from its interaction with the $\underset{\sim}{P}$, wiggly line. The $\underset{\sim}{P}$ interacts with itself. For the usual reasons only triple couplings are considered.

Figure 5.1 Kinematics associated with the double Regge limit of the five point amplitude. In this limit s_{12}, s_{13}, $s_{23} \to \infty$ with Q_1^2, Q_2^2 and $\eta_{12} = s_{12}/s_{13}s_{23}$ held fixed.

Figure 5.2 A hybrid Feynman graph and its Reggeon graph contribution to the double Regge limit of the five point function. Two distinct partial wave terms enter; one has simultaneous discontinuities in s_{12} and s_{13}; the other, in s_{12} and s_{23}.

Figure 5.3 A Reggeon graph with branch points in J_1 and J_2 which contributes to the double Regge limit of the $2 \to 3$ process.

Figure 5.4 The picture of the basic Pomeron ($\underset{\sim}{P}$) as generalized ladder graph.

Figure 5.5 The cut across the $\underset{\sim}{P}$ reveals a multiperipheral production process in the s-channel.

Figure 5.6 (a) Absoptive corrections to the basic production process, production from two chains, and production with a large rapidity gap - these amplitudes are revealed by the cut of the two Reggeon graph contri-

bution to the elastic amplitude. One cuts one, two, or zero Reggeons respectively.

(b) The production processes revealed by cutting up the Reggeon graph of Figure 2.6.

Figure 5.7 (a) The distribution in number (n) of particles produced by the graphs with multiple non-interacting exchanged $\underset{\sim}{P}$. Figure 1.2 is an example of this.

(b) The expected smoothing of the σ_n distribution of Fig. 5.7a which will come from $\underset{\sim}{P}$ interactions.

Figure 5.8 A cut part way through a Reggeon which leaves a hanging chain with rapidity spread y. The particle line carrying momentum q will have mass $q^2 \alpha e^y$, which must be large since a Reggeon is cut. Since large q^2 is presumed to be absent, so is the partial cut of this Reggeon.

Figure 5.9 Reggeon graph contributions to the 3→3 amplitude whose discontinuity in $M^2 = (P_a + P_b - P_c)^2$ gives the single particle inclusive distribution $a + b \to c + X$ in the central region.

Figure 6.1 Reggeon graphs which contribute to the leading behavior of the total cross section. The expansion parameter here is (r_0^2/α_0') log s. When it is of order one, the whole series must be summed to give the strong coupling scaling solution of RFT. Indications are that at present energies this parameter is only of order 1/8 or so.

Figure 6.2 The triple Regge region of the inclusive process A + B → A + anything, where one may estimate the triple Regge coupling.

Figure 6.3 Elastic amplitudes study the two time correlation function for sources (called particles) to emit Reggeons and reabsorb them. The times are 0 and log s for the elastic process. For long times the scaling solution of RFT is applicable. It averages over enormous numbers of s-channel inelastic processes and over the hadron coordinates which are at the heart of Reggeon building.

Figure 6.4 Single particle inclusive amplitudes (as in Fig. 6.2) involve three times: 0, log M^2, and log s. The study of many time correlation functions reveals how Pomerons behave at intermediate times. Such correlation functions are equivalent to learning about s-channel physics in RFT.

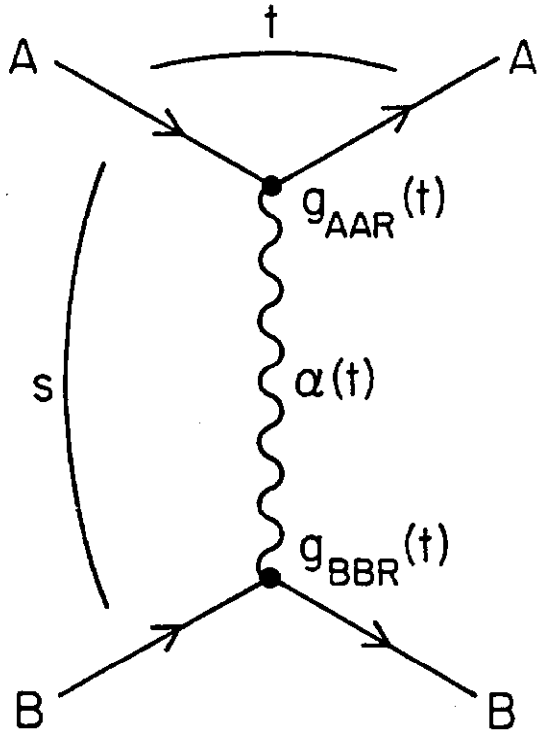

Fig. 1.1

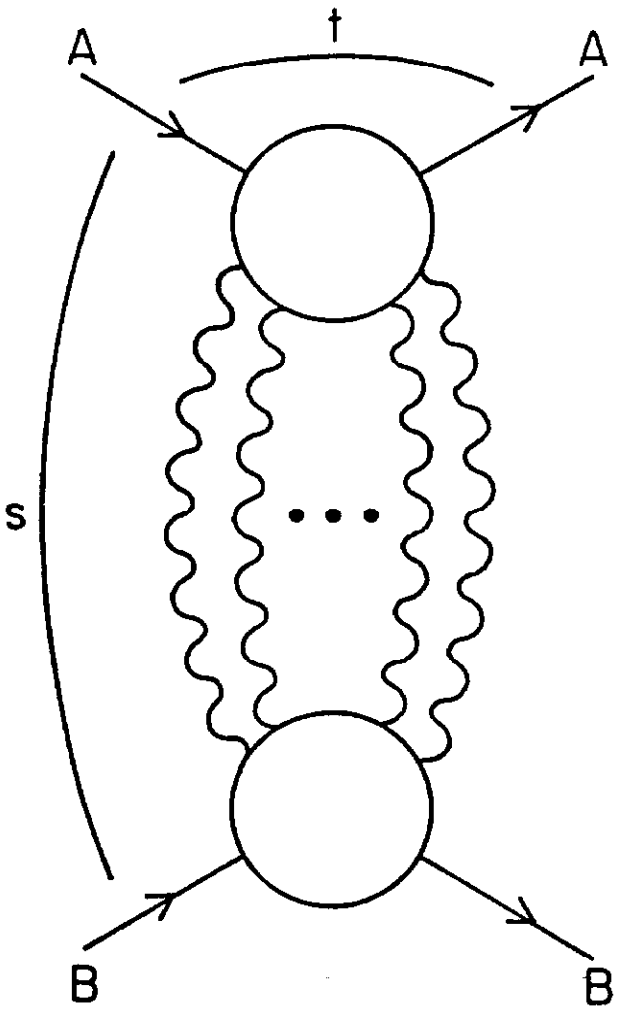

Fig. 1.2

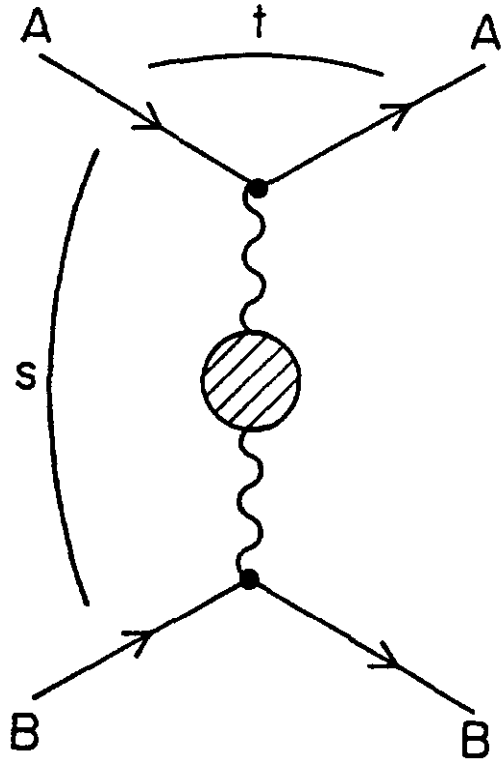

Fig. 1.3

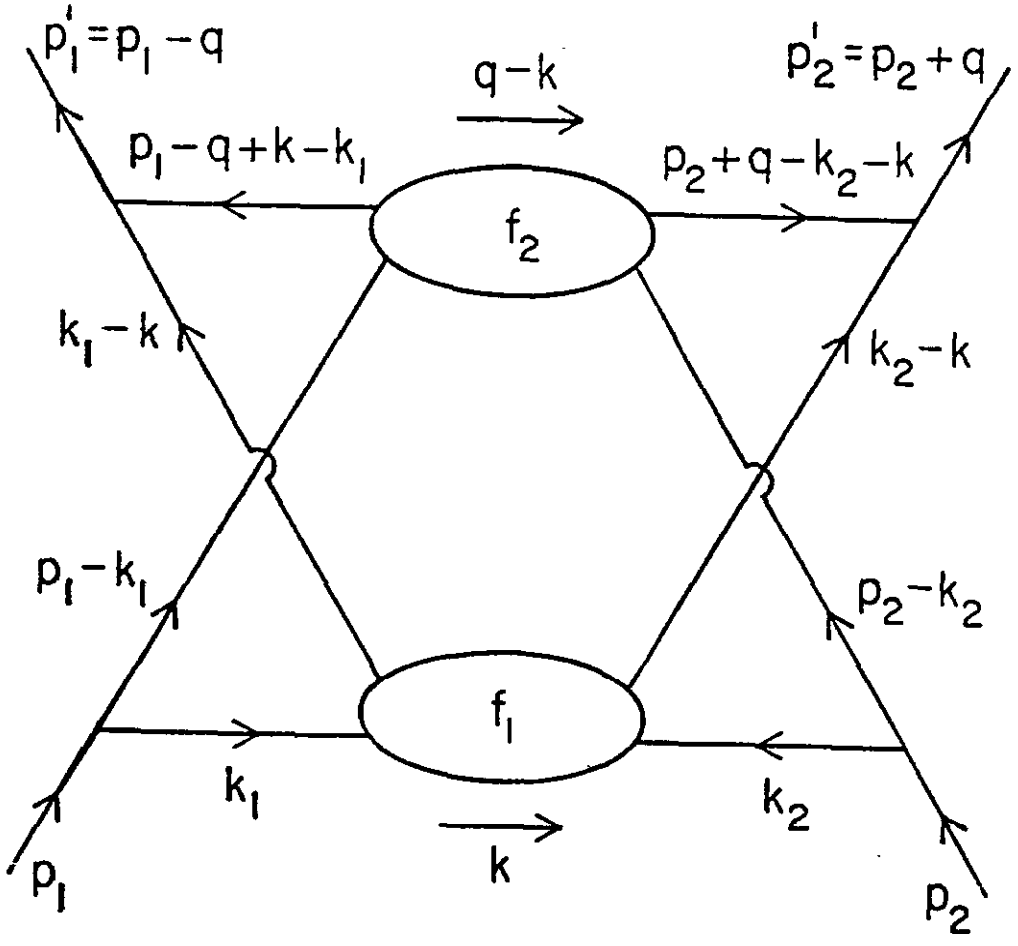
$p_1' = p_1 - q$
$q - k$
$p_2' = p_2 + q$
$p_1 - q + k - k_1$
$p_2 + q - k_2 - k$
f_2
$k_1 - k$
$k_2 - k$
$p_1 - k_1$
$p_2 - k_2$
f_1
k_1
k_2
k
p_1
p_2

Fig. 2.1

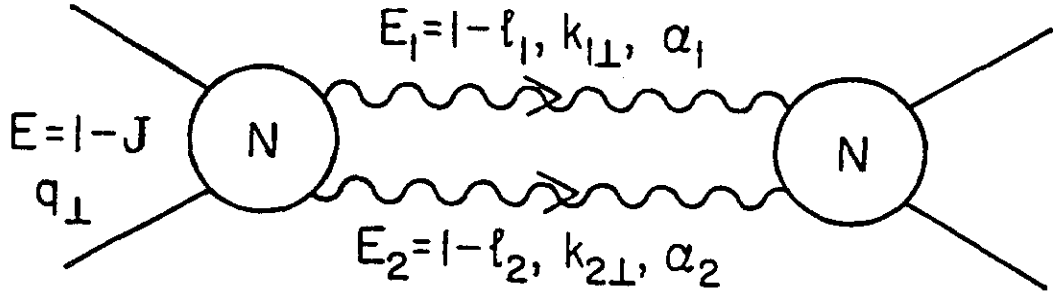
$E_1 = 1 - \ell_1,\ k_{1\perp},\ \alpha_1$
$E = 1 - J$
$q_\perp$
N
N
$E_2 = 1 - \ell_2,\ k_{2\perp},\ \alpha_2$

Fig. 2.2

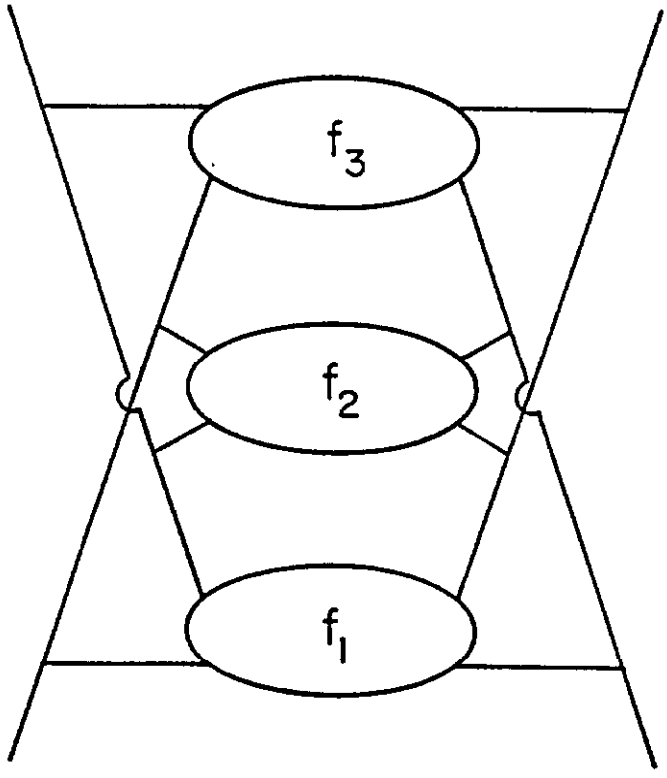
f_3
f_2
f_1

Fig. 2.3

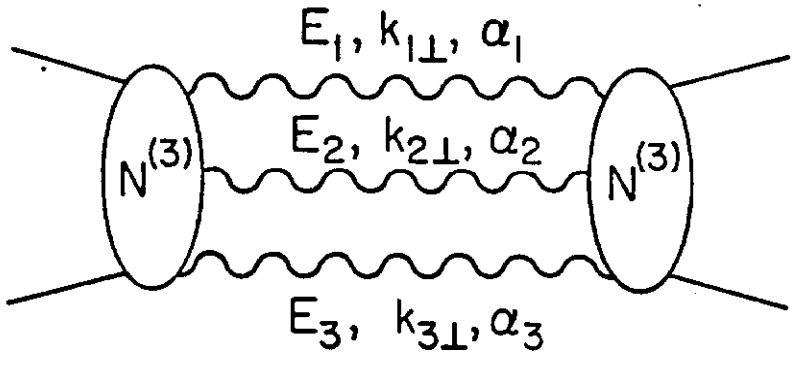
$E_1, k_{1\perp}, \alpha_1$
$N^{(3)}$
$E_2, k_{2\perp}, \alpha_2$
$N^{(3)}$
$E_3, k_{3\perp}, \alpha_3$

Fig. 2.4

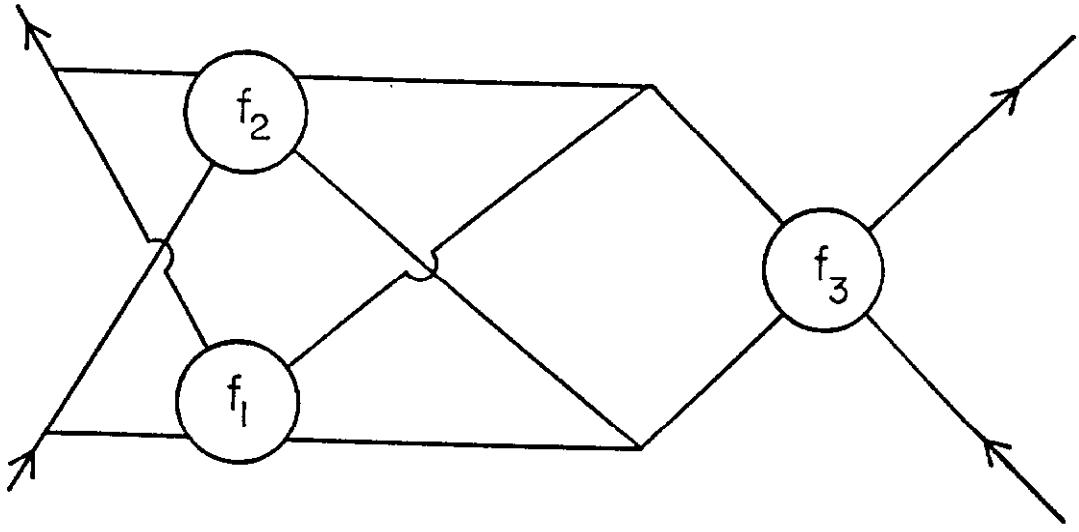
f_2
f_1
f_3

Fig. 2.5

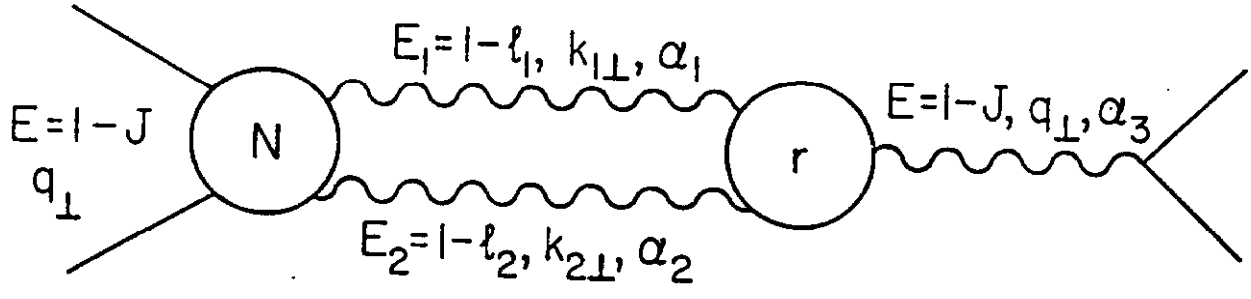
$E_1 = 1 - \ell_1,\ k_{1\perp},\ \alpha_1$
$E = 1 - J$
$q_\perp$
N
r
$E = 1 - J,\ q_\perp, \alpha_3$
$E_2 = 1 - \ell_2, k_{2\perp}, \alpha_2$

Fig. 2.6

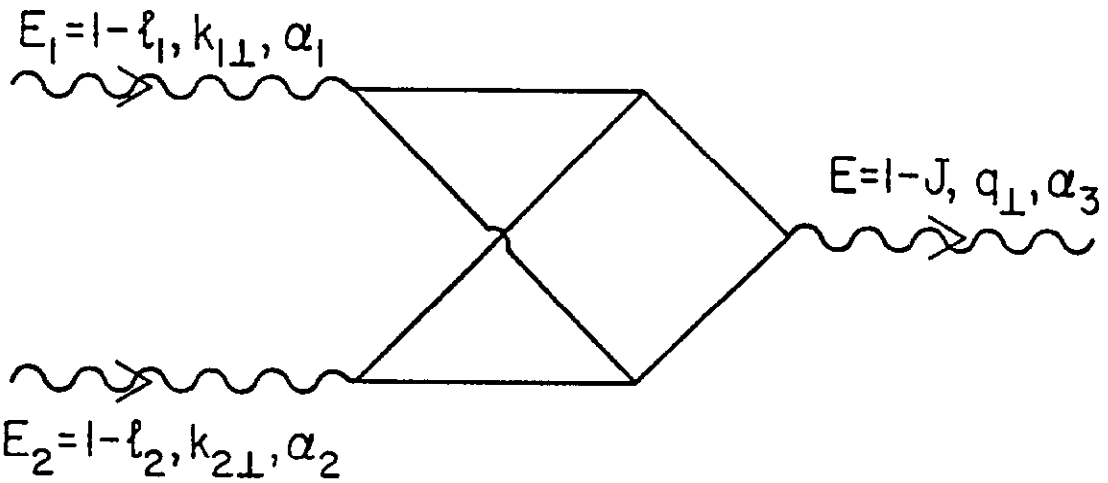
$E_1=1-\ell_1, k_{1\perp}, \alpha_1$
$E=1-J, q_\perp, \alpha_3$
$E_2=1-\ell_2, k_{2\perp}, \alpha_2$

Fig. 2.7

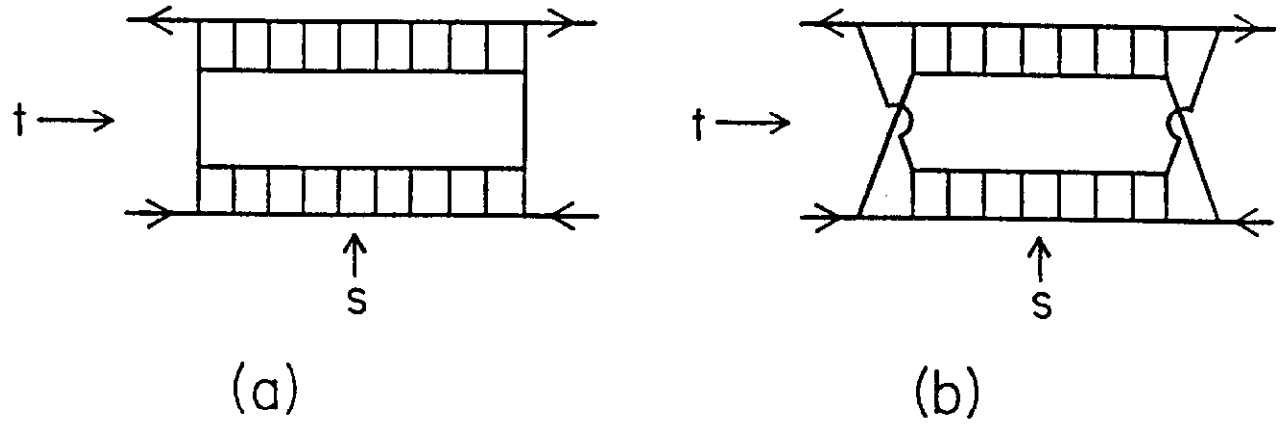

Fig. 3.1

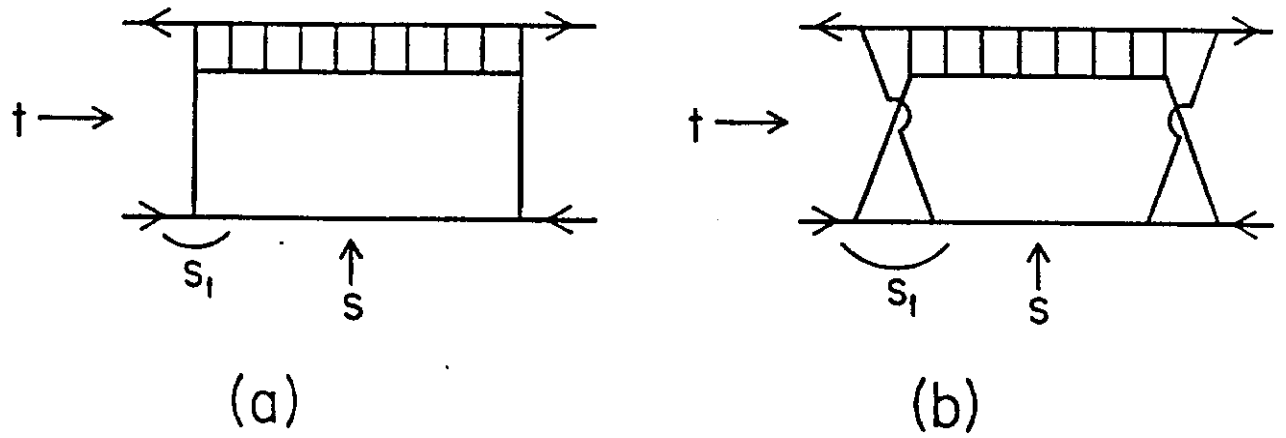

Fig. 3.2

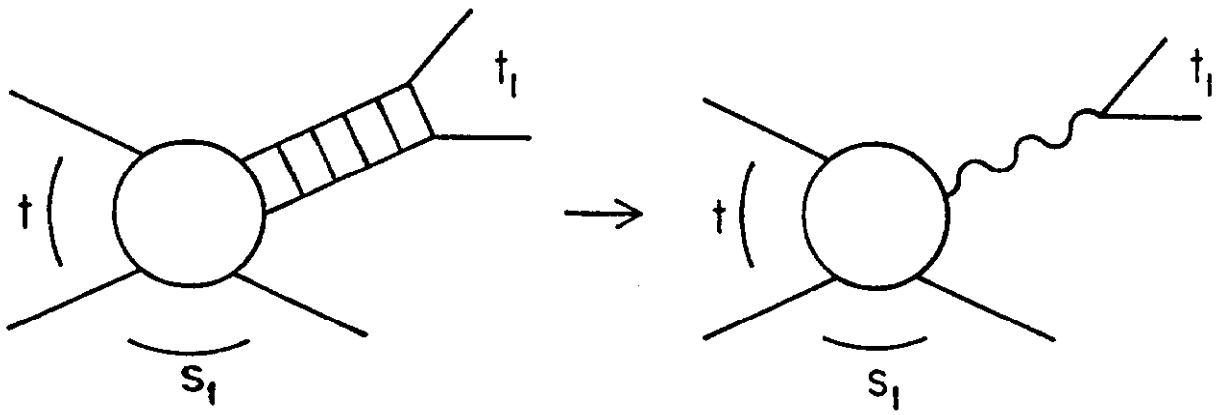

Fig. 3.3

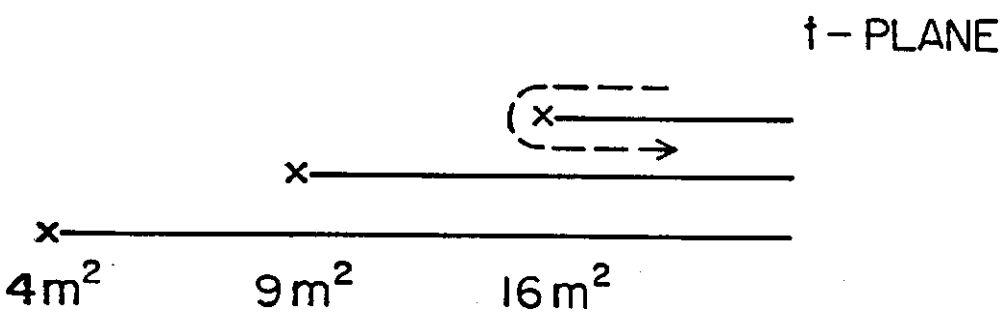

Fig. 3.4

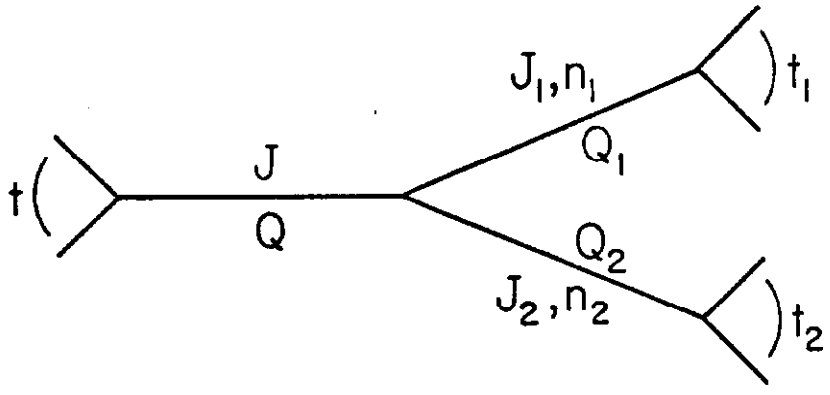
t
J
Q
J1,n1
Q1
t1
Q2
J2,n2
t2

Fig. 3.5

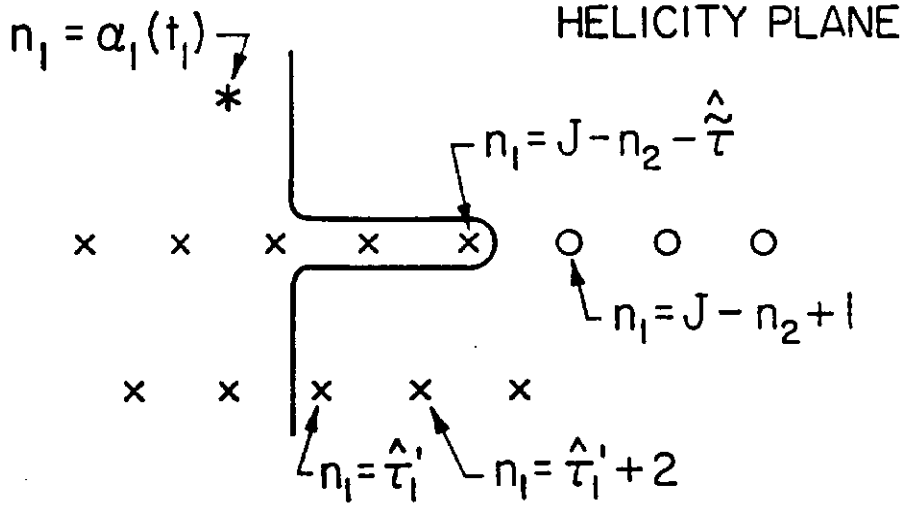
n1 = α1(t1)
HELICITY PLANE
n1 = J − n2 − τ̃
n1 = J − n2 + 1
n1 = τ̂1'
n1 = τ̂1' + 2

Fig. 3.6

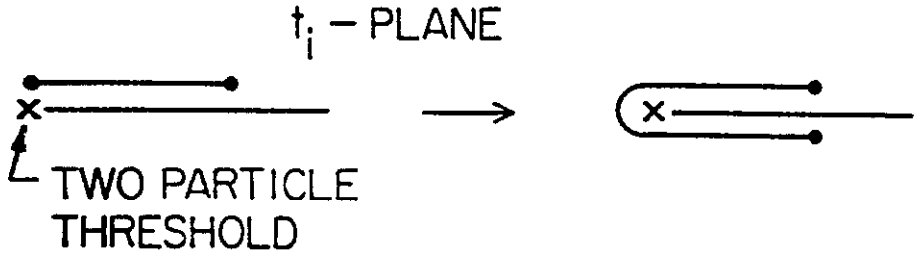
t_i – PLANE
TWO PARTICLE
THRESHOLD

Fig. 3.7

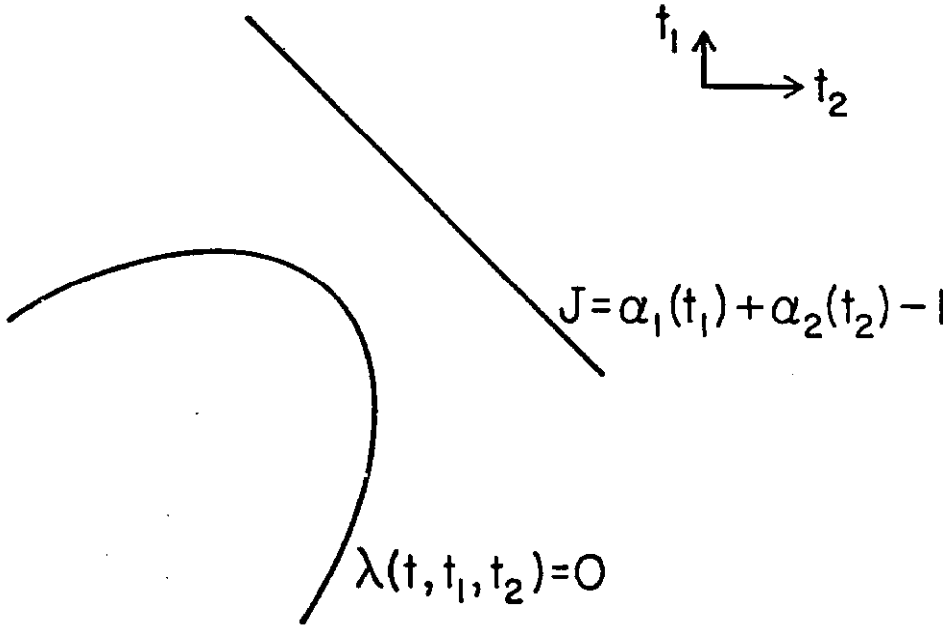
t_1
t_2
$J=\alpha_1(t_1)+\alpha_2(t_2)-1$
$\lambda(t,t_1,t_2)=0$

Fig. 3.8

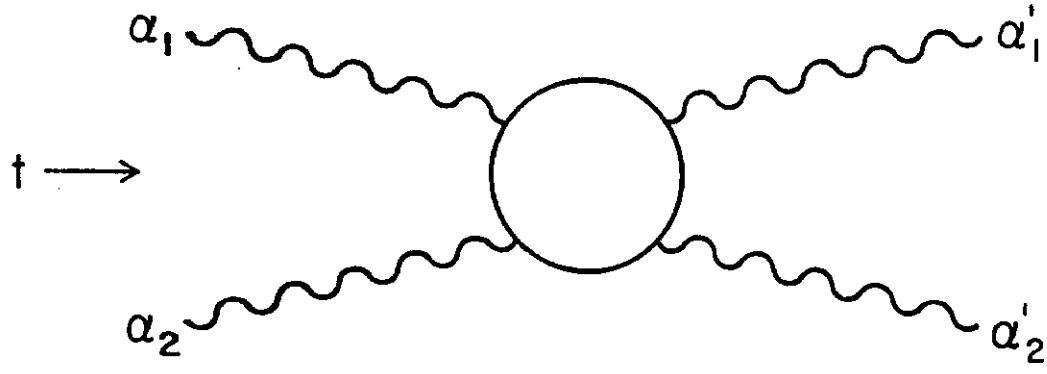

Fig. 3.9

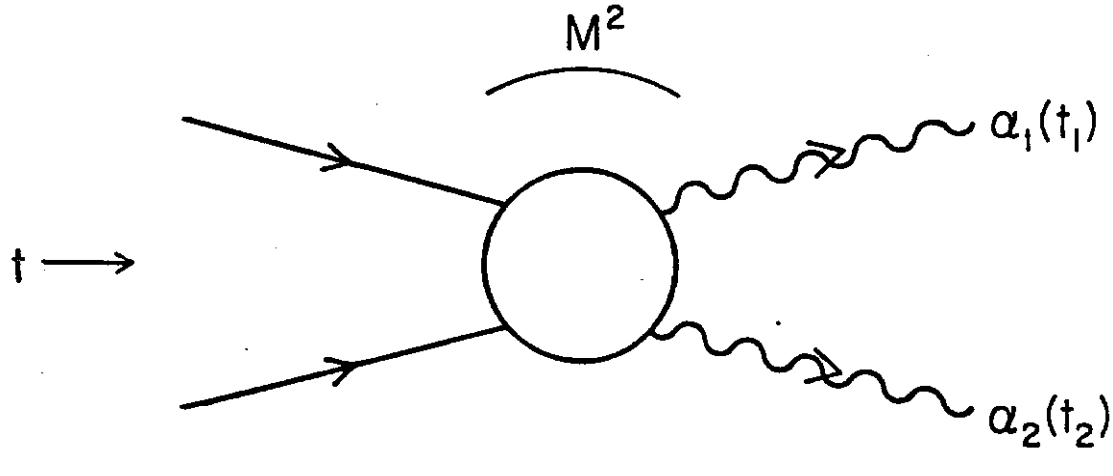

Fig. 3.10

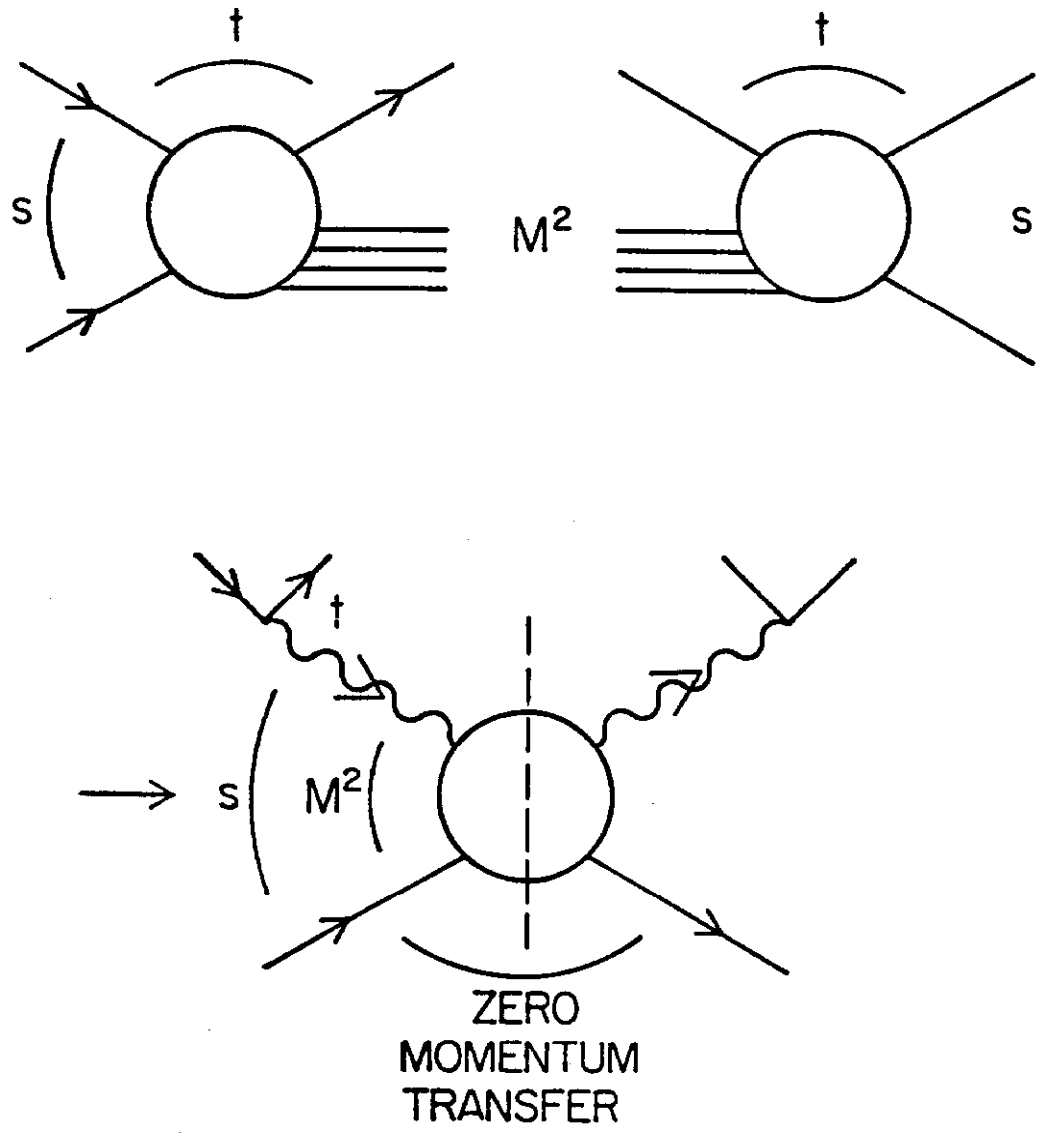

Fig. 3.11

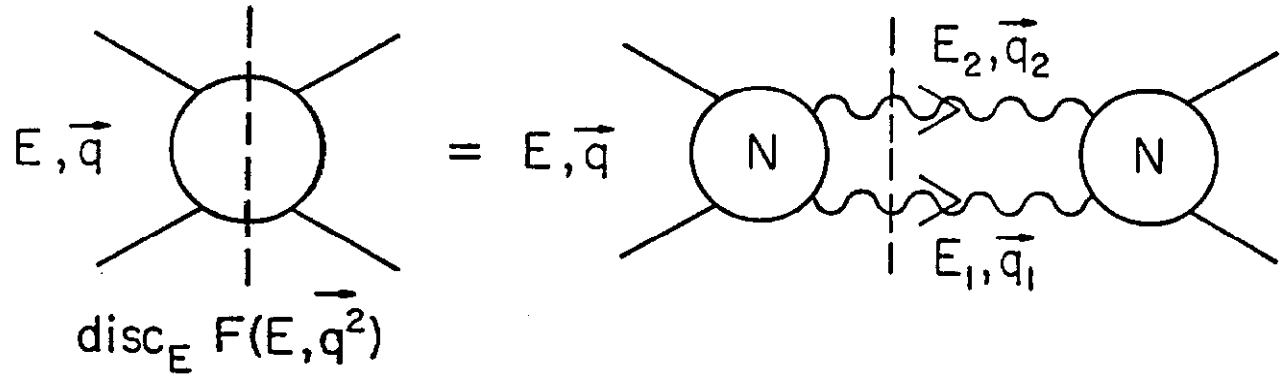

Fig. 3.12

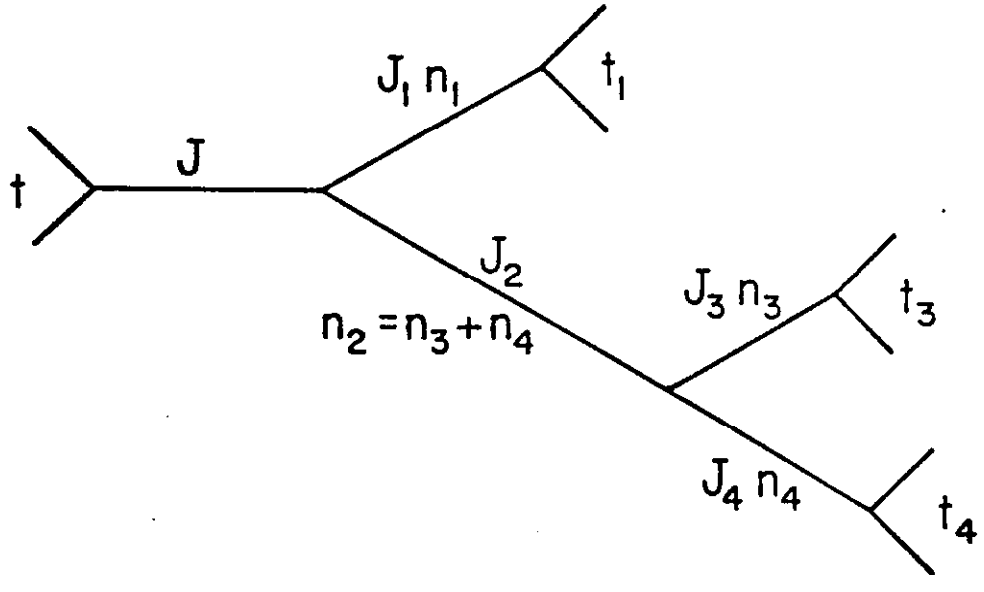

Fig. 3.13

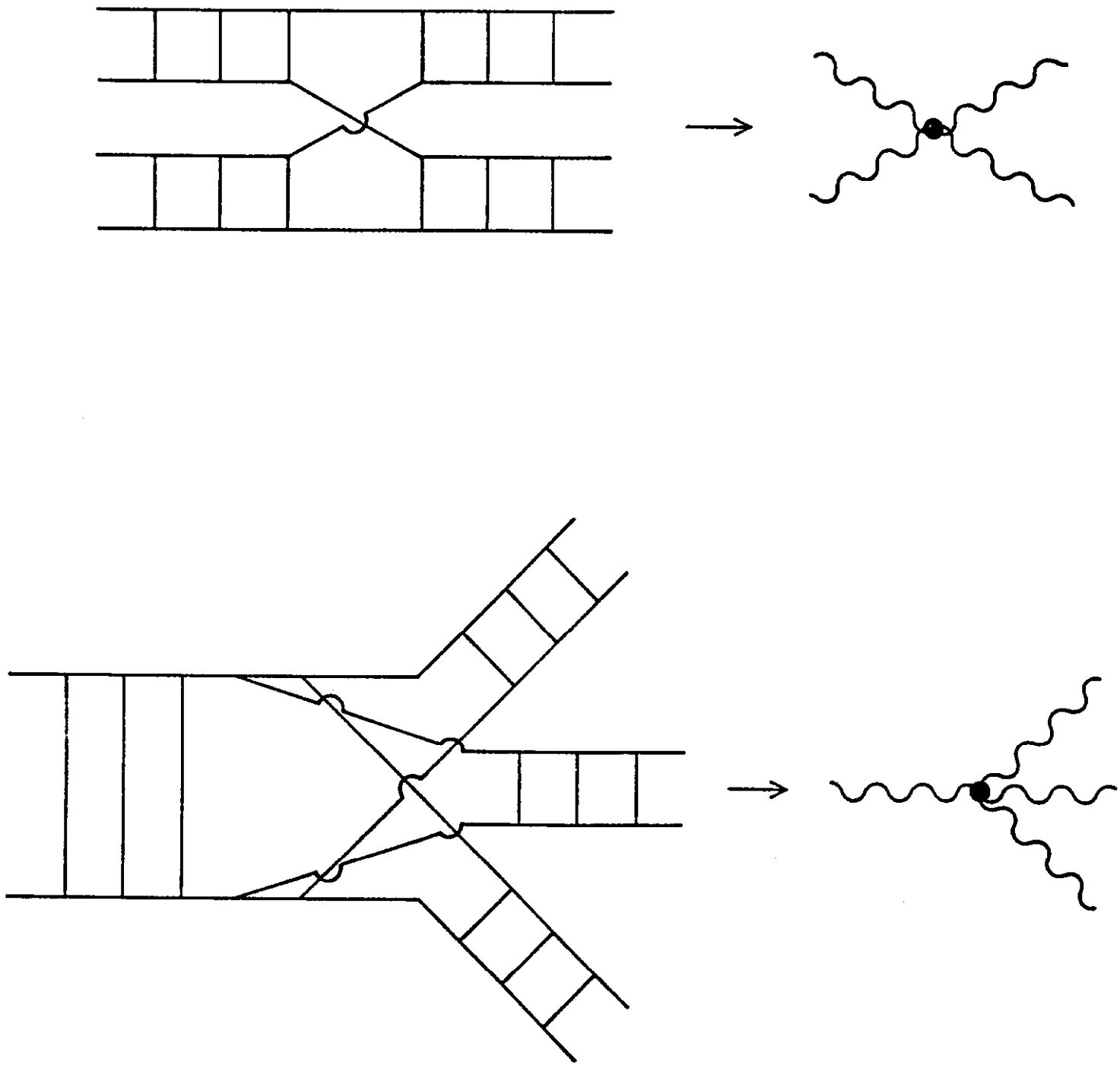

Fig. 4.1

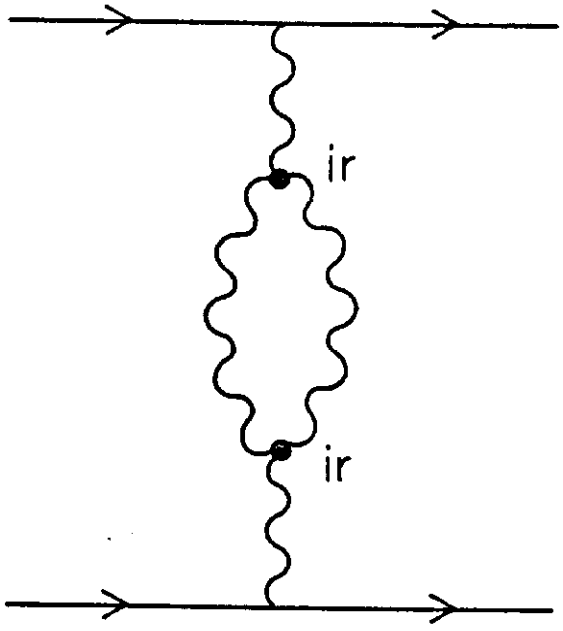

Fig. 4.2

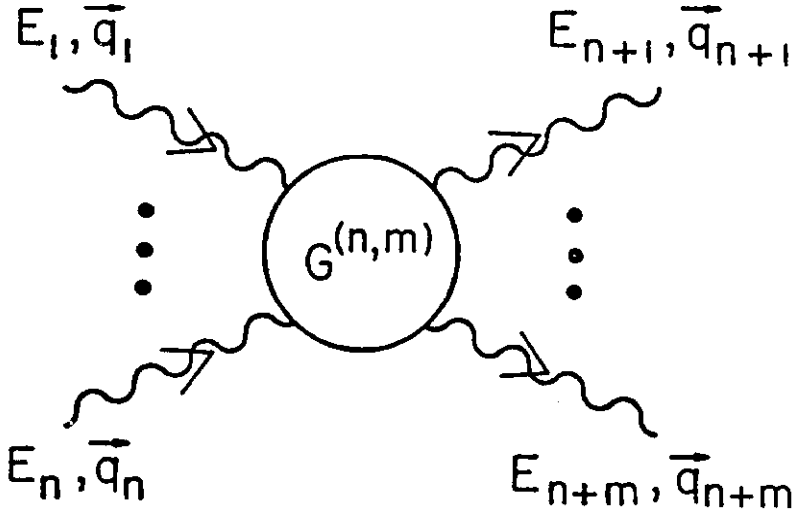

Fig. 4.3

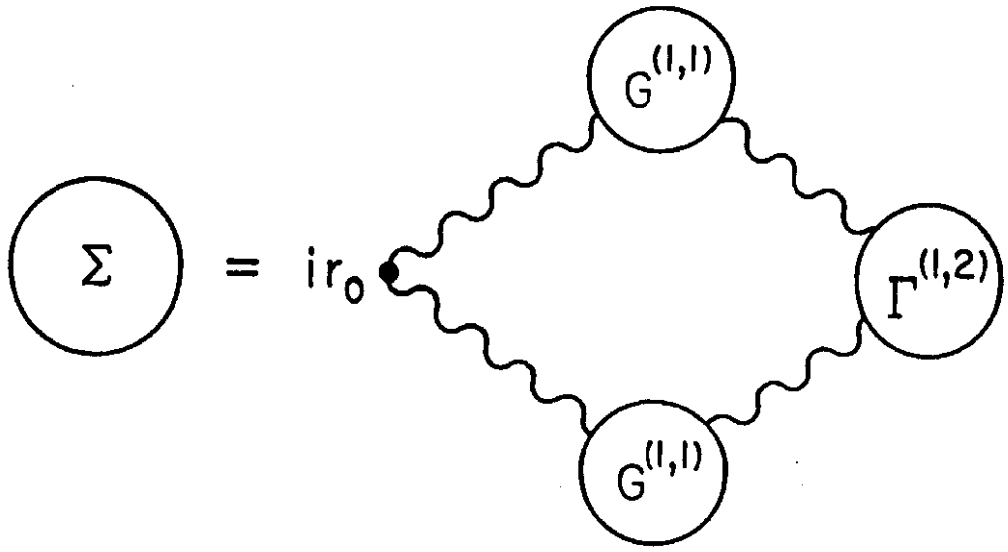

Fig. 4.4

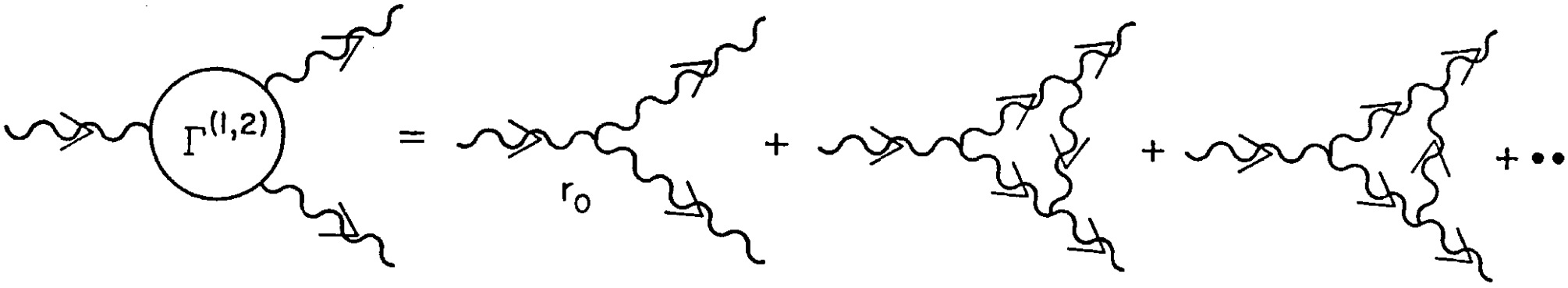

Fig. 4.5

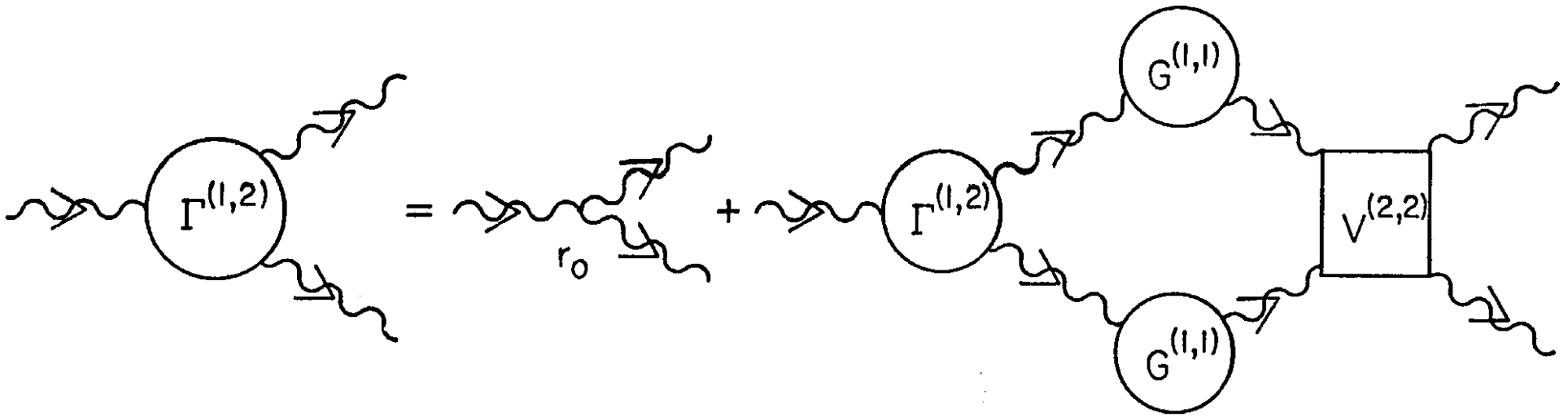

Fig. 4.6

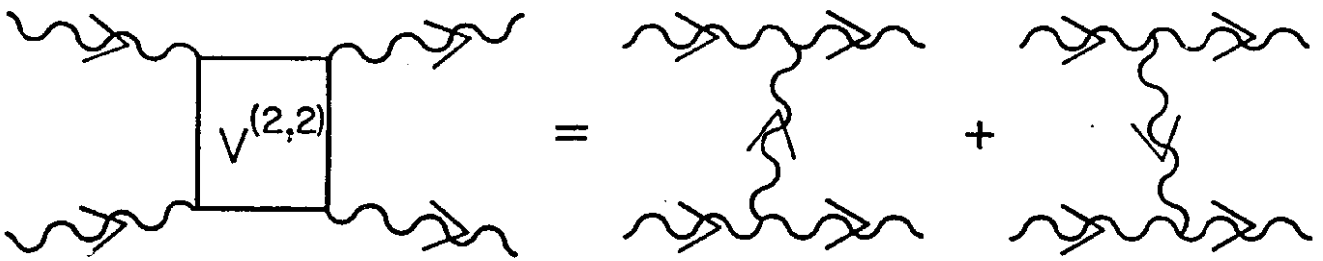

Fig. 4.7

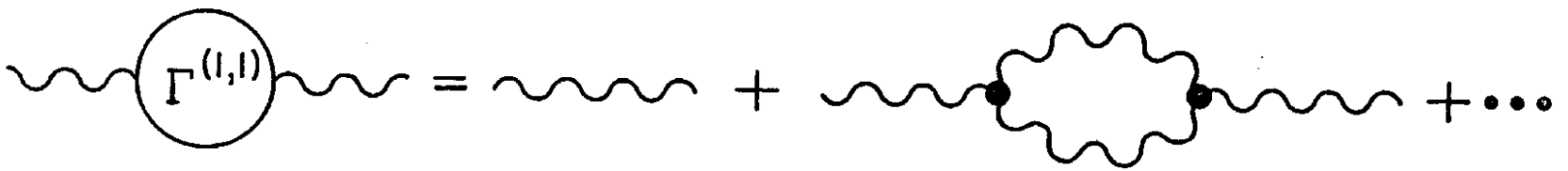

Fig. 4.8

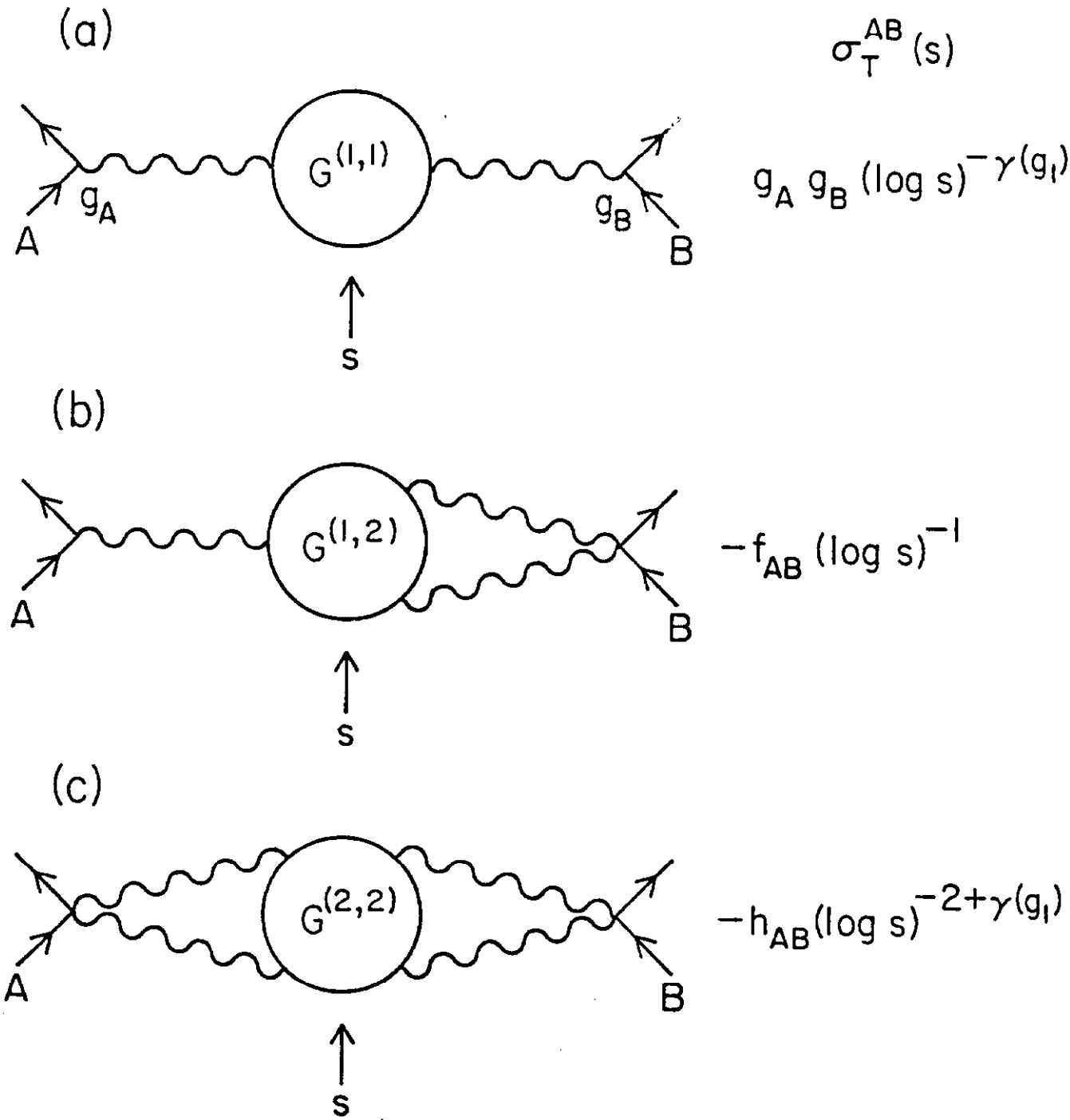
(a)
$\sigma_T^{AB}(s)$
$G^{(1,1)}$
g_A
g_B
A
B
s
$g_A\, g_B\, (\log s)^{-\gamma(g_1)}$
(b)
$G^{(1,2)}$
A
B
s
$-f_{AB}\, (\log s)^{-1}$
(c)
$G^{(2,2)}$
A
B
s
$-h_{AB}(\log s)^{-2+\gamma(g_1)}$

Fig. 4.9

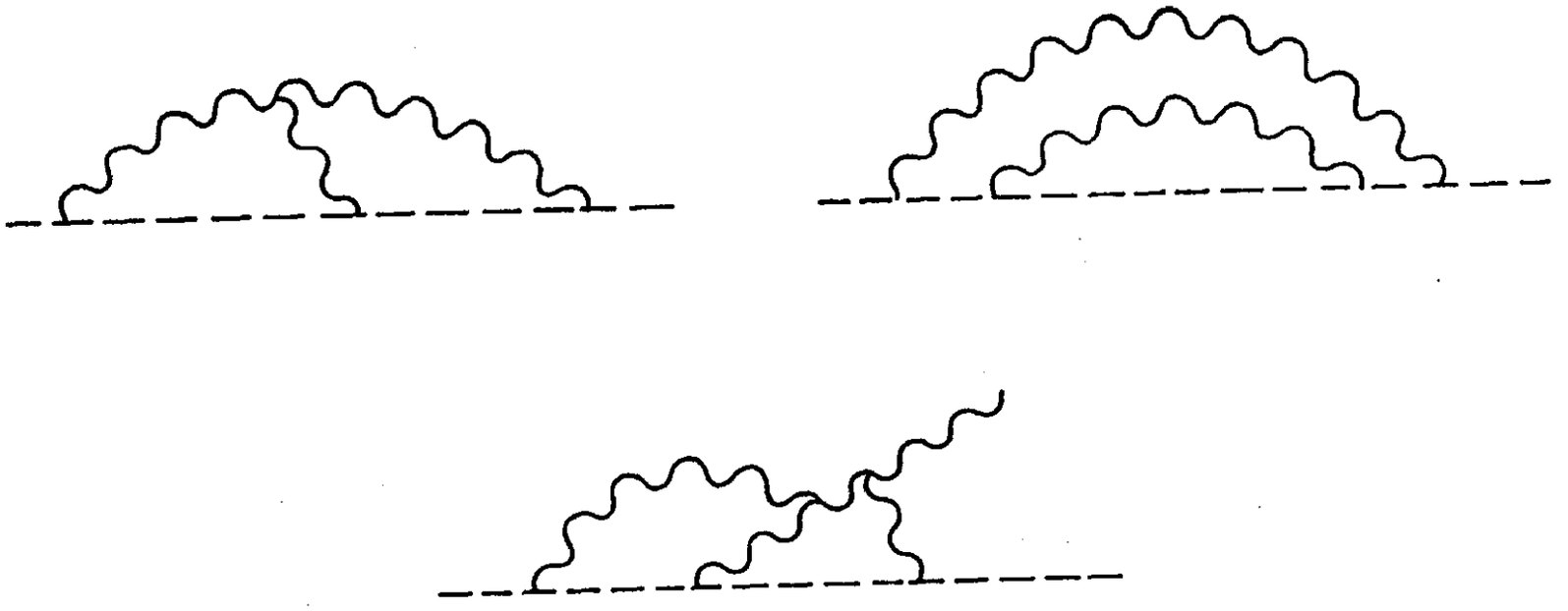

Fig. 4.10

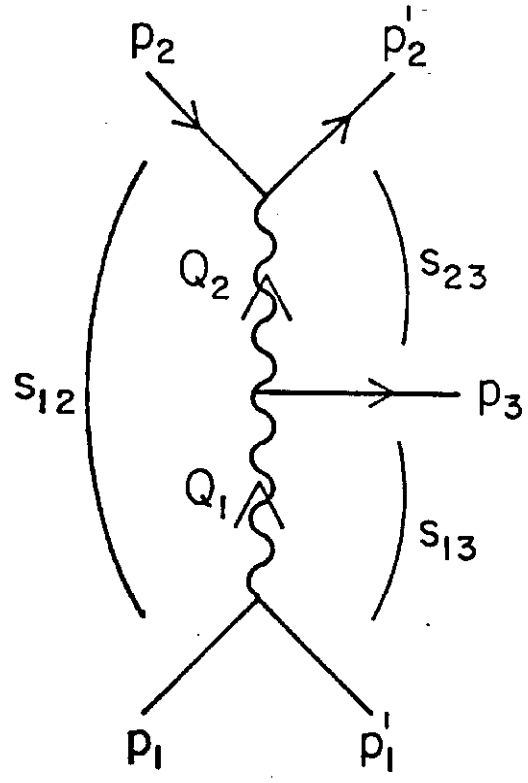

Fig. 5.1

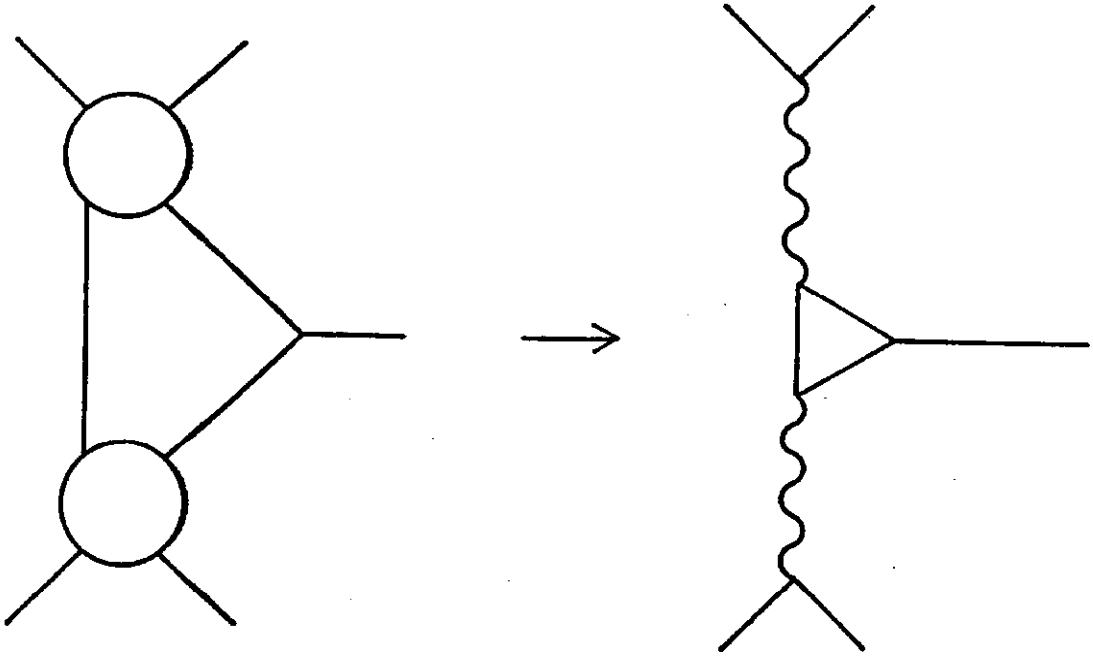

Fig. 5.2

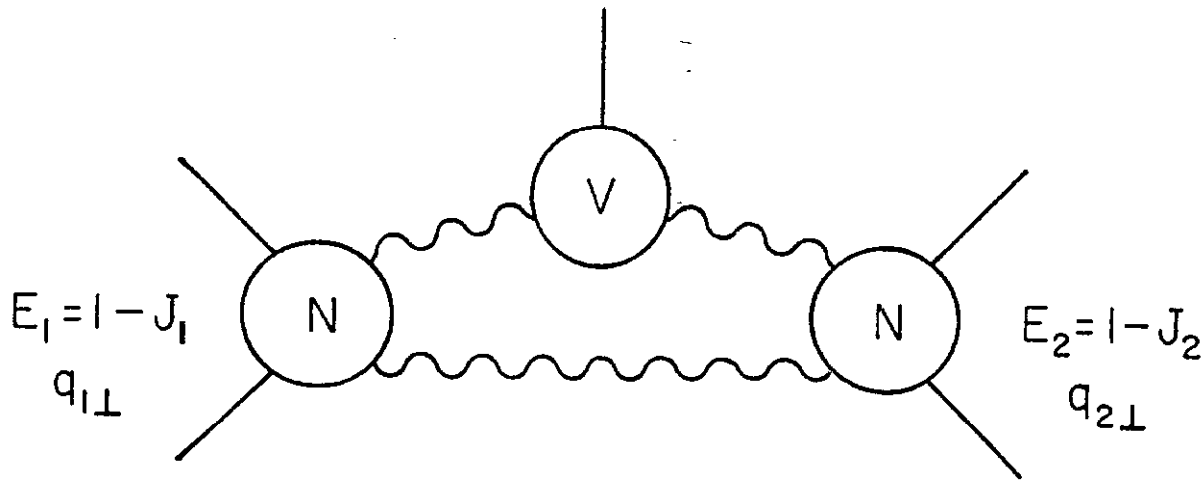

Fig. 5.3

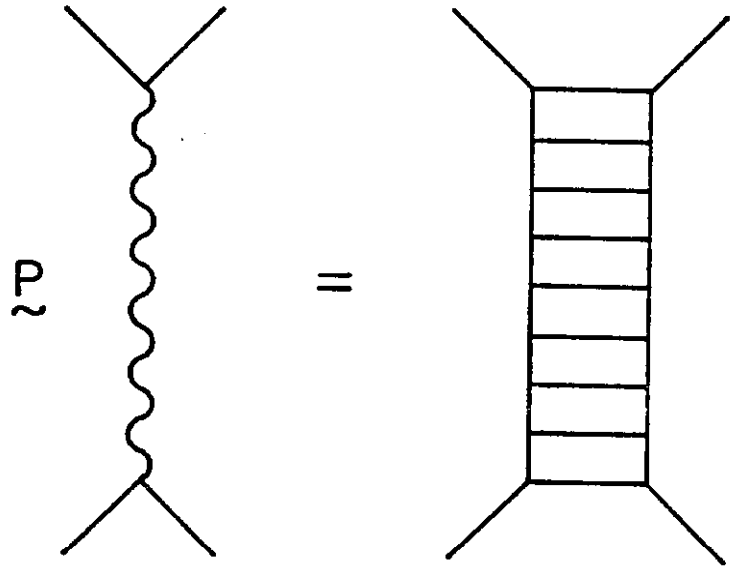

Fig. 5.4

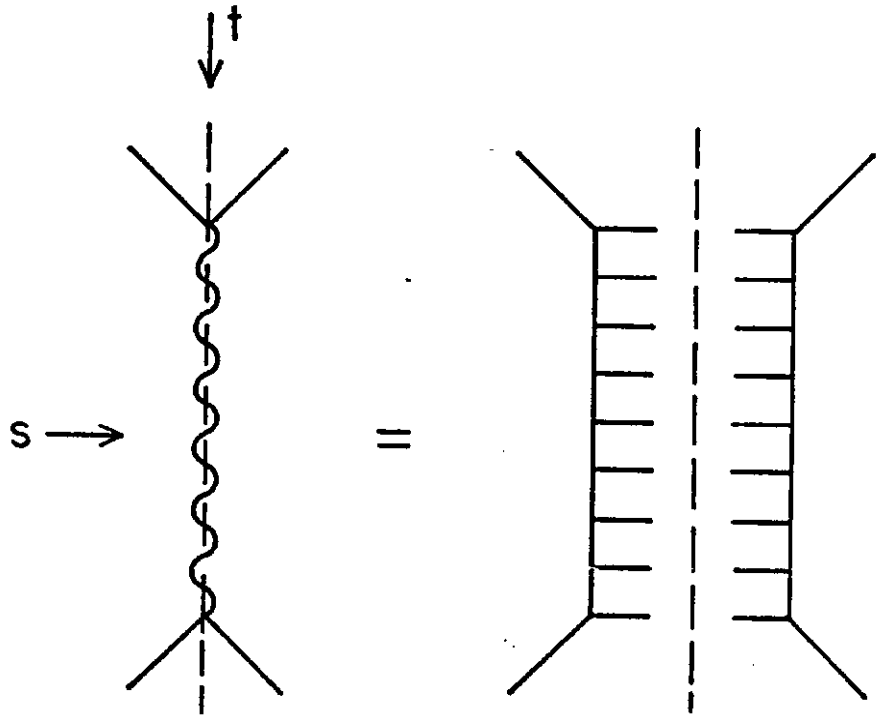

Fig. 5.5

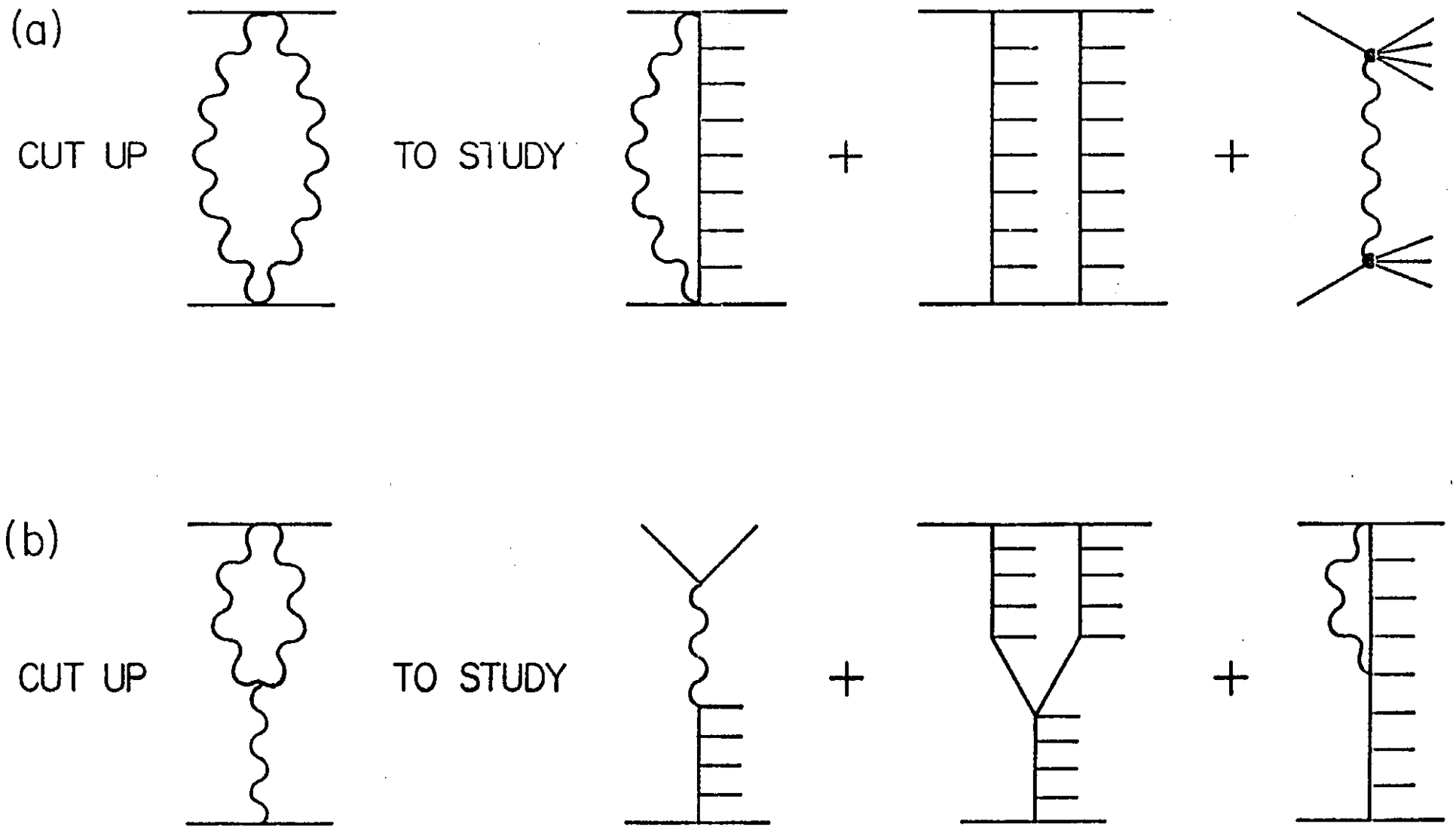

Fig. 5.6

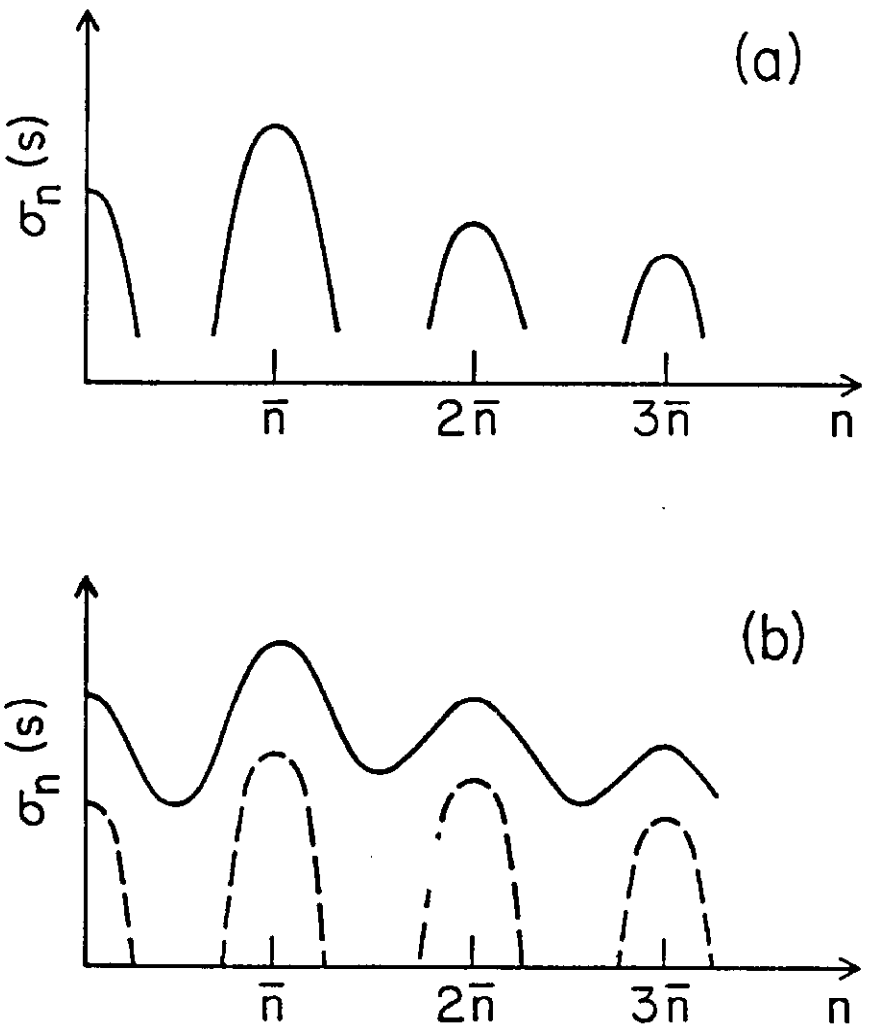

Fig. 5.7

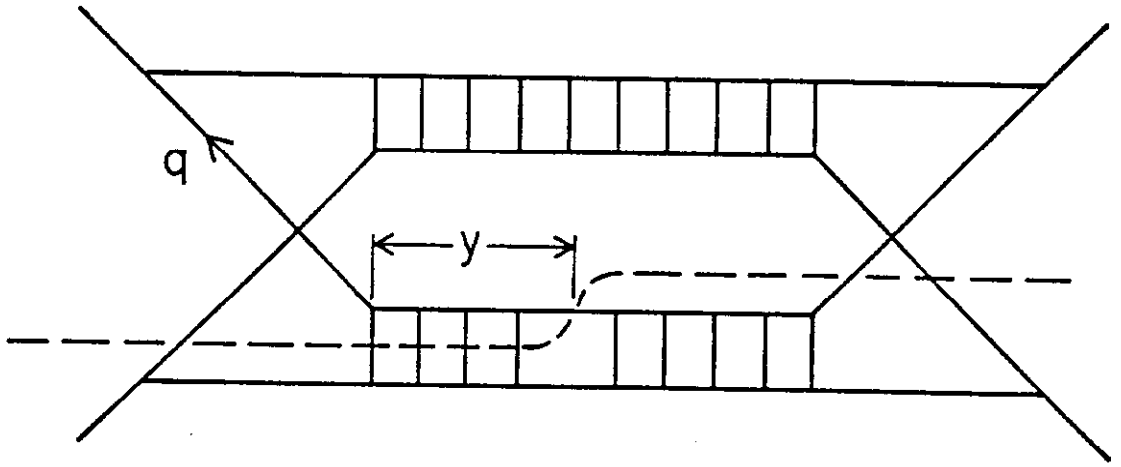

Fig. 5.8

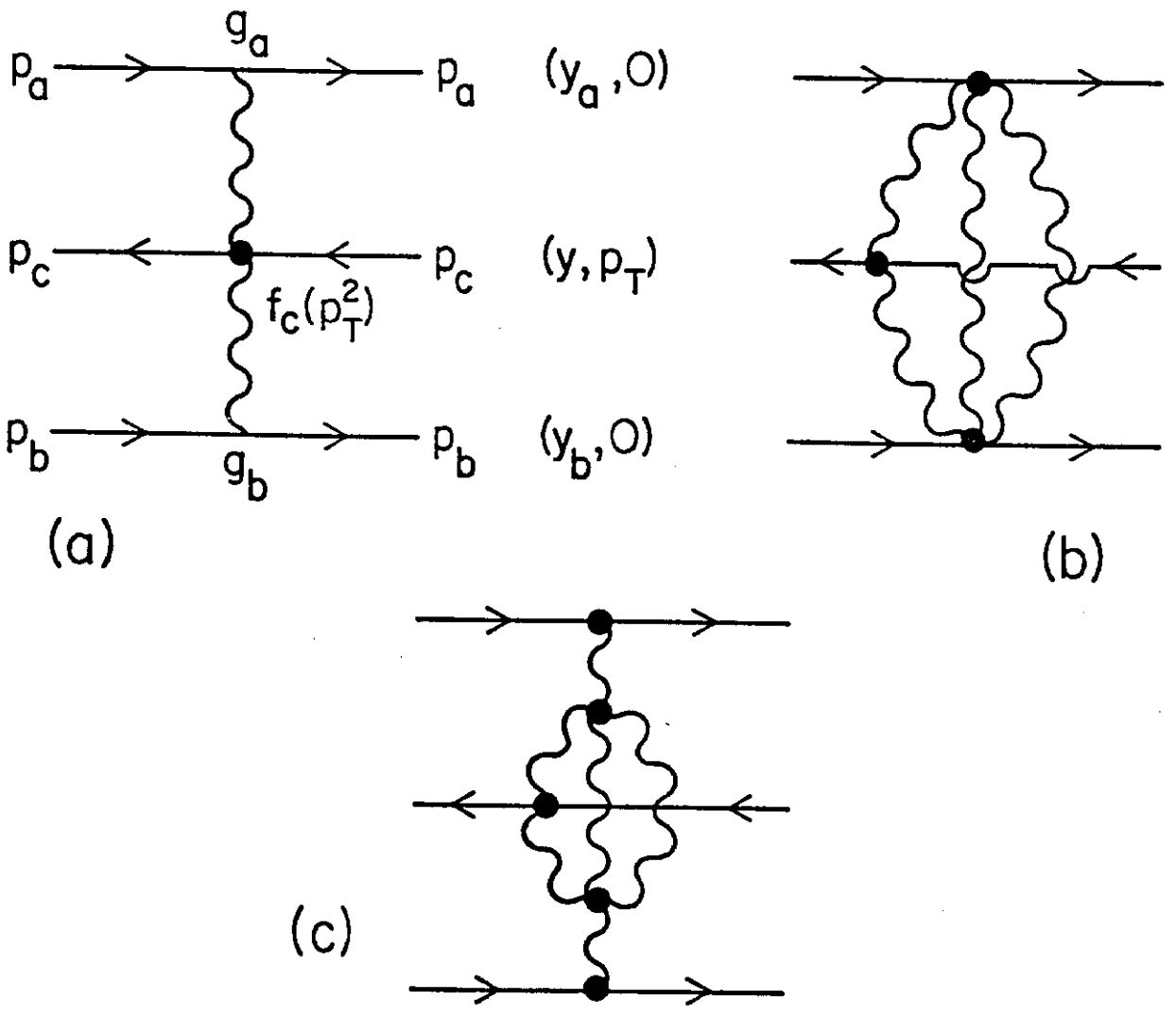

Fig. 5.9

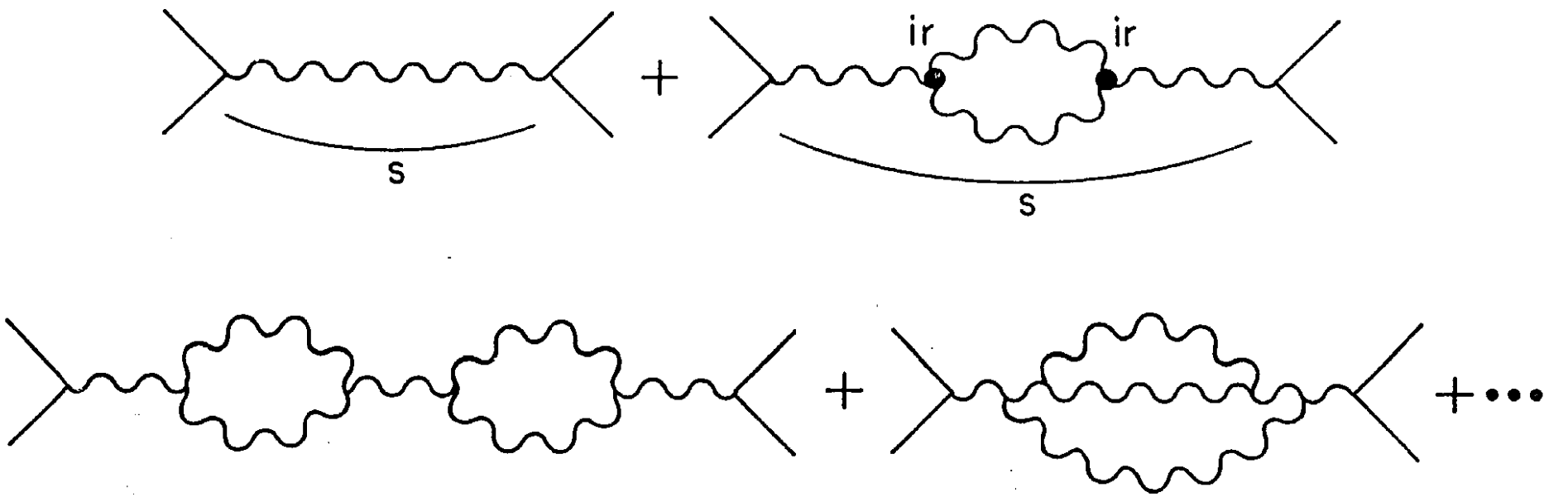

Fig. 6.1

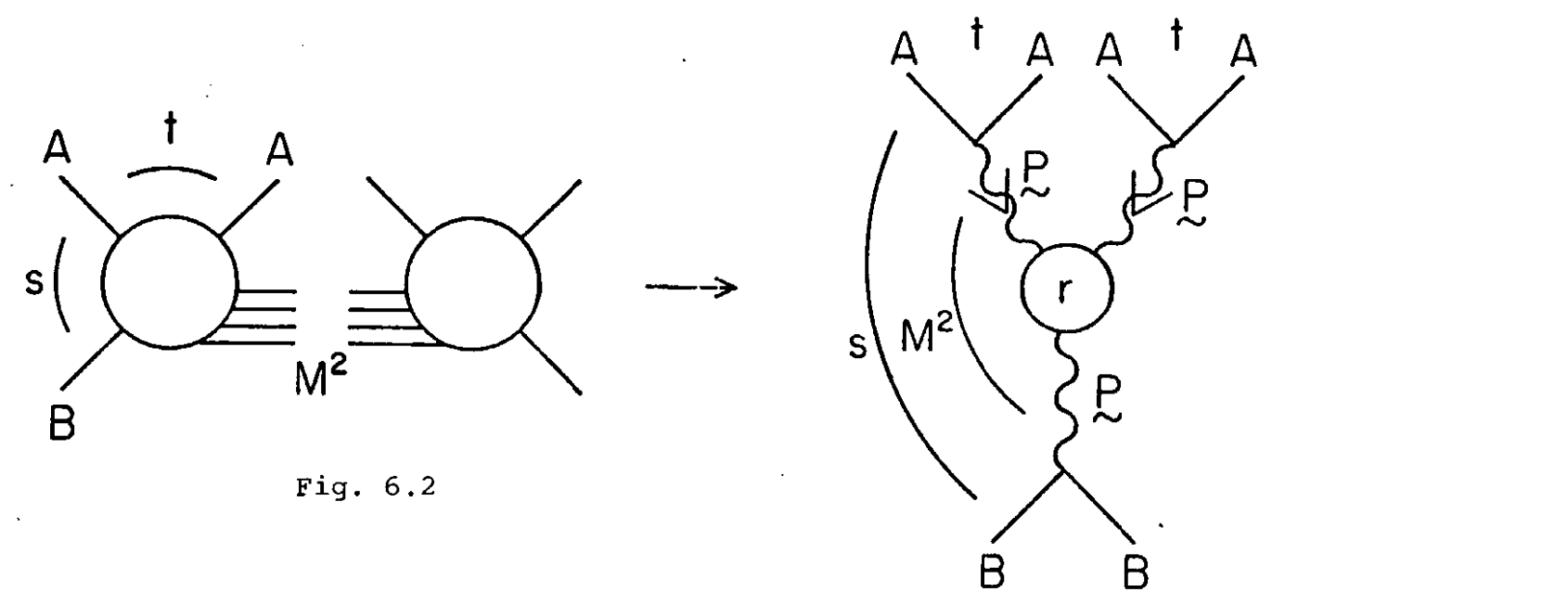

Fig. 6.2

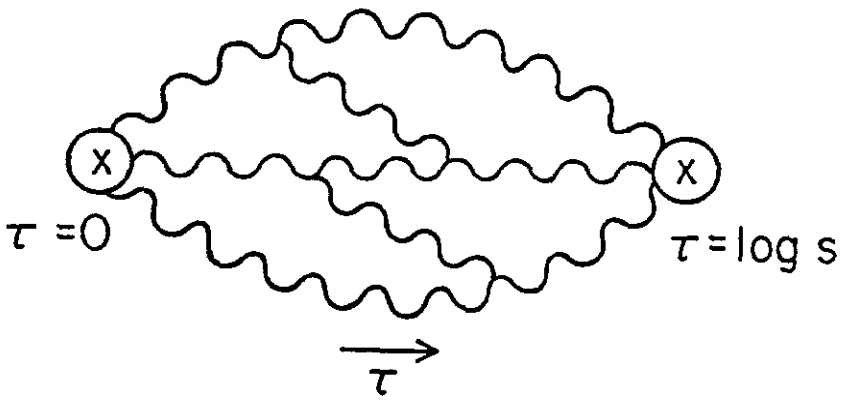

Fig. 6.3

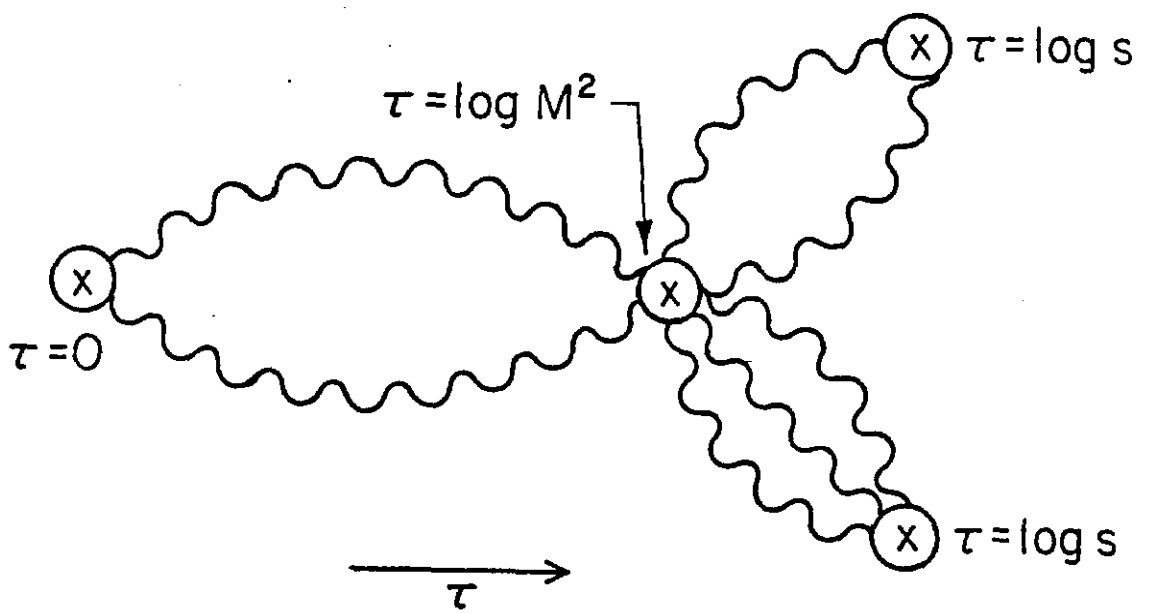

Fig. 6.4